AD-A081 180 IOWA INST OF HYDRAULIC RESEARCH IOWA CITY F/G 20/4
EXPERIMENTS ON TRANSITIONAL OSCILLATORY PIPE FLOW,(U)
AUG 79 B R RAMAPRIAN, S W TU DAAG-29-79-G-0017
UNCLASSIFIED IIHR-221 NL

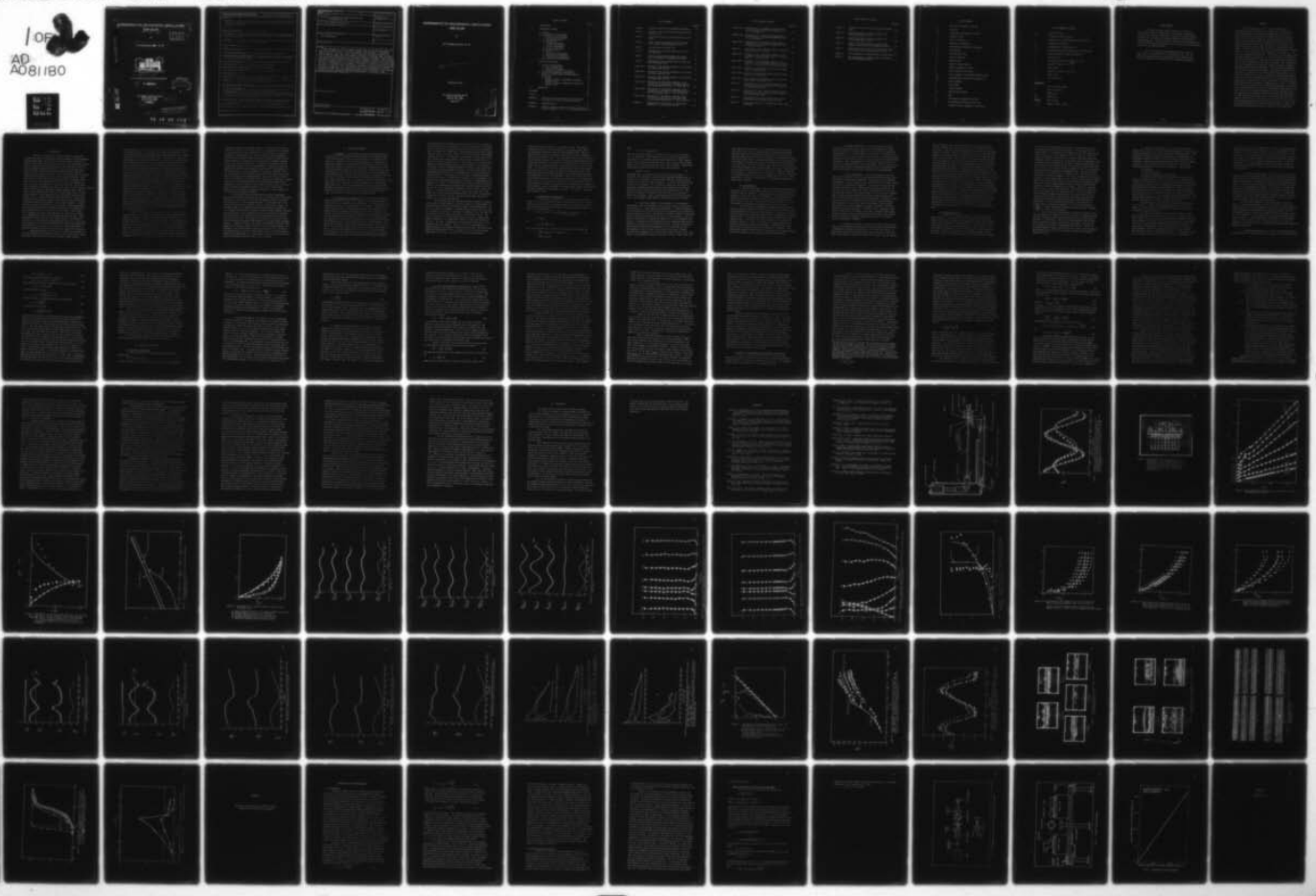

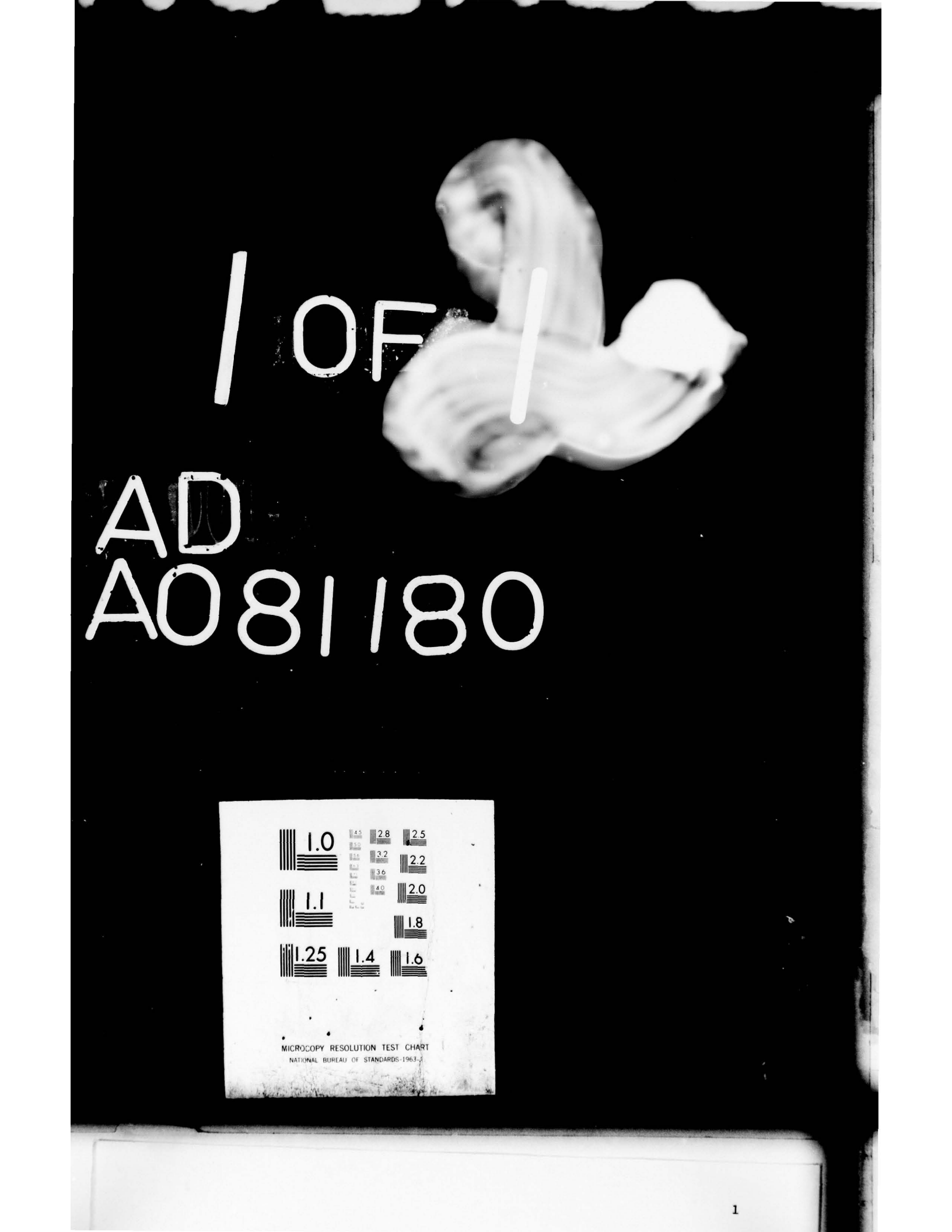
1 OF
AD
A081180
1.0
1.1
1.25
1.4
1.6
1.8
2.0
2.2
2.5
2.8
3.2
3.6
4.0
MICROCOPY RESOLUTION TEST CHART
NATIONAL BUREAU OF STANDARDS-1963-A

EXPERIMENTS ON TRANSITIONAL OSCILLATORY PIPE FLOW

by

B. R. Ramaprian and S. W. Tu

ADA081180

LEVEL II

Contract DAAG-29-79-G-0017

IIHR Report No. 221

DTIC ELECTE FEB 2 6 1980 S D

A

DDC FILE COPY

Iowa Institute of Hydraulic Research
The University of Iowa
Iowa City, Iowa 52242

August 1979

125

188 300

DISTRIBUTION STATEMENT A
Approved for public release;
Distribution Unlimited

79 10 04 024

INSTRUCTIONS FOR COMPLETING FORM NTIS-35 (Bibliographic Data Sheet based on COSATI Guidelines to Format Standards for Scientific and Technical Reports Prepared by or for the Federal Government, PB-180 600).

1. **Report Number.** Each individually bound report shall carry a unique alphanumeric designation selected by the performing organization or provided by the sponsoring organization. Use uppercase letters and Arabic numerals only. Examples FASEB-NS-73-87 and FAA-RD-73-09.

2. Leave blank.

3. **Recipient's Accession Number.** Reserved for use by each report recipient.

4. **Title and Subtitle.** Title should indicate clearly and briefly the subject coverage of the report, subordinate subtitle to the main title. When a report is prepared in more than one volume, repeat the primary title, add volume number and include subtitle for the specific volume.

5. **Report Date.** Each report shall carry a date indicating at least month and year. Indicate the basis on which it was selected (e.g., date of issue, date of approval, date of preparation, date published).

6. **Performing Organization Code.** Leave blank.

7. **Author(s).** Give name(s) in conventional order (e.g., John R. Doe, or J.Robert Doe). List author's affiliation if it differs from the performing organization.

8. **Performing Organization Report Number.** Insert if performing organization wishes to assign this number.

9. **Performing Organization Name and Mailing Address.** Give name, street, city, state, and zip code. List no more than two levels of an organizational hierarchy. Display the name of the organization exactly as it should appear in Government indexes such as Government Reports Index (GRI).

10. **Project/Task/Work Unit Number.** Use the project, task and work unit numbers under which the report was prepared.

11. **Contract/Grant Number.** Insert contract or grant number under which report was prepared.

12. **Sponsoring Agency Name and Mailing Address.** Include zip code. Cite main sponsors.

13. **Type of Report and Period Covered.** State interim, final, etc., and, if applicable, inclusive dates.

14. **Sponsoring Agency Code.** Leave blank.

15. **Supplementary Notes.** Enter information not included elsewhere but useful, such as: Prepared in cooperation with . . . Translation of . . . Presented at conference of . . . To be published in . . . Supersedes . . . Supplements . . . Cite availability of related parts, volumes, phases, etc. with report number.

16. **Abstract.** Include a brief (200 words or less) factual summary of the most significant information contained in the report. If the report contains a significant bibliography or literature survey, mention it here.

17. **Key Words and Document Analysis. (a). Descriptors.** Select from the Thesaurus of Engineering and Scientific Terms the proper authorized terms that identify the major concept of the research and are sufficiently specific and precise to be used as index entries for cataloging.
(b). Identifiers and Open-Ended Terms. Use identifiers for project names, code names, equipment designators, etc. Use open-ended terms written in descriptor form for those subjects for which no descriptor exists.
(c). COSATI Field/Group. Field and Group assignments are to be taken from the 1964 COSATI Subject Category List. Since the majority of documents are multidisciplinary in nature, the primary Field/Group assignment(s) will be the specific discipline, area of human endeavor, or type of physical object. The application(s) will be cross-referenced with secondary Field/Group assignments that will follow the primary posting(s).

18. **Distribution Statement.** Denote public releasability, for example "Release unlimited", or limitation for reasons other than security. Cite any availability to the public, other than NTIS, with address, order number and price, if known.

19 & 20. **Security Classification.** Do not submit classified reports to the National Technical Information Service.

21. **Number of Pages.** Insert the total number of pages, including introductory pages, but excluding distribution list, if any.

22. **NTIS Price.** Leave blank.

BIBLIOGRAPHIC DATA SHEET	1. Report No.	2.	3. Recipient's Accession No.

4. Title and Subtitle

Experiments on Transitional Oscillatory Pipe Flow
IIHR Report No. 221

5. Report Date
August 1979

6.

7. Author(s) B.R. Ramaprian and S.W. Tu

8. Performing Organization Rept. No.

9. Performing Organization Name and Address

10. Project/Task/Work Unit No.

11. Contract/Grant No.

12. Sponsoring Organization Name and Address

U.S. Army Research

13. Type of Report & Period Covered

14.

15. Supplementary Notes

16. Abstracts

Fully developed oil flow in a smooth circular pipe at a mean Reynolds number of about 2100 was subjected to a nominally sinusiodal flow modulation at frequencies ranging from 0.05 - 1.75 Hz. It was observed that flow oscillation increased the critical Reynolds number and, under certain conditions, even brought about linearization of the flow, which would be intermittently turbulent at the mean Reynolds number under quasi-steady (infinitely small oscillation frequency) conditions. The occurrence and extent of laminarization was, however, found to depend on factors such as the intermittency of turbulent puffs in the mean quasi-steady flow, frequency of oscillation,etc. Two series of experiments were performed. In one series, the oscillatory flow was fully turbulent. In both the cases, instantaneous velocities in the flow were measured using Laser Doppler anemometry. The instantaneous velocity was decomposed into time-mean periodic and random components employing ensemble averaging techniques. The experiments indicated that the laminarized oscillatory flow behaves (continued in book)

17. Key Words and Document Analysis. 17a. Descriptors

17b. Identifiers/Open-Ended Terms

17c. COSATI Field/Group

18. Availability Statement	19. Security Class (This Report) UNCLASSIFIED	21. No. of Pages 125
	20. Security Class (This Page UNCLASSIFIED	22. Price

FORM NTIS-35 (REV. 10-73) ENDORSED BY ANSI AND UNESCO. THIS FORM MAY BE REPRODUCED USCOMM-DC 8265-P74

EXPERIMENTS ON TRANSITIONAL OSCILLATORY PIPE FLOW

by

B. R. Ramaprian and S. W. Tu

Approved for public release; distribution unlimited.

IIHR Report No. 221

Iowa Institute of Hydraulic Research
The University of Iowa
Iowa City, Iowa 52242

August 1979

Accession For
NTIS GRA&I
DDC TAB
Unannounced
Justification
By
Distribution/
Availability Codes
Dist | Avail and/or special
A

TABLE OF CONTENTS

		Page No.
I	INTRODUCTION	1
II	EXPERIMENTAL PROGRAM	4
	A. General	4
	B. Description of the Apparatus	4
	C. Performance of the Apparatus	6
	1. Quasi-steady performance	6
	2. Unsteady performance	7
	D. Instrumentation	8
	1. Pressure measurement	8
	2. Discharge measurements	9
	3. Velocity measurements	9
	4. Reference time signal	9
	E. Experimental Details	10
	1. General	10
	2. Quasi-steady measurements	12
	3. Unsteady flow measurements	13
	4. Intermittency measurements	13
	F. Data Acquisition and Processing	14
III	RESULTS AND DISCUSSION	16
	A. Steady Flow Measurements	16
	1. Axial pressure drop	16
	2. Velocity distribution	17
	3. Turbulence intensity distribution	18
	B. Velocity Distribution in Unsteady Flows	19
	C. Effect of Flow Modulation on Turbulence and Transition	22
	1. General	22
	2. Results of Series 1 experiments (turbulent unsteady flow)	23
	3. Results of Series 2 experiments (laminarized unsteady flow)	28
IV	CONCLUSIONS	34
REFERENCES		36
FIGURES		38
APPENDIX A	Description of the LDA System at IIHR and Sample Calculations of Velocity from the LDA Signal	73
APPENDIX B	Experimental Data	83
APPENDIX C	Assembler Language Program for Sampling and Processing Periodic Turbulent Flows, on the IIHR IBM/1800 System	89

LIST OF FIGURES

		Page No.
Figure 1.	Schematic layout of the experimental apparatus.	38
Figure 2.	Variation of the cross sectional average velocity during a cycle.	39
Figure 3.	Oscilloscope traces of velocity signals from LDA (r=0).	40
Figure 4.	Static pressure drop along the pipe in steady flow; results from experiments of series 2.	41
Figure 5.	Friction factor in steady flow.	42
Figure 6.	Distributions of mean and turbulent velocities in steady flow.	43
Figure 7.	Velocity distribution in steady flow in wall-layer coordinates θ=0 (Maximum slot opening).	44
Figure 8.	Distribution of the time-mean velocity across the pipe in unsteady flow.	45
Figure 9(a).	Variation of the periodic component of the velocity with phase angle (Run 13).	46
Figure 9(b).	Variation of the periodic component of the velocity with phase angle (Run 23).	47
Figure 9(c).	Variation of the periodic component of the velocity with phase angle (Run 24).	48
Figure 10(a).	Distribution of the periodic component of the velocity across the pipe at fixed phase angle in oscillating turbulent flow; f = 1.75 Hz (Run 13).	49
Figure 10(b).	Distribution of the periodic component of the velocity across the pipe at fixed phase angle in oscillating laminar flow; f = 1.75 Hz (Run 23).	50
Figure 10(c).	Distribution of the periodic component of the velocity across the pipe at fixed phase angle in oscillating laminar flow; f = 0.057 Hz (Run 24).	51
Figure 11.	Distribution of the amplitude of the periodic component of velocity across the pipe.	52

LIST OF FIGURES (continued)

		Page No.
Figure 12(a).	Distribution of the ensemble average velocity across the pipe in oscillatory turbulent flow, f = 1.75 Hz (Run 13).	53
Figure 12(b).	Distribution of the ensemble average velocity across the pipe in oscillatory laminarized flow, f = 1.75 Hz (Run 23).	54
Figure 12(c).	Distribution of the ensemble average velocity across the pipe in oscillatory laminarized flow, f = 0.057 Hz (Run 24).	55
Figure 13.	Distribution of the turbulent intensity across the pipe in run 13 (f = 1.75 Hz).	56
Figure 14(a).	Variation of the longitudinal component of the turbulent velocity with phase angle in oscillatory flow at f = 1.75 Hz (r = 0).	57
Figure 14(b).	Variation of the longitudinal component of the turbulent velocity with phase angle in oscillatory flow at f = 1.75 Hz. [r=23.4 mm (2 mm from wall)].	58
Figure 15(a).	Variation of the Reynolds shear stress with phase angle in oscillatory flow.	59
Figure 15(b).	Variation of the Reynolds shear stress with phase angle in oscillatory flow.	60
Figure 15(c).	Time variation of the Reynolds shear stress with phase angle in oscillatory flow.	61
Figure 16.	Distribution of total, laminar and Reynolds shear stresses across the pipe in wall-layer coordinates at prescribed phase angles.	62
Figure 16.	Distribution of total, laminar and Reynolds shear stresses across the pipe in wall-layer coordinates at prescribed phase angles.	63
Figure 17.	Distribution of the time-averaged total, laminar and Reynolds shear stresses across the pipe.	64
Figure 18.	Velocity distribution in unsteady flow in wall-layer coordinates.	65

LIST OF FIGURES (continued)

		Page No.
Figure 19.	Variation of the rate of shear work with the phase angle.	66
Figure 20.	Oscilloscope traces of velocity signals from LDA from experiment series 2.	67
Figure 20.	Oscilloscope traces of velocity signals from LDA from experiment series 2.	68
Figure 21.	Typical strip chart records of the LDA output signal in steady flow from experimental series 2.	69
Figure 22.	Typical strip chart records of the LDA output signal in oscillatory flow from experiment series 2.	70
Figure 23.	The intermittency of turbulent puffs in steady flow.	71
Figure 24.	The intermittency of turbulent puffs in oscillatory flow from experiment series 2.	72

LIST OF SYMBOLS

A	area of cross-section of the pipe
A_e	exit area
C_D	coefficient of discharge of the slot
D	diameter of pipe
F	factor in equation 3
f	frequency of oscillation
f_t	characteristic frequency of turbulence
H	constant head
h_t	frictional head loss
K	factor in equation 4
L	length of pipe
M	number of cycles sampled
N	number of samples in a cycle
P	static pressure at any point
P_A	static pressure at an upstream reference point
ΔP^*	non-dimensional pressure drop (Equation 17)
R_e	Reynolds number
r	local radius
S	Strouhal number
ΔT	sampling time interval
t	time
U	instantaneous longitudinal velocity
U^+	non-dimensional velocity in wall layer
u	turbulent velocity component in x-direction

LIST OF SYMBOLS (continued)

u_*	friction velocity
V	instantaneous radial velocity
v	turbulent velocity component in radial direction
x	longitudinal coordinate
x*	non-dimensional x-coordinate = x/D
Y^+	non-dimensional radial coordinate in the wall layer
β	pressure gradient parameter (Equation 23)
λ	friction factor
η	non-dimensional radial coordinate = 1-2r/D
Ω	frequency parameter, $[D/2 \sqrt{\frac{2\pi f}{\nu}}]$
ρ	fluid density
ν	kinematic viscosity of the fluid
τ	shear stress
τ_w	wall shear stress

Subscripts:

m	cross-sectional average
p	periodic component
q	quasi-steady
max	maximum value
overbar	time average
< >	ensemble (phase) average

ACKNOWLEDGEMENTS

This study was made possible initially by a Grant from the Graduate College of The University of Iowa under the Biomedical Research Grants Program. Subsequently, the project has been supported internally by the Institute of Hydraulic Research and the Division of Energy Engineering. The final stages of the study and the preparation of this report have been supported in part by the United States Army Research Office Grant No. DAAG29-79-G-0017.

The authors gratefully acknowledge the support from all these sources. The authors wish to thank Professor V.C. Patel for many useful discussions and Mr. Dale Harris and his workshop staff for their support in the construction of the experimental apparatus.

ABSTRACT

Fully developed oil flow in a smooth circular pipe at a mean Reynolds number of about 2100 was subjected to a nominally sinusoidal flow modulation at frequencies ranging from 0.05 - 1.75 Hz. It was observed that flow oscillation increased the critical Reynolds number and, under certain conditions, even brought about laminarization of the flow, which would be intermittently turbulent at the mean Reynolds number under quasi-steady (infinitely small oscillation frequency) conditions. The occurrence and extent of laminarization was, however, found to depend on factors such as the intermittency of turbulent puffs in the mean quasi-steady flow, frequency of oscillation, etc. Two series of experiments were performed. In one series, the oscillatory flow was almost completely laminarized. In the other series, the oscillatory flow was fully turbulent. In both the cases, instantaneous velocities in the flow were measured using Laser Doppler anemometry. The instantaneous velocity was decomposed into time-mean, periodic and random components employing ensemble averaging techniques. The experiments indicated that the laminarized oscillatory flow behaves very similar to laminar oscillatory flow at either end of the Strouhal number range studied. The oscillatory turbulent flow was found to depend on both the Strouhal number and the ratio of the oscillation frequency (f) to some characteristic frequency (f_t) of turbulence in the flow. The design of the present experimental facility made it possible to study the flow at $f/f_t \approx 1$, a condition that could not be attained in most previous investigations. It was found, that at this frequency of oscillation, the Reynolds stresses generally remained frozen at an average state during the entire oscillation cycle. The turbulent structure showed significant departures from equilibrium at all times during the oscillation cycle. As a result, there was a net change in the time-mean velocity profile near the wall and a net increase in the time-mean wall shear stress and power loss due to friction. The data also indicated that the direct interaction between oscillation and the turbulent structure was essentially confined to the Stokes layer.

The study suggests that quasi-steady turbulence models may not be adequate to describe unsteady flows when the time scale of unsteadiness is comparable to that of dominant turbulent eddies.

I. INTRODUCTION

The study of unsteady shear flows is relevant to many areas of application such as aerodynamics, ship hydrodynamics, biofluid mechanics and wind engineering. Much of the study reported in the literature on unsteady flows, however, concerns laminar flows. Exact solutions are available for relatively simple unsteady laminar flow situations in the classical literature [(see Rosenhead 1963)]. Laminar flows in pipes due to periodic pressure gradients have been studied by Richardson and Tyler (1929), and Uchida (1956) and others. The situation with regard to unsteady transitional and turbulent flows is, however, less satisfactory. While there have been some attempts to analyze the problem of stability in periodic flows (e.g., Kerczek and Davis 1974, 1975, Hino and Sawamoto 1975, Hino et al 1976), much remains to be studied in this area. Of the laboratory experiments on periodic pipe channel flow that have been reported in the literature, most pertain to high Reynolds number turbulent flows. The earliest of such experiments were reported by Schulz-Grunow (1940). More recent experiments in this category are those performed by Hirose and Oka (1969), Lu et al, (1973), and Acharya and Reynolds (1975). In all these experiments fully developed turbulent pipe flow was perturbed by imposing a periodic modulation in discharge at a prescribed frequency. Of these, the work of Acharya and Reynolds involved the most detailed measurements such as Reynolds shear stress, though the amplitude of flow modulation in their experiments was less than 5 per cent of the mean. These experiments suggested that even at that amplitude, the structure of turbulence can be significantly affected in the Stokes layer near the wall. Their measurements in this layer were very limited because of the thinness of the layer. Lu et al experienced considerable difficulty in the use of hot film anemometry as well as in analog data processing in their experiments on oscillatory flow of water in a circular pipe. Their measurements of mean and turbulent velocities did not lead to any significant conclusions.

One would intuitively expect that the effects of unsteadiness on the flow structure will be stronger on flows in the neighborhood of transition than on flows at very large Reynolds numbers. This is because

transition process can be sensitive to the strong acceleration/deceleration in the unsteady flow. The experience with steady flows subjected to spatial pressure gradients has confirmed that pressure gradients have a significant effect on the critical Reynolds number. Strong effects of periodic flow modulation on the flow characteristics at transitional Reynolds numbers have, indeed, been observed in the experiments of Sarpkaya (1966) and in the more recent studies of Gerrard (1971) and Hino and Sawamoto (1975). From a study of the growth of disturbances in sinusoidally modulated pipe flow in the mean flow Reynolds number range of 2000-5000, Sarpkaya concluded that flow pulsation increases the critical Reynolds number. Gerrard's experiments related to periodic pipe flow at a mean Reynolds number of 3700 while the experiments of Hino and Sawamoto pertaineed to purely oscillatory pipe flow (i.e., at a mean Reynolds number of zero). These latter two studies were mainly qualitative but they indicated that, in general, turbulence is inhibited during the acceleration part of the modulation cycle and enhanced during the retardation part. In fact, the flow, under certain circumstances, appeared to remain laminar during the acceleration part of the cycle. Indications of inhibition of turbulence or delayed transition have also been observed in some of the in-vivo studies of pulsatile blood flow in the aorta of mamals (e.g., Falsetti et al 1972, Kiser et al 1976). However, the instrumentation and data reduction techniques used in the blood flow studies, as well as in the other laboratory studies mentioned above, were not sufficiently sophisticated to yield detailed quantitative information on the flow structure.

There is one class of unsteady turbulent flows, however, that has been studied in fair detail using moderate to highly sophisticated data reduction techniques. This is the unsteady turbulent boundary layer in a periodic free stream. Most of these studies (Karlsson 1959, Houdeville et al 1976, Cousteix et al 1977, and Patel 1977) pertain to zero pressure gradient boundary layers though some experiments on adverse pressure gradient flows have been reported recently (Kenison 1977, Houdeville and Cousteix 1978). The experiments on the zero pressure gradient boundary layers have, generally, lead to the conclusion that flow modulation has no effect on the average behavior of the flow and that the turbulent structure can still be

described by quasi-steady turbulence models. A careful study of these investigations, however, reveals that in all these experiments, the frequency of flow modulation was small compared with the characteristic frequency of turbulence in the boundary layer. One can expect to find a significant effect of flow modulation on the average flow structure only when the modulation frequency is comparable to the characteristic turbulent frequency in the flow. The very recent report of Houdeville and Cousteix (1978) on the unsteady boundary layer in the neighborhood of separation (where this condition is satisfied) does indicate strong effects of flow modulation on the flow structure. Hence, the behavior of an unsteady turbulent flow is not only determined by the Strouhal number (ratio of the time scale of mean flow to the time scale of unsteadiness), but also by the ratio of the time scale of unsteadiness to the characteristic time scale of turbulence. Further, since most of the interaction between the impressed oscillation and the turbulence structure is likely to occur within the Stokes layer, it is necessary to design the experiment carefully so as to get a thick enough Stokes layer and yet keep the modulation frequency at a value comparable to the characteristic turbulent frequency.

The present study was directed towards obtaining experimental data on fully developed oscillatory pipe flow at transitional Reynolds numbers. The nature of the periodic flow was found to depend strongly on the nature of the steady flow at the mean Reynolds number. It was found that if the steady mean flow was fully turbulent (with an intermittency of unity), the flow would remain fully turbulent when the Reynolds number was modulated at a frequency large enough to approach the characteristic turbulent frequency. On the other hand, if the steady mean flow was not turbulent but contained turbulent puffs at a low intermittency, the flow would tend to laminarize on periodic oscillation. Both these flow situations were studied in detail using Laser Doppler anemometry (LDA) together with a digital phase averaging technique. Important features of the present experiments, particularly with regard to the turbulent unsteady flow are (i) the oscillation frequency was comparable to the characteristic turbulence frequency in the flow and (ii) the viscous sublayer (2 mm) and Stokes sublayer (6 mm) were thick enough to permit detailed measurements in a region where the interaction of flow oscillation and turbulence have been found to be very strong.

II. EXPERIMENTAL PROGRAM

A. General. A test facility for producing sinusoidally oscillating pipe flow at transitional Reynolds numbers was designed and built for the present study. This facility used Eureka oil (of kinematic viscosity, $\nu = 1.384\times10^{-5}$ m^2/s at 26°C) and consisted of a long pipe of 50 mm diameter in which the oscillating flow was maintained. The flow oscillation was produced by varying the flow exit area sinusoidally by a rotating sleeve situated at the exit end of the pipe. The design of the rotating sleeve was very similar to that used in the classical experiments of Schultz-Grunow (1940). The exit area was kept small in comparison with the pipe area so that most of the head loss in the system occurred at the exit. Under such conditions, it is possible to obtain a discharge rate nearly proportional to the exit area. Velocity measurements were made using a single channel LDA. The data was acquired and processed using the IIHR IBM/1800 Data Acquisition System and a data processing technique developed by Mueller and Ramaprian (1977) for the analysis of unsteady turbulent flows. The details are described in the following sections

B. Description of the Apparatus. The experimental apparatus is shown schematically in figure 1. Oil is pumped by the circulating pump from the sump tank to the constant level overhead tank. The overhead tank is a cylindrical reservoir of 0.5 m diameter × 0.75 m height. The head is maintained constant (about 4 m above the ground level) by providing a 50 mm diameter overflow pipe which returns the extra oil to the sump tank. Oil from the constant head tank flows down through the 100 mm diameter inlet pipe and then through the 200 mm diameter curved pipe. A set of turning vanes is provided in the curved pipe to distribute the flow uniformly in the pipe. The horizontal section of the 200 mm pipe acts as a calming chamber. This section is followed by a bell-shaped contraction nozzle of 50 mm exit diameter. The test pipe is made of copper and has a nominal inlet diameter of 50 mm. It has a total length of 8.8 m, (i.e., L/D = 176) which ensures full development of flow even under laminar flow conditions. The pipe has been assembled from sections. The joints between the different sections

have been matched with special care insuring that there are no irregularities in the surface. Twenty-eight wall static pressure taps of 1 mm diameter have been provided at regular intervals along the pipe for the measurement of pressure loss through pipe. These pressure taps have been provided along the bottom of the tube in order to prevent air bubbles from accumulating near the holes. Provision has also been made for flush mounting pressure transducers at three locations along the pipe. The first one is at a point 1.3 m from the contraction exit. The second one is at a point 50 mm upstream from the measurement location and the third at 1.3 m upstream of the second. Pressure transducers mounted at locations 2 and 3 can be used to obtain the pressure gradient in the pipe. The test section where velocity measurements were made is a plexiglass tube, 0.3 m long and 50 mm in internal diameter. The upstream end of the tube is machined and matched with the copper pipe. The other end is connected to a 50 mm diameter × 300 mm long copper tube whose downstream end is closed. Two longitudinal rectangular slots, 50 mm × 3.2 mm, milled on the surface of this tube along two generators 180 degrees apart from each other, provide the exit for the oil. The oil falls into a rectangular plexiglass collection chamber (vented adequately to the atmosphere) from where it flows into a weigh tank. The weigh tank rests on a platform weighing machine and is used for measuring the mass rate of flow of the oil. The oil from the weigh tank can be drained via a valve into the sump tank.

The technique used for producing discharge oscillation is similar to that used by Schultz-Grunow. The device consists of a hollow copper cylindrical sleeve rotating over the slotted copper tube mentioned above. One end of the sleeve is profiled on a milling machine in such a way as to form, on development, two cycles of a sine wave of amplitude 12 mm. The other end of the sleeve is closed and is attached to a 13 mm diameter shaft. The shaft is connected to a variable speed motor, by means of a coupling that permits adjustment of the longitudinal position of the sleeve relative to the slots. The shaft is supported by a bearing housed in the wall of the plexiglass collection chamber. The motor is mounted independently on a bracket secured to the framework supporting the apparatus. The motor is manufactured by Bodine Electric and is a geared D.C. motor having an output speed range of 1.2-55 rpm. Its speed is regulated electronically by

controlling the motor voltage via a feed-back circuit. The regulator maintains the speed of the motor within 1% of the preset speed, which is continuously selectable within the range mentioned above. When the sleeve rotates, the area of opening of the pair of slots is continuously varied by the profiled sleeve. It is seen that the exit area variation will be a sinusoidal function of time with the variation going through two cycles during each revolution of the sleeve. The mean exit area can be adjusted within limits by changing the axial location of the sleeve relative to the slots. In the present study, this location has been chosen (after several trial runs) such that the mean flow Reynolds number would be about 2100. The sleeve profile was initially designed for an estimated discharge modulation amplitude of 0.35 × mean discharge. Later tests showed that the actual discharge modulation at infinitely low frequencies (i.e., quasi-steady state), was in fact, quite close to this calue. With the present design, it is possible to produce fully laminar flow at the minimum slot opening and fully turbulent flow at the maximum slot opening (under steady flow conditions). At higher frequencies, the amplitude is reduced. This aspect is discussed next in greater detail.

C. Performance of the Apparatus

1. Quasi-steady performance. If H is the gross head available (about 2.7 m), h_f the overall head loss in the system, V_e the exit velocity, V the test section velocity, A_e the exit area, A the cross sectional area of the test section and C_D the discharge coefficient (assumed constant), we have, for quasi-steady flow,

$$H - h_f = V_e^2/2g - V^2/2g \cong \frac{V_e^2}{2g} \quad \text{(Since V is very much smaller than } V_e\text{)} \qquad (1)$$

$$AV = C_D A_e V_e$$

or

$$V = C_D \frac{A_e}{A} \sqrt{2g(H - h_f)} \qquad (2)$$

If $h_f = K\, V^2/2g$, where K is a constant for the system, one finally gets

$$V = \sqrt{2gH}\ (C_D A_e/A)\ [1/\{1 + K(C_D A_e/A)^2\}^{1/2}] \qquad (3)$$

$$= \sqrt{2gH}\ C_D\ (A_e/A) F$$

where

$$F = [1/\{1 + K(C_D A_e/A)^2\}]^{\frac{1}{2}}$$

Since C_D is assumed constant, V is proportional to A_e, if F is constant; i.e., if $K(A_e/A)^2 \ll 1$. The frictional loss in the various components of the system can be estimated using standard handbook data. These estimates yield a value of $K \doteq 2$ for the present system. The ratio A_e/A has a maximum value of 0.1 in the present case (for fully "open" position). Substituting these values, one gets, for the fully "open" sleeve position,

$$K(A_e/A)^2 = 0.02 \qquad (4)$$

This means that F varies from 1.0 to 0.98 from the fully closed to fully open sleeve positions. Thus an almost sinusoidal discharge rate (or velocity) can be expected. The quasi-steady discharge variation with the rotation of the sleeve is shown in figure 2. It is seen that the modulation is very nearly sinusoidal. It is possible to improve the wave shape of modulation by departing slightly from an exact sinusoidal sleeve profile. The required sleeve profile can then, be calculated from Eq. (3). This requires a knowledge of the precise values of K and C_D as functions of quasi-steady discharge. These can be obtained after the steady flow operation. In the present design, however, this procedure was not followed.

2. Unsteady performance. The performance of the system will be described by Eq. (3) only when the exit area is constant or varied infinitely slowly (i.e., under quasi-steady conditions). At finite frequencies of area variation, the flow in the system will be governed by the appropriate unsteady euations of motion. Specifically, the dynamic response of the system will be affected by the inertia of the fluid. As a consequence, as the frequency of oscillation is increased the amplitude of the flow modulation will decrease, the modulation will be distorted from the sinusoidal shape and the pressure at any point in the system will oscillate. Further, the discharge and pressure oscillations will generally be out of phase with the exit area variation. Some of these effects are seen from figure 2 showing the shape of the discharge (or cross sectional average velocity, U_m) Vs. time curve, at two different oscillation frequencies; 0.057 Hz and 1.75 Hz. In

this figure, the distribution of U_m is normalized with respect to the quasi-steady cross sectional average velocity at the mid slot opening. The quasi-steady velocity distribution (U_q) as well as an exact sinusoidal distribution are also shown in the figure. The reduction in amplitude and the phase shift of discharge modulation, as well as the distortion in the shape of the modulation curve can be easily seen from the figure. It is seen that at the lower frequency, these effects are very small while at the higher frequency, they are perceptible. We, however, regard the distortion from the sinusoidal shape to be still small enough to be ignored for the purpose of the present study. Likewise, the reduction in amplitude at the higher frequency is no cause for concern, since it is still large enough (20% of the mean) to allow useful and meaningful measurements to be made at this frequency.

D. Instrumentation

1. Pressure measurement. Wall static pressure distribution along the pipe in steady flow was measured using the static pressure taps and an inverted U-tube oil manometer. The most upstream static pressure hole was connected to one of the limbs of the manometer. The other limb could be connected to any static pressure hole via a manifold with which all the static pressure holes were in communication through individual stop cocks. The manometer thus measured the pressure drop from the first hole.

In the unsteady flow experiments, pressure was measured using a pressure transducer mounted flush with the inner surface of the pipe. Pressure measurements were made at only one position viz. at station 2 in Fig. 1. Unsteady pressure drop measurements were, however, not made due to instrumentation problems. The pressure transducer used was an ENDEVCO 8510 semiconductor type, of range 0-15 psi, with a sensitivity of 9.5 mv/psi at an excitation voltage of 5 volts. An IIHR-built straingage balance and 5-volt-power supply was used with the transducer. The unbalanced voltage output from the bridge was amplified by a PRESTON D.C. amplifier. The instantaneous amplified output which was proportional to the static pressure was measured using the data acquisition technique described later.

2. Discharge measurements. The time averaged flow rate was measured using the weigh tank. The flow rate was measured by clocking the time required for a preset weight of oil to flow into the weigh tank. Unfortunately, due to the small capacity of the tank, it was necessary to limit the duration of oil collection to 15-20 s only. This resulted in some inaccuracy in the estimate of the flow rate, especially in the unsteady flow experiments. These measurements of flow rate were, however, neither critical nor extremely important in the present study. In fact, the flow rate could be more accurately determined in specific cases by integrating the velocity distribution across the pipe obtained from LDA measurements.

3. Velocity measurements. Velocity measurements in unsteady flow studies reported so far in the literature have been made using either pitot-tubes or hot-wire/film anemometry. These probes have two important disadvantages; (i) they disturb the flow and (ii) they do not allow reversals in velocity to be detected or measured. In addition, the Pitot tube has the added limitations that it cannot measure turbulent intensity nor can it even by used in any except very slowly oscillating flows. One of the most important features of the present study is the use of LDA, a technique that can measure instantaneous flow velocities without disturbing the flow. The LDA has also the additional advantages that its signal is proportional to the velocity and that it does not require calibration against other standards. One can, thus, avoid the calibration drift problems associated with hot-film anemometry in liquids. Reversal of flow can be detected and measured using LDA if a "frequency shift" technique is used. The LDA system used in the present studies used a frequency-shift feature though flow reversal did not actually occur in the range of flows studied. The single channel LDA system of IIHR and the details of the traverse system are described in appendix A.

4. Reference time signal. In the present report, the time history of the flow during the oscillation cycle was studied using the instant of maximum slot opening as the reference ($t = 0$) point in the cycle. As will be seen later, the Data Acquisition System was designed to use this point as the instant at which data sampling should begin. For this purpose

an electromagnetic device was used to produce a voltage pulse at the instant of maximum slot opening once during each revolution of the profile sleeve. (Note that this corresponds to once in every two oscillation cycles). The device included an electromagnetic pick up (1.5 mm) diameter) mounted on the support frame and a thin steel rod (1.5 mm diameter) attached to the motor shaft. The position of the rod was carefully adjusted such that during its rotation the tip passed within 1 mm of the pick up, cutting the magnetic field. The voltage induced in the pick up was used as the reference time signal. The intensity and duration of the pulse would depend upon the diameter of the rod and its rotational speed. The diameter of the rod (1.5 mm) was determined from the requirement that a signal of sufficient strength to drive the Data Acquisition System was to be produced at the lowest speed studied. With this diameter and with the radius of rotation of the rod of about 150 mm, the pulse duration was found to vary from about 2.5 degrees, at the lowest speed, to about 3.5 degrees at the highest speed of rotation. This corresponds to the range 5-7 degrees when referred to an oscillation cycle and represents the overall uncertainty in the reference time signal. The phase angle measurements reported in this study are all subjected to this uncertainty. The angular position of the rod was adjusted such that the rod was aligned with the pick up in the maximum slot opening position. A 360-degree graduated protractor fixed to the plexiglass collection chamber and a pointer attached to the shaft enabled setting up the sleeve at any desired position (θ) relative to the maximum slot opening position ($t = 0$ or $\theta = 0$) in steady flow experiments.

E. Experimental Details

1. General. As already mentioned, two series of experiments were carried out. In both the series, the steady flow had a Reynolds number of about 2900 at maximum slot opening ($\theta=0°$) and a Reynolds number of about 1300 at minimum slot opening ($\theta=180°$). The mean steady flow Reynolds number was about 2100 and this occured at $\theta\cong90°$. However, in the first series, the steady flow at $\theta=90°$ was found to be fully turbulent at all times. In fact, the intermittency of turbulence remained at unity for $\theta\leq 100°$. When this flow was oscillated at the highest possible frequency

of 1.75 Hz, the flow remained fully turbulent. Instantaneous velocity measurements were obtained across the pipe for this situation (Run 13). A rough estimate of the turbulent burst frequency in this flow using the criterion of Rao et al, (1971) indicates a value of about 2 Hz. Thus the oscillation frequency can be expected to interact significantly with the turbulent structure in this flow. In the second series of experiments, while the steady flow at the maximum and minimum slot opening behaved exactly as in the first series, the mean flow at $\theta=90°$ exhibited an intermittent turbulent structure. The structure strongly resembled the puff type transitional structure studied by Wygnanski and Champagne (1973). In fact, the steady flow became fully turbulent only at values of $\theta \lesssim 60°$. When this flow was oscillated (at whatever frequency) it was found to laminarize with the intermittency of puffs dropping almost to zero. This is clearly seen from figure 3 where a photograph of the storage oscilloscope traces corresponding to the center line velocity signals obtained from the LDA under three different conditions are shown superimposed on one another. These are: i) steady flow at $\theta=0°$, Re = 2872 (fully turbulent), ii) steady flow at $\theta=180°$, Re = 1278 (fully laminar) and (iii) oscillatory flow at 0.057 Hz between the above two Reynolds numbers (laminarized). The peak velocity in the oscillatory flow is different from the velocity in steady turbulent flow because the steady flow is laminar and hence has a different velocity distribution. Velocity measurements were made in this laminarized unsteady flow at oscillation frequencies of 1.75 Hz (Run 23) and 0.057 Hz (Run 24). These frequencies correspond to Strouhal numbers S (defined as $\frac{2\pi fD}{\bar{U}_m}$) of 1.0 and 0.032 respectively.

In both the series, measurements of velocity distribution in the pipe were made for the steady flows at $\theta=0$ and $\theta=180°$. In addition, steady flow axial pressure drop data were obtained for several (fixed) angular positions, θ of the sleeve. These steady flow experiments can be considered to approximate closely to quasi-steady experiments. They are used as a reference in the study of the unsteady flow behavior. The use of these data instead of steady flow data from other sources is both necessary and desirable in view of the very low Reynolds numbers and transitional nature of the flow.

2. Quasi-steady measurements. One of the features of the present design is that it allows one to make measurements at steady flow conditions corresponding to any desired point on the oscillation cycle. These measurements closely approximate to quasi-steady flow measurements, i.e., measurements obtained in unsteady flow oscillating at infinitesimally low frequencies. These quasi-steady measurements form the basis for studying the effect of flow oscillation at finite frequencies. Quasi-steady measurements were made in both series of experiments. These included:

(1) discharge

(2) pressure drop and

(3) velocity distribution across the pipe.

The discharge measurements were made using the weigh tank and have been already referred to earlier in Section D.2. As mentioned previously, it was found that due to the small collection time used, there was some inaccuracy introduced into the discharge measurements. The discharge data obtained from the weigh tank measurements were compared with the more accurate values obtained from the integration of velocity profiles in the test section and a correction factor for the former was arrived at. This was used for the rest of the discharge data from the weigh tank. These discharge measurements were made for several fixed slot openings (i.e., for several fixed values of θ) in both the experimental series.

The distribution of static pressure along the pipe was measured only in series 2. Pressure drop measurements were made for several values of θ. These pressure measurements were made using the inverted oil manometer mentioned earlier.

The velocity measurements were made in both series. However, they were made only for two values of θ; $\theta=90°$ and $\theta=0°$ (Runs 11, 12; 21, 22). Further, the velocity profiles were measured at 16 points across the pipe in series 1. In series 2, velocities were measured at a fewer number of points. Since these measurements appeared to reproduce closely the first series of measurements, it was felt unnecessary to obtain data at finer intervals. The velocity measurements were made using the IIHR Data Acquisition System, as described in Section F. Measurements at $\theta=90°$ (i.e., in laminar flow) served to check the accuracy of measurement as

well as the quality of flow (axisymmetry) in the pipe by comparing the observation with the theoretical parabolic profile. Measurements in fully turbulent flow (θ=0°) provided the basis for studying the effect of flow oscillation. The turbulent velocity distribution in the pipe at low Reynolds numbers is strongly dependent on the Reynolds number and possibly on the characteristics of the specific experimental apparatus. It is thus necessary to use the quasi-steady measurements in the same apparatus at similar Reynolds numbers in order to make any comparisons with unsteady flow measurements.

3. Unsteady flow measurements. The flow was oscillated at the desired frequency by setting the voltage control of the motor at the appropriate position. The rotational speed (equal to twice the oscillation frequency) was measured by clocking the time taken for 50 revolutions of the sleeve. Several minutes were allowed to elapse after starting the oscillations before the measurements were made. As in the case of quasi-steady flow, velocity measurements were made at 16 points across the pipe. The instantaneous velocity signal from the LDA, was read on to he IIHR Data Acquisition System and processed using the procedure described in section F. The reference time signal from the magnetic pick-up was used as the synchronizing signal in the data acquisition process.

An oscillation frequency of 1.75 Hz was studied in series 1. (Run 13). As already mentioned, the flow was observed to be fully turbulent in this case. At lower frequencies (say <1 Hz), the flow was found to switch intermittently between laminar and turbulent regimes. This was accompanied by large variations in the "mean" velocity of the flow. Hence, it was not possible to make any quantitative velocity measurements under these conditions. In the second series of experiments, the flow remained laminar or nearly laminar at 1.75 Hz (Run 23) as well as at a very low frequency, viz. 0.057 Hz (Run 24). Detailed velocity profiles were obtained at these two frequencies.

4. Intermittency measurements. A careful and extended study did reveal that even in the second series of experiments, the flow did not remain

fully laminar at all oscillation frequencies. It became turbulent intermittently and this intermittency was found to depend on the oscillation frequency. In order to study this aspect in some detail, the velocity signal from the LDA was recorded on a strip chart recorder for a duration long enough to allow one to estimate the intermittency of turbulence from the record. This duration corresponded approximately to 300 cycles or 5 minutes whichever was larger. Such records were obtained for several oscillation frequencies in the range of 0.05 Hz - 1.75 Hz and for two points in the pipe, viz., $r = 0$ mm, and $r = 18.4$ mm.

F. Data Acquisition and Processing. The procedure used in the present study for the analysis of unsteady turbulent flows is based on that used by Nakato (1974) and is essentially similar to that used by many recent investigators of oscillatory turbulent boundary layers. The author considers it to be superior and more informative than the analog procedures used by previous investigators of pulsating flows in arteries or rigid walled-tubes. The analysis can be used in a degenerate form for unsteady laminar flows, steady turbulent and steady laminar flows also. The analysis is briefly described below.

Let the instantaneous velocity $U(y, ,t)$ be written as:

$$U(r,\theta,t) = \bar{U}(r) + U_p(r,\theta) + u(r,\theta,t) = < U(r,\theta) > + u(r,\theta,t) \quad (8)$$

where $\bar{U}$ is the time mean velocity, u is the turbulent (random) velocity, and <U> is the deterministic velocity. The deterministic velocity can be obtained by a process of ensemble averaging. In the present periodic flow, ensemble averaging is equivalent to phase averaging i.e., averaging over the values obtained at identical values of r and θ in a large number of cycles. Thus,

$$< U(r,\theta) > = \frac{1}{N} \sum_{i=1}^{N} U_i(r,\theta,t) \quad (9)$$

where N is the total number of cycles being averaged and U_i is the velocity in the ith cycle. The time mean value $\bar{U}(r)$ is obtained by long time averaging or equivalently by averaging <U> (r,θ) over a cycle. Thus,

$$\bar{U}(r) = \frac{1}{2\pi} \int_0^2 <U \quad (r,\theta)> d\theta \quad (10)$$

If M descrete samples are taken during a cycle, we can write

$$\bar{U}(r) = \frac{1}{M} \sum_{j=1}^{M} <U_j(r,\theta_j)> \tag{11}$$

The random velocity component u is obtained as

$$u(r,\theta,t) = U(r,\theta,t) - <U(r,\theta)> \tag{12}$$

The ensemble average value of turbulent velocity u_p' defined by

$$u_p'(r,\theta) = \sqrt{<u^2(r,\theta,t)>} \tag{13}$$

is obtained from the process

$$u_p'(r,\theta) = \sqrt{[\frac{1}{N} \sum_{i=1}^{N} u^2{}_i(r,\theta,t)]} \tag{14}$$

and the rms value of turbulent velocity u'(y), defined by

$$u'(r) = \sqrt{\overline{u_p'^2(r,\theta)}} \tag{15}$$

is obtained from the process

$$u'(r) = \sqrt{\frac{1}{M} \sum_{j=1}^{M} u_p'^2(r,\theta_j)} \tag{16}$$

In the present experiments, the Data Acquisition System was programmed to sample the LDA output once at the end of each sampling interval (ΔT), starting from the instant when the synchronizing signal (reference time signal) was received. ΔT was so chosen that 100 $\Delta T \leq$ the period of oscillation. This would ensure that 100 samples could be taken per cycle. However, only 96 samples were taken, no samples being taken at the end of 97th, 98th, 99th, and 100th time intervals. These "holes" in the data were required in order to allow for the fact that the period of oscillation might not be exactly equal to but less than 100 ΔT. It may be noted that with the present program, data would be acquired actually from two consecutive oscillation cycles, the first cycle yielding 50 (No. 1 - No. 50) samples and the second cycle yielding 47 (No. 50 - No. 96) samples. A total of 100 revolutions were used for phase averaging (N = 100) at the higher oscillation frequency. At the lower frequency, 25 revolutions were used. From the sampled data, the various velocities $\bar{U}$, U_p, u', etc were computed according to Eqs (8) through (12). In most cases, the experiments were repeated thrice and the results averaged over the three experiments. If the results in consecutive experiments differed significantly from one

another, the experiments were repeated till three consecutive experiments gave nearly the same results. (Such repititions were, however, rarely necessary). The value of $\bar{U}$ varied insignificantly among consecutive repititions, while the scatter in <U> was within 1% and the scatter in u' within 5%. The computer programs in Assembler Language used in the present experiments for both the acquisition and the subsequent processing of the data were developed by Mueller (see Mueller and Ramaprian 1977) from an earlier version developed by Nakato (1974). A listing of the program package used in the present experiments is given in Appendix C. One of the important features of the present program was that it would detect the LDA signal drop-out and reject the samples taken during such a cycle. Data acquisition would then proceed until N valid revolutions were sampled. However, with the use of frequency shift technique, there was virtually no "signal dropout" problem and this feature in the program was never made use of.

The above program package was also used for processing unsteady laminar flows, the value of u' in this case being used as a measure of the noise in the optics and electronics. It was found that u' ranged from 2-5 parts per 1000 in these cases, indicating the acceptability of the experimental procedure. The program package was also used for processing steady flow (laminar and turbulent) data, the quantities $\bar{U}$ and u' being the only quantities sought for in these cases. While experimenting with steady flows, a fictitious synchronizing signal was provided from a square wave generator with a period of approximately 3 seconds. With 100 "cycles" of sampling, this would result in an overall averaging time of 5 minutes.

The unsteady data acquisition program package was also used for the unsteady pressure measurements referred to in section D.1.

III. RESULTS AND DISCUSSION

A. Steady Flow Measurements

1. Axial pressure drop. The nondimensional pressure drop ΔP^* defined by

$$\Delta P^* = (P_A - P)/(1/2\ \rho \bar{U}_{qm}^2) \qquad (17)$$

is shown in figure 4 for various values of θ (i.e., for various Reynolds

numbers). P_A is the static pressure at an upstream reference point, x=0 (see figure 1). P is the static pressure at a longitudinal location x and ρ is the fluid density. The values shown are from the second series of experiments. The figure shows that mean flow has attained full development at all Reynolds numbers for $x^* = x/D \geq 70$. The quasi-steady friction factor, λ_q is defined in the usual way as

$$\lambda_q(\theta) = -\left[\frac{dP}{dx}(\theta)\, D\right]/\left[1/2\ \rho \bar{U}_{qm}^{\,2}\right] = \frac{d(\Delta P^*)}{dx^*} \qquad (18)$$

and thus, is given by the slope of the lines in figure 4. The values of λ_q at different Reynolds numbers are shown in figure 5. Also shown for comparison are the laminar relation, $\lambda = 64/Re$ and the Blasius relation for low Reynolds number turbulent flows, $\lambda = 0.3165\ Re^{-1/4}$ (Schlichting 1968). The value of $\bar{U}_{qm}$ used in figures 4 and 5 were obtained from discharge measurements made using the measuring tank. Figure 5 is presented to show that the apparatus was functioning as expected and that the flow was transitional.

2. Velocity distribution. The results of velocity measurement at θ=180° (minimum slot opening) and θ=0° (maximum slot opening) are shown in figure 6. In each case, data obtained in both the series of experiments are shown even though fewer points are shown for series 2. This is considered adequate in view of the excellent repeatability observed between the two series of steady flow experiments. In the case of laminar flow (θ=180°), the data are seen to agree well with the theoretical parabolic profile. This good agreement, however, has been obtained, as already mentioned, by applying a constant "zero correction" to the apparent location of the measurement point. The adjustment is justified by the fact that a constant zero correction brings the measured profile in agreement with the parabolic profile. The same correction was applied to the turbulent flow (θ=0°) measurements also. It is seen from the figure that the mean velocity profiles in turbulent flow obtained from the two series of experiments also indicate agreement with each other. The agreement between the two sets of data obtained with a gap of several months in between establishes the accuracy of the measurement procedure. It also confirms that the behavior of the

quasi-steady flow at both the maximum and minimum end of the oscillation cycle did not change even though the transitional character at intermediate Reynolds numbers had changed.

The velocity profile for the turbulent flow at $\theta=0°$ is shown in figure 7 in the usual wall layer coordinate U^+ $(=\bar{U}/u_*)$ vs. $Y^+[=(D/2-r)u_*/\nu]$ u_* being the shear velocity, $\sqrt{\tau_w/\rho}$ where τ_w is the wall shear stress. The value of u_* was obtained from the quasi-steady pressure drop and discharge data for $\theta=0°$ using the relation,

$$\lambda_q = \frac{1}{8}\frac{u_*^2}{U_{qm}^2} \tag{19}$$

The measured velocity distribution is compared with the universal law of the wall, namely $U^+ = Y^+$ in the viscous sub-layer and $U^+ = 5.75 \log Y^+ + 5.5$ in the fully turbulent region. The deviation of the experimental data from the universal log law is to be expected in view of the very low Reynolds number of the flow. On the other hand, the fact that the first data point near the wall falls on the linear $U^+ = Y^+$ curve indicates not only that this point is in the viscous sub-layer but also that the value of u_* and r are accurate.

3. Turbulence intensity distribution. Figure 6 introduced earlier, also shows the distribution of the rms intensity, u' of the longitudinal turbulent velocity fluctuations in the steady turbulent flow at $\theta=0$. The distribution is normalized using the velocity and length scales, u_* and $D/2$ respectively. Consequently, the distribution can be expected to show Reynolds number dependence in the inner region. This is, in fact, the case as is seen from the comparison with the data of Laufer (1954) obtained at a Reynolds number of 5×10^5. The distribution in the region $0.5 < (1-2r/D) < 1$ seen to coincide reasonably well with Laufer's data while in the region $(1-2r/D) < 0.5$, a strong Reynolds number effect is observed. In fact, the large viscous region in the present case allows one to observe the gradual decrease of u' from a maximum towards zero at the wall, a feature which is usually difficult to observe in higher Reynolds number laboratory flows. The purpose of presenting the steady flow

turbulence distribution in figure 6 is to provide a basis for the comparison with the unsteady turbulent flow data. It is clear that it is very important to make comparisons in approximately the same Reynolds number range in order to arrive at reliable conclusions.

B. Velocity Distribution in Unsteady Flow. Figure 8 shows the distribution of the time-averaged velocity $\bar{U}$ across the pipe in the three runs 13, 23, and 24. The velocities, in each case, are normalized with respect to the corresponding velocity at the pipe axis ($\bar{U}_{max}$). The distributions are compared with the quasi-steady velocity distributions corresponding to $\theta=180°$ and $\theta=0°$. It is seen from the figure that the unsteady flows in run 23 and run 24 that appeared to be laminar were, indeed, very nearly laminar i.e., they exhibit nearly parabolic velocity distributions. In fully developed oscillatory laminar pipe flow of a Newtonian fluid, the time-mean velocity distribution should be identical to that of the steady Poiseuille flow since the velocity field is determined from the linear equation

$$\frac{\partial U}{\partial t} = -\frac{1}{\rho}\frac{\partial P}{\partial x} + \nu\left[\frac{\partial^2 U}{\partial r^2} + \frac{1}{r}\frac{\partial U}{\partial r}\right] \tag{20}$$

It is seen that, in the high frequency run 23, in which the intermittency of turbulent puffs was negligibly small (see figure 23), the time-mean unsteady flow behaves almost exactly like laminar flow. The deviation of the experimental data of run 24 from the parabolic profile has been caused by the flow becoming turbulent with a larger intermittency than in run 23. It is, however, important to observe from figure 8 that the effect of flow oscillation on the time-mean velocity gradient and hence the wall shear stress, is negligible in both these runs.

When the oscillatory flow is turbulent, the total shear stress (τ) distribution in the pipe is given by the linear equation

$$\frac{\partial U}{\partial t} = -\frac{1}{\rho}\frac{\partial P}{\partial x} + \frac{1}{\rho r}\frac{\partial(\tau r)}{\partial r} \tag{21}$$

and hence the distribution of time averaged shear stress, $\bar{\tau}$ is now given by

$$\bar{\tau}/\rho = \nu\frac{\partial \bar{U}}{\partial r} - \overline{uv} \tag{22}$$

(where u and v are the turbulent velocity fluctuations in the x and r

directions, respectively), the velocity field is not determined by a linear equation. The time averaged velocity distribution, and hence the time averaged wall shear stress need not, therefore, be necessarily the same as in the steady flow at the mean Reynolds number. It is, in fact, seen from figure that the time-mean velocity distribution in the unsteady turbulent flow of run 13 exhibits a point of inflection near the wall and thus differs from the steady state turbulent velocity profile. The time mean velocity gradient at the wall is slightly larger than in the steady case resulting in a larger time-mean wall shear stress. This observation differs from those reported by previous investigators of oscillatory turbulent boundary layers, who concluded that unsteadiness has no effect on the time-mean properties (or even the turbulent structure) of the flow. However, as already mentioned, a significant difference between the present experiment and the earlier experiments is that the oscillation frequency in the present case is comparable to the characteristic turbulent frequency.

Figure 9 presents the variation of the periodic component U_p of the velocity through the oscillation cycle at a few typical points across the pipe. The velocity is normalized with respect to the amplitude $(U_{qmp})_{max}$ of the quasi-steady cross sectional average periodic velocity. The variations are shown only for 700 degrees of oscillation cycle, short record gaps being present (for reasons mentioned earlier) from 0 - 7.2° and 698.4 - 720°, i.e., a total of 4 sampling periods. For run 13, the data are shown only for 600 degrees of oscillation cycle, due to some difficulties encountered during data acquisition. These difficulties were subsequently removed before the second series of experiments were started. However, since data over only 360 degrees of oscillation cycle are sufficient for the purpose of analysis, the loss of redundant data is not serious. In each of the figures 9 (a), (b), (c), the distributions of the unsteady cross sectional average periodic velocity, U_{mp} and quasi-steady cross sectional average periodic velocity, U_{qmp} (proportional to the effective modulation in exit area) are also shown for comparison. The latter curve is the same as the periodic part of the velocity distribution shown in figure 2. A comparison of the laminar flow data for runs 23 and 24 shows that the phase-wise variations are strongly dependent on the oscillation frequency. The variations

appear to be very nearly sinusoidal at the lower frequency while significant distortion in the wave shape can be observed at the higher oscillation frequency. The distortion at the higher frequency is, as mentioned earlier, due to nonlinear effects.

It is also clear from the figures 9 (a), and 9 (b), that at the higher oscillation frequency, there is a significant phase shift between the velocity variation and the exit area opening. Most of this phase shift is brought about by the global dynamics of the system and is observable as the phase shift of unsteady cross sectional average flow. However, there is also a relative phase shift between the local velocity and the cross sectional average velocity. The flow in the wall region leads the cross sectional average flow while the flow in the core region lags behind the average flow. Unfortunately, owing to the uncertainty in phase angle measurement ($\pm$ 3.5°) and the distortion in the modulation profile, it is not possible to make a precise quantification of the phase differences nor is it possible to look for differences between the laminar and turbulent flow.

Figures 10 (a), (b), and (c) show cross plots of the distribution of the periodic velocity, U_p across the pipe for a few typical fixed phase angles in the oscillation cycle. It is seen that at the higher oscillation frequency, the variations in U_p are confined essentially to $\eta = (1-2r/D) \leq 0.25$ (i.e., the Stokes layer), the rest of the flow oscillating virtually as one solid mass at all times. At the lower frequency, U_p varies across the entire pipe at all times. The responses of turbulent and laminar flows appear to be qualitatively similar.

Figure 11 shows the distribution of the "amplitude", $(U_p)_{max}$ of the periodic velocity across the pipe for the three experiments. Since the velocity modulation is distorted from a sine wave especially at the higher frequency, it is not strictly appropriate to use the term "amplitude" without making a formal harmonic analysis. However, in the present case, $(U_p)_{max}$ denotes one half of the peak to peak variation in the periodic velocity U_p. In the figure $(U_p)_{max}$ is normalized with respect to the amplitude $(U_{mp})_{max}$ of the cross sectional average periodic velocity. It is more clearly seen from this figure that at the higher frequency, the amplitude variations are confined to a small region($\eta \lesssim 0.25$) near the wall while at the lower frequency the variations extend over the entire pipe cross section.

Also, it is seen that an overshoot occurs in the amplitude distribution. The dominant effect of oscillation frequency is clearly seen from this figure. At the same time, it is possible to notice, in this figure, a difference between the responses of laminar and turbulent flow in the near-wall region. The turbulent flow data of run 13 exhibit a larger overshoot than the laminar flow data of run 23. Also shown in the figure are the results computed from the exact solution of Uchida (1956) for fully developed laminar periodic flow in a pipe under the influence of a pressure gradient sinusoidally varying with time. The pressure gradient variation in the present experiments at the higher frequency differs significantly from that assumed in Uchida's analysis. The experiment at the lower frequency, however, approximates closely to the theoretical case. The data for this experiment are seen to agree reasonably well with the exact solution, any apparent discrepancy being possibly due to the intermittency effects mentioned earlier.

Lastly, the distribution of the ensemble average velocity <U> at prescribed phase angles are shown in figures 12 a, b, and c, for a few typical points in the oscillation cycle, for each of the runs. The distribution of the time-mean velocity, $\bar{U}$ is also shown, in each case, for comparison. The velocities are normalized with respect to the time-mean velocity at the center line ($\bar{U}_{max}$) corresponding to each run. The distributions at the higher frequency indicate simple displacement but very little distortion from the shape of the time-mean profile in the core region. Near the wall, (in the Stokes layer) however, the profiles cross over and suffer some distortion. However, no reverse flows were observed in the present experimrnts. At the lower frequency, the different profiles of <U> show distortion with respect to the time mean profile across the entire pipe because of the variation of both the amplitude and phase angle of the periodic velocity continuously across the pipe.

C. Effect of Flow Modulation on Turbulence and Transition

1. General. The data obtained in the two series of present experiments provide some insight into the effects of impressed unsteadiness on the structure of turbulence and transition in pipe flow. For convenience, the two series of experiments will be discussed one by one.

2. Results of Series 1 experiments (turbulent unsteady flow): The distribution of the rms turbulent intensity u', normalized with respect to $\bar{u}_*$[1] is shown in figure 13. Comparison with the steady flow data for $\theta=0$ shows that in the oscillatory flow there is a slight decrease in the maximum turbulence intensity near the wall, while the turbulence intensity farther away from the wall is not affected. The near-wall region where the turbulent intensity is affected extends approximately over 25 per cent of the pipe radius and this region coincides with the Stokes layer where significant effects of flow oscillation are observed on the time-mean and periodic structures of the flow also. This result is in agreement with the conclusions of Acharya and Reynolds (1975) that the structure of turbulence is primarily affected within the Stokes layer. The distributions of the ensemble averaged turbulence intensity $u_p'(\theta)$ normalized with respect to the corresponding shear velocity $u_{*p}(\theta)$ are also shown in figure 13 for a few typical fixed phase angles of the oscillation cycle. Large variations in the distributions from one another and from the distribution of $u'/\bar{u}_*$ indicate that the turbulence structure is highly disturbed from equilibrium. The variations in the relative turbulent intensity (u_p'/u_{*p}) with time are shown in figure 14 for two typical locations across the pipe. These figures suggest that the flow was undergoing rapid structural distortion in time. Actually, the wall shear stress (u_{*p}) could nearly follow the changes through the discharge cycle while the turbulent u-fluctuations could not. This is seen clearly from figure 14 which also shows the variation of u_{*p} and the variation of u_p' (not normalized) at these two typical points in the pipe. It is seen that u_{*p} oscillates with a slight phase lead with respect to the cross sectional average periodic velocity U_{mp}, while u_p' remains

---

[1] The shear velocity $u_{*p}(\theta)$ in unsteady flow was obtained from the ensemble average velocity gradient at the wall. The velocity gradient at the wall was calculated from the measured $\langle U(\theta)\rangle$ at the first point near the wall assuming a linear velocity distribution in the viscous sublayer at all instants. This procedure was found to be generally satisfactory as verified from checks made in steady laminar and turbulent flow. In these cases, the wall shear stress obtained by this method compared well (within 3%) with the value obtained from pressure drop measurements. From the ensemble averaged value u_{*p}, the time averaged value $\bar{u}_*$ was obtained from the discrete analog of the relation,

$$\bar{u}_*^2 = \frac{1}{2\pi}\int_0^{2\pi} u_{*p}^2 \, d\theta$$

practically constant throughout the oscillation cycle. Such a freezing of the turbulent normal stress can be expected to occur when the flow is subjected to rapid strain rates, i.e., when changes occur at time scales comparable to some important characteristic time scale of turbulence. In a wall-bounded flow, we can regard the turbulent burst frequency, f_t to determine such a characteristic time scale (at least near the wall). In the present case the estimated burst frequency is about 2.3 Hz, (using the criterion $\frac{\bar{U}_m}{f_t D} \cong 5$ of Rao et al 1971). The estimate is rough but is sufficient to indicate that one can expect to find interaction between the external oscillation and the internal turbulence structure when the flow pulsates at a frequency of 1.75 Hz. Stress-freezing is well documented in rapidly accelerated steady flows but studies of rapidly decelerated steady flows are difficult to perform, since the flow in such cases would separate very quickly. One of the interesting features of the present experiments is that the flow experiences large pressure gradients of alternating sign but yet does not actually separate. An estimate of the severity of the pressure gradient in the present case can be made by calculating the value of the Clauser pressure gradient parameter β defined by (neglecting the shear effects),

$$\beta = \frac{D}{2\rho u_*^2} \frac{\partial P}{\partial x} \approx \frac{D}{2u_*^2} \frac{dU_m}{dt} \tag{23}$$

Such a calculation shows that β varies from about -40 to about +40 during a cycle. The magnitudes of β attained during the cycle are comparable with the values for some of the severe adverse pressure gradient steady flows reported in the Proceedings of the Stanford Conference (Coles and Hirst 1978). Not only are the pressure gradients very large but they vary rapidly, the value of $d\beta/dt$ being of the order of 100 sec^{-1}, (based on a variation in β from 40 to -40 in half the period of oscillation). It is thus clear that the turbulent structure will be in a highly disturbed state. Hence, quasi-steady turbulence models based on local equilibrium assumption cannot be expected to describe the flow at such oscillation frequencies.

The quantity which is of greater value than u' in understanding the structure of turbulence is the Reynolds shear stress $-\rho\,\overline{uv}$. Unfortunately,

on account of instrumentation limitations, it was not possible to make direct measurements of the Reynolds shear stress. However, it is possible to compute it, perhaps with some loss of accuracy, from the measured wall shear stress and velocity distribution. For this purpose, we write the instantaneous x-momentum equation for pipe flow as

$$\rho \frac{\partial U}{\partial t} + \rho U \frac{\partial U}{\partial x} + \rho V \frac{\partial U}{\partial r} = - \frac{\partial P}{\partial x} + \frac{1}{r} \frac{\partial (\tau r)}{\partial r} \tag{24}$$

where V is the instantaneous velocity in the radial direction. Performing an ensemble average on this equation, one gets, for fully developed unsteady turbulent flow,

$$\rho \frac{\partial \langle U \rangle}{\partial t} = - \frac{\partial \langle P \rangle}{\partial x} + \frac{1}{r} \frac{\partial \langle (\tau r) \rangle}{\partial r} \tag{25}$$

$$\text{where } \langle \tau \rangle = \tau_{\text{laminar}} - \rho \langle uv \rangle \tag{26}$$

We define $- \rho \langle uv \rangle$ as the ensemble averaged Reynolds shear stress. Mutliplying both sides of the equation (25) by $2\pi r$ and integrating across the pipe, one gets (after inserting the phase average notations introduced earlier)

$$\rho \frac{\partial U_m(\theta)}{\partial t} = - \frac{\partial \langle P \rangle}{\partial x}(\theta) + \frac{4\tau_w(\theta)}{D} \tag{27}$$

Eliminating $\frac{\partial P}{\partial x}$ between equations (25) and (27) one gets

$$\frac{\tau}{\rho}(r,\theta) = \frac{1}{r} \int_0^r \frac{\partial}{\partial t} [\langle U(r,\theta) \rangle - U_m(\theta)] \cdot r \, dr + \frac{2\tau_w(\theta) r}{D} \tag{28}$$

and

$$- \langle uv \rangle (r,\theta) = \frac{\tau}{\rho} (r,\theta) - \nu \frac{\partial \langle U(r,\theta) \rangle}{\partial r} \tag{29}$$

The ensemble (phase) averaged Reynolds shear stress $- \langle uv \rangle$ was obtained from Equations (28) and (29) using measured velocity and wall shear stress data. The process required differentiation with respect to time and integration across the pipe both of which were performed numerically on a computer. The velocity-time data were smoothed in order to reduce the numerical noise in differentiation. The procedure was found to work reasonably well because the velocity values were available at very close time intervals (50 values per cycle), velocity gradients in the radial direction were not severe (due to the low Reynolds number of the flow), sufficient cycles were used for phase averaging (effectively 300) and lastly, the three terms in equation (28) were all of similar order of magnitude.

Variation of the ensemble averaged Reynolds shear stress during the cycle is shown in figures 15 a, b, c for three typical locations in the pipe, viz; 1, 2 and 10 mm from the wall. Although there is some scatter in the data, the results are still good enough to allow one to arrive at meaningful conclusions especially in the region of flow where the Reynolds shear stress is significant. Very near the wall, $\langle uv \rangle$ shows a cylical variation but lags behind U_m (and hence behind u_{*p} also). As the distance from the wall increases, the amplitude of variation of $\langle uv \rangle$ decreases until it becomes almost indistinguishable from scatter beyond the Stokes layer (as seen from figure 15c). The well-defined cylical variation of $\langle uv \rangle$ in the inner layer (figures 15 a, b) is in contrast to the frozen structure of u'_p. This suggests that the modulation in $\langle uv \rangle$ might have originated from modulations in the ensemble averaged intensity, v'_p. This is possible since the v-fluctuations are likely to be of finer scale than the u-fluctuations (by a factor of nearly 5 as observed by Ramaprian, 1975) and hence can respond more readily to the impressed oscillations. Since the time scale gets larger as the distance from the wall increases, the response of $\langle uv \rangle$ must be expected to diminish eventually in the core region. The nearly frozen structure of $\langle uv \rangle$ in the core region (figure 15c) thus indicates rapid strain rates. The departure from local equilibrium is again seen from the variations in $\langle uv \rangle / u^2_{*p}$ during the oscillation cycle.

Figure 16 a, b, c, and d are cross plots of the above data and show some typical distributions of the total, laminar and ensemble averaged Reynolds shear stresses, across the pipe for fixed phase angles during the cycle. The distributions are normalized using the relevant inner layer scales of velocity, (u_{*p}) and length, (ν/u_{*p}). The large variations in the distribution of the stresses from one point in the cycle to the other (seen more clearly from these figures) again indicate that the turbulence structure is far from equilibrium and hence cannot be described by quasi-steady models. Figure 17 shows the time averaged distributions of each of the above stresses using $\bar{u}_*$ as the scaling velocity. These distributions were obtained by averaging the computed distributions at 50 phase positions in the cycle. It is seen that except for a slight discrepancy near the wall, the time-averaged total shear stress $\bar{\tau}$ shows the expected

linear distribution. This indicates that there were no significant errors in the numerical procedure used for calculating the shear stresses from the experimental data. Some of the important features pertaining to figures 16 and 17 that require comments are:

(i) The laminar shear stress is significant upto a considerable distance from the wall. This is to be expected in view of the low Reynolds number of the flow.

(ii) The time averaged turbulent shear stress reaches a maximum at about 6 mm (η=0.25) from the wall i.e., at about the same location where u' reaches a maximum. It is important to note that this is within the Stokes layer.

(iii) The time averaged laminar shear stress distribution exhibits a local minimum near the wall. This is due to the presence of a point of inflection in the time-mean velocity profile.

(iv) The distribution of the time-mean Reynolds shear stress also exhibits a kink within the Stokes layer. Also, it is observed that, in the region very close to the wall, the time-mean Reynolds shear stress attains a value larger than in steady flow.

(v) The time-mean distributions of the stresses are not significantly different from the corresponding distributions in steady flow, in the region beyond the Stokes layer. However, by affecting the distributions within the Stokes layer, the imposed unsteadiness produces an increase in the time-mean velocity gradient at the wall and hence increases the wall shear stress. This is seen from figures 14 a, b, where the quasi-steady time-mean value, u_{*qm} (obtained from pressure drop measurements at the mean Reynolds number of 2100) is shown as a horizontal dashed line against the distribution of u_{*p} in unsteady flow. The time-mean value of u_{*p} is clearly larger than the quasi-steady mean value of u_*.

Figure 18 shows a few typical distributions of the ensemble average velocity <U> in the inner layer co-ordinates $\langle U\rangle/u_{*p}$ vs $(D/2-r)u_{*p}/\nu$. The time-mean distribution $\bar{U}/\bar{u}_*$ vs $(D/2-r)\bar{u}_*/\nu$ is also shown in the figure.

The data display exactly the trend that one would expect to see. In the region very close to the wall $y^+ < 10$, the ensemble average velocity scales with the corresponding u_{*p} but at larger distances from the wall, the flow structure does not keep in step with u_{*p} and hence the data at different phase angles exhibit different distributions. It is also important to note that there is a net difference between time averaged velocity distribution in the unsteady flow (shown by open circles) and the velocity distribution in steady flow (shown by the full line). This difference is seen more clearly in this figure than in figure 8, discussed earlier.

The quantity, $E_p = \int_0^R \{\langle\tau\rangle \frac{\partial\langle U\rangle}{\partial r}\} 2\pi\, r\, dr$ represent the rate of work done per unit length of pipe by the shear stress and hence its average value over an oscillation cycle represents the power loss in the pipe. The term E_p normalized with respect to $(\rho \bar{U}_{qm}^3 \pi D/4)$ is shown in figure 19 as a function of the phase angle. The corresponding power loss in a hypothetical quasi-steady turbulent flow can be obtained for the same Reynolds number modulation using the Blasius relation, $\lambda = 0.3165\ Re^{-\frac{1}{4}}$. Also, for the actual transitional quasi-steady flow, the power loss for the same Reynolds number can be obtained from the quasi-steady pressure drop data of figure 4 (or alternately the friction factor data of figure 5). Both these distributions are also shown in figure 19. It is seen that flow oscillation in run 13 at a high frequency results in an increase in average power loss when compared with the quasi-steady transitional flow. This is, however, to be expected since the unsteady flow is fully turbulent during the entire cycle, whereas the quasi-steady flow is not. However, it is interesting to observe that the unsteady flow has a slightly higher average power loss when compared to the hypothetical fully turbulent quasi-steady flow also.

3. Results of Series 2 experiments (laminarized unsteady flow) During the second series of experiments, the unsteady flow remained nearly laminar. Since this was a very significant observation, it was carefully verified to insure that the laminarization was not due to any obvious reasons such as an increase in fluid viscosity, reduction in flow velocity, etc. Starting from a fully turbulent flow at the fully open slot position, the flow could be laminarized by just rotating the sleeve at the lowest possible speed (0.057 Hz). The photographs in figure 20 show a few typical

oscilloscope traces obtained from the LDA at several oscillation frequencies and include data from two radial locations, r = 0 and r = 18.4 mm. In each photograph, three traces are shown: (i) fully turbulent steady flow at θ=0 corresponding to a Reynolds number of about 2900, (ii) fully turbulent laminar flow at θ=180°, and (iii) fully or partially laminarized oscillatory flow. The photographs generally confirm that the oscillatory flow had a strong tendency towards laminarization under the operating conditions of the series 2 experiments.

A careful study of the traces at several oscillation frequencies indicated that laminarization was not always complete, and that the oscillatory flow did, in fact, become turbulent at times (as seen in some of the photographs in figure 20). The intermittency of this occurence depended on the oscillation frequency. In order to make a more detailed study of this phenomenon, several long-time records of the LDA signal were obtanined using a strip chart recorder. The record length in all the cases was equal to 300 cycles or 5 minutes whichever was longer. Records were obtained for r = 0 and r = 18.4 mm. Similar records were obtained in quasi-steady flow for comparison. A few typical records are shown in figures 21 and 22. It is seen that the flow does become turbulent several times during the duration of the record. Estimating the intermittency of turbulence from such records is no doubt difficult and subjective; particularly when turbulent and oscillation frequencies are not well separated. The following procedure was arbitrarily selected for making a rough estimate of the intermittency. The procedure is based on the observation (and assumption) that whenever the flow became turbulent, its velocity level would jump upwards or downward from the laminar value depending on whether the point under consideration was in the wall region or on the centerline. In both the cases, a distortion would be observed in the velocity signal recorded on the strip chart. The dynamic response of the recorder (5 Hz) was adequate for indicating this distortion. A short length of the laminar record traced out on a transparent sheet would be moved over the record and portions of the record that did not coincide with the laminar record would be marked out as turbulent intervals. The intervals marked T in the photographs of figure 22 correspond to typical turbulent intervals. The intermittency factor, γ was defined as the ratio of the total turbulent interval to the

total record length. In the case of steady flow, the turbulent intervals could be easily recognized without much ambiguity.

The intermittency factor is plotted in figure 23 for quasi-steady flow as a function of quasi-steady Reynolds number. It is seen that the mean quasi-steady flow ($\theta=90^\circ$, i.e., Re $\cong$ 2100) has an intermittency of about 0.2. The intermittency factor for oscillatory flow is shown in figure 24 as a function of oscillation frequency. A parameter often used in characterizing laminar oscillatory pipe flows is Ω defined as $[D/2\sqrt{\frac{2\pi f}{\nu}}]$. It is seen that Ω is proportional to the ratio of the pipe radius, to the thickness of the Stokes layer. The values of Ω are also shown in figure 24. The data for unsteady transitional flow show some interesting trends. The intermittency is very low at either end of the frequency range studied (Ω=4-22). However, it increases fairly significantly and appears to reach a maximum around an oscillation frequency of about 0.4 Hz ($\Omega\cong$12). This maximum intermittency factor attained, is not very small, and, at r=18.4 mm, is indeed comparable to that of the mean quasi-steady flow. Lastly, the data indicate different values for intermittency near the wall and at the center. It is interesting to note that Yellin (1966) also observed that when transition occurred in pulsatile flows, the disturbances were typically restricted to the core. However, the authors have no explanation at this time for this behavior of the flow. The other aspects of transition in oscillatory flows are examined in some detail below.

Wygnanski and Champagne (1973) have reported detailed study of the steady transitional pipe flow. They divide intermittent transitional turbulence into two categories - the "puff" type and the "slug" type. Puffs are caused by large disturbances at the inlet region of the pipe and are actually remnants of a partial relaminarization process. Slugs, on the other hand, originate from the instability of the boundary layer and represent various stages of amplification of these disturbances. The puffs usually occur in the Reynolds number range of 2000-2700 while the slugs appear generally at very much larger Reynolds numbers. The intermittency measurements in steady flow in the present case are compared in figure 23 with the puff flow data from Wyganski and Champagne. The qualitative agreement between the two sets of data suggests that the present transitional flow can be regarded as a 'puff' type flow. This is further borne out by the

fact that the turbulent puffs are of approximately the same intensity near the wall as at the center line (as seen from the strip chart record), unlike a slug type flow which is known to exhibit an increase in intensity from the centerline to the wall. It may be noted also that the flow is fully turbulent at about Re = 2700.

The development of turbulence through a puff-type transition process does not depend on shear layer instability near the pipe wall since the disturbance is provided by the inlet conditions but depends on the existence of a Reynolds number above a critical value so that the initial turbulence can be sustained. This threshold critical value is about 2000 and transition to turbulence can not occur below this Reynolds number. In a flow subjected to a favorable pressure gradient, this critical Reynolds number is known to increase. But, in an adverse pressure gradient, it will not decrease significantly below the threshold value. Hence, if the Reynolds number of flow oscillates around 2000, the net effect would be an increase in the critical Reynolds number and hence a partial or complete laminarization of the initial turbulent puffs. The increase in the critical Reynolds number will be larger at larger favorable pressure gradients and hence one would expect to find a greater degree of laminarization as the oscillation frequency increases. This is, exactly what is observed in figure 24 as a decrease in the intermittency in the range of 0.4 Hz - 1.75 Hz (Ω=12-22) with the flow being almost completely laminar at 1.75 Hz. The existence of a maximum intermittency (almost equal to the intermittency in the mean steady flow) at about 0.4 Hz ($\Omega \cong 12$) appears somewhat to contradict the above argument. It is, however, important to note that at low frequencies, (0 - 0.4 Hz), (Ω = 0-12) the favorable pressure gradients are very small (at the amplitude of modulation employed) and consequently, the effect on the critical Reynolds number is negligibly small at these frequencies. On the other hand, the extent of laminarization of the puffs depends not only on the critical Reynolds number but also on the length of time in a cycle the puffs are exposed to a Reynolds number lower than the critical Reynolds number. At low frequencies the latter effect becomes dominant and since the residence time of the puffs below the critical Reynolds number increases as the oscillation frequency is reduced, the intermittency of puffs would

decrease with frequency in this range. The results in this range agree qualitatively with those of Sarpkaya (1966) whose experiments extended over the range Ω = 4-7.8. He found that at small amplitudes of modulation (λ = 0.2 - 0.3) there was only a slight increase in critical Reynolds number above the steady state value and that increase in the oscillation frequency in this range reduced the rise in critical Reynolds number. Sarpkaya noticed negligible effect of oscillation on the transition characteristics at Ω = 7.8 (which, incidentally, he regarded as 'rapid' oscillation). It is interesting to note that at about 0.4 Hz corresponding to $\Omega \cong 12$ the present unsteady flow exhibits the maximum intermittency. The present observations are thus in qualitative agreement with those of Sarpkaya. There is, however, quantitative disagreement between the present data and those of Sarpkaya with respect to the actual magnitudes of the critical Reynolds number at the various values of Ω. This is due largely to the difference between the definitions of critical Reynolds number used in the two cases. In the present case, the critical Reynolds number is taken to be the Reynolds number at which the puffs (external disturbances) disappear whereas Sarpkaya defined it as the Reynolds number at which the external disturbances cease to amplify. It is thus clear that the present definition describes the lower bound for the puff-type transition process.

The major difficulty with studies connected with puff-type transition is that the process is very sensitive to the nature of external disturbances and other ambient conditions. It is thus very difficult to find repeatability in observations over a period of time. This is especially true when an additional factor, namely flow oscillation, is introduced. This has been clearly demonstrated by the two series of experiments reported in this paper. The two series gave entirely different results under what apparently appeared to be identical conditions. It is worth examining the reasons for this at least in a qualitative way. As mentioned already, the mean steady flow (θ=90°) was fully turbulent in the Series 1 experiments. In fact, it was fully turbulent even at θ=100° (corresponding to $Re \cong 2000$). Unfortunately, intermittency measurements were not made in these series. However, one can visualize (without much error) the intermittency variation with Reynolds number to be as shown in figure 23. It is very clear that

in this flow, transition occurred within a very narrow range of Reynolds numbers, unlike in the second series of experiments in which it was spread over a much wider range of Reynolds numbers. The reason for this is not known with certainty but a reasonable guess is as follows. The first weries of experiments were conducted in summer during which time, the laboratory temperature was about 30°C while the fluid temperature remained at about 26°C. Since the pipe was not insulated, there was heat transfer from the ambient to the fluid. This would aid the process of transition. On the other hand, the second series of experiments were conducted in winter when the laboratory temperature was around 20°C while the fluid temperature still remained at 26°C. There was, thus, a heat transfer from the fluid to the surroundings. This loss of energy to the surroundings would reduce the energy available for producing and completing the transition and hence would tend to stabilize the flow.

The two intermittency distributions shown in figure 23 for the two series can be used to explain qualitatively the observed difference in response of the flow to oscillate at a high frequency in the two cases. Flow oscillation at a high frequency would raise the critical Reynolds number from its value of about 2000 at quasi-steady state by an amount, say, ΔRe. This is equivalent to moving the operating line, i.e., mean flow Reynolds number of the unsteady flow to the left by ΔRe in figure 23. It is seen that in the series 2 experiments, the new operating line corresponds to a laminarized flow (of very small intermittency) while in the series 1 experiments, it corresponds to fully turbulent flow (of intermittency 1). It is to be mentioned here that laminarized oscillatory flow can be observed only under very restricted conditions. These include puff-type transition (i.e., transition brought about by inlet disturbances), a relatively small intermittency of puffs at the mean Reynolds number and either strong pressure gradient fluctuations (high frequency, large amplitude oscillation) or large puff-residence time (long enough pipe). These conditions are often found in the pulsatile flow of blood in the mammalian aorta and hence laminarization of the flow can be expected to occur in such cases. This is, in fact, corroborated by some of the recent in-vivo aorta experiments mentioned at the beginning of this paper.

IV. CONCLUSIONS

The present study has lead to the following conclusions:

(i) Periodic oscillation of discharge tends to increase the critical Reynolds number of puff-type transitional pipe flow. Under certain conditions, the transitional flow may be laminarized on periodic oscillation. For a given amplitude of flow modulation the extent of laminarization depends on factors such as the intermittency of puffs in the quasi-steady mean flow, the oscillation frequency and the residence time of the puffs in the pipe.

(ii) The laminarized periodic flow behaves very much like laminar periodic flow. For example, the time-mean flow properties remain unchanged from those of quasi-steady mean flow and the phase lag and amplitude of the periodic velocity component depend strongly on the Strouhal number.

(iii) When the oscillatory flow is fully turbulent, its time mean and periodic structure qualitatively resemble those of oscillatory laminar flow at the same Strouhal number. However, the behavior of the oscillatory turbulent flow is also influenced by an additional parameter, namely the ratio of the oscillation frequency to some characteristic frequency of turbulence. When this ratio is of the order unity, the oscillations interact with the turbulent structure. Important differences can be observed between laminar and turbulent flows at such oscillation frequencies. For example, the time-mean velocity profile in the oscillatory flow exhibits a point of inflection near the wall, and the time mean wall shear stress and power loss increase from their quasi-steady values. Also, the periodic velocity component exhibits an overshoot in the Stokes layer, the magnitude of the overshoot being larger than in laminar oscillatory flows at the same Strouhal number.

(iv) At the interactive frequency of scillation, mentioned above, the ensemble averaged turbulence intensity is frozen everywhere in the pipe. The ensemble averaged Reynolds shear stress is able to follow the oscillation cycle (with some lag) only very close to the wall. However, beyond the Stokes layer, it is also frozen at some average value. The stress freezing

is brought about by the large and rapidly varying strain rates. The ensemble averaged Reynolds stresses as well as the ensemble averaged velocity do not scale with the corresponding ensemble averaged wall shear stress indicating significant departures from local structural equilibrium.

REFERENCES

Acharya, M. and Reynolds, W.C. (1975). Measurements and predictions of a fully developed turbulent channel flow with imposed controlled oscillations. Stanford University Thermosciences Division, Tech. Report No. TF-8.

Cousteix, J., Desopper, A., and Houdeville, R. (1977).. Structure and development of a turbulent boundary layer in an oscillatory external flow," Proceedings of Symposium on Turbulent Shear Flows, Penn State University, University Park, Pa.

Falsetti, H.L., Kiser, K.M., Francis, J.P., and Belmore, E.R. (1972). Sequential velocity development in the ascending aorta of the dog. Cir. Research 31, pp. 328-338.

Gerrard, J.H. (1971). An experimental investigation of the pulsating turbulent flow in a water tube. Journal of Fluid Mechanics, 46, Pt. 1, pp. 43-64.

Hino, M., and Sawamoto, M. (1975). Linear stability analysis of an oscillatory flow between parallel plates. Proceedings of the Seventh Symposium on Turbulence (ed. Sato, H., and Ohji, M.) Institute of Space and Aeronautics, University of Tokyo, pp. 1-7.

Hino, M., Sawamoto, M., and Takasu, S. (1976). Experiments on transition to turbulence in oscillatory pipe flow. Journal of Fluid Mechanics, 75, Pt. 2, pp. 193-207.

Houdeville, R. and Cousteix, J. (1978) "Premiers Resultats d'une etude sur les couches limites turbulentes en ecoulement pulse avec gradient de pression moyen defavorable", 15e Colloque D'Aerodynamique Appliquee, Marseille, November 7-8.

Lu, S.Z., Nunge, R.J., Erian, F.F. and Mohajery, M. (1973). Measurements of pulsating turbulent water flow in a tube. Proceedings of the Third Symposium on Turbulence in Liquids, University of Missouri, Rolla, pp. 375-392.

Mueller, A. and Ramaprian, B.R. (1977). Velocity measurements in a transitional oscillatory boundary layer. Proc. of 2nd Annual ASCE EMB Specialty Conference, Raleigh, N.C.

Nakato, T. 1974. Wave-induced sediment entrainment from rippled beds, Ph.D. Thesis, Mechanics and Hydraulics Program, University of Iowa, Iowa City.

Patel, M.H. (1977). On turbulent boundary layers in oscillatory flow. Proceedings of the Royal Society of London. A353, pp. 121-144.

Ramaprian, B.R. (1975). Turbulence measurements in an 'equilibrium' axisymmetric wall jet. Journal of Fluid Mechanics, 71, Pt. 2, pp. 317-338.

Rao, K.N., Narasimha, R. and Badri Narayanan, M.A. (1971). The 'bursting' phenomena in a turbulent boundary layer. Journal of Fluid Mechanics, 48, pp. 339-352.

Richardson, E.G., and Tyler, E. (1929). The transverse velocity gradient near the mouthes of pipes in which an alternating or continuous flow of air is established. Proceedings of Physical Society of London, 43, pp. 1-15.

Rosenhead, L. (1963). (ed). Laminar Boundary Layers, Oxford Univ. Press, London.

Sarpkaya, T. (1966). Experimental determination of the critical Reynolds number for pulsating Poiseuille flow. Journal of Basic Engineering, Trans. ASME 88, pp. 589-598.

Schlichting, H. (1968). Boundary Layer Theory. McGraw-Hill, New York.

Schulz-Grunow, (1940). Pulsierender Durchfluss durch Rohre, Forschung 11, 4, pp. 170-187. Translated as "Pulsation Flow Through Pipes", NASA Technical Translation, NASA-TT-F-14881, 1973, 50 p.

Tu, S.W. (1978). An experimental study of oscillatory pipe flow at transitional Reynolds numbers, M.S. Thesis, Mechanics and Hydraulics Program, The University of Iowa, Iowa City, Iowa.

Coles, D.A. and Hirst, E.A. (1968). (ed.) Proceedings of the 1968 Stanford Conference on Boundary Layers.

Uchida, S. (1956). The pulsating viscous flow superposed on the steady motion of incompressible fluid in a circular pipe. ZAMP, 7, pp. 403-421.

Wygnanski, I.J., and Champagne, F.H. (1973). On transition in a pipe. Part I, The origin of puffs and slugs and the flow in a turbulent slug. Journal of Fluid Mechanics, 59, Pt. 2, pp. 281-336.

Yellin, E.L. (1966). Laminar turbulent transition process in pulsatile flow. Circ. Res. 19; pp. 791-804.

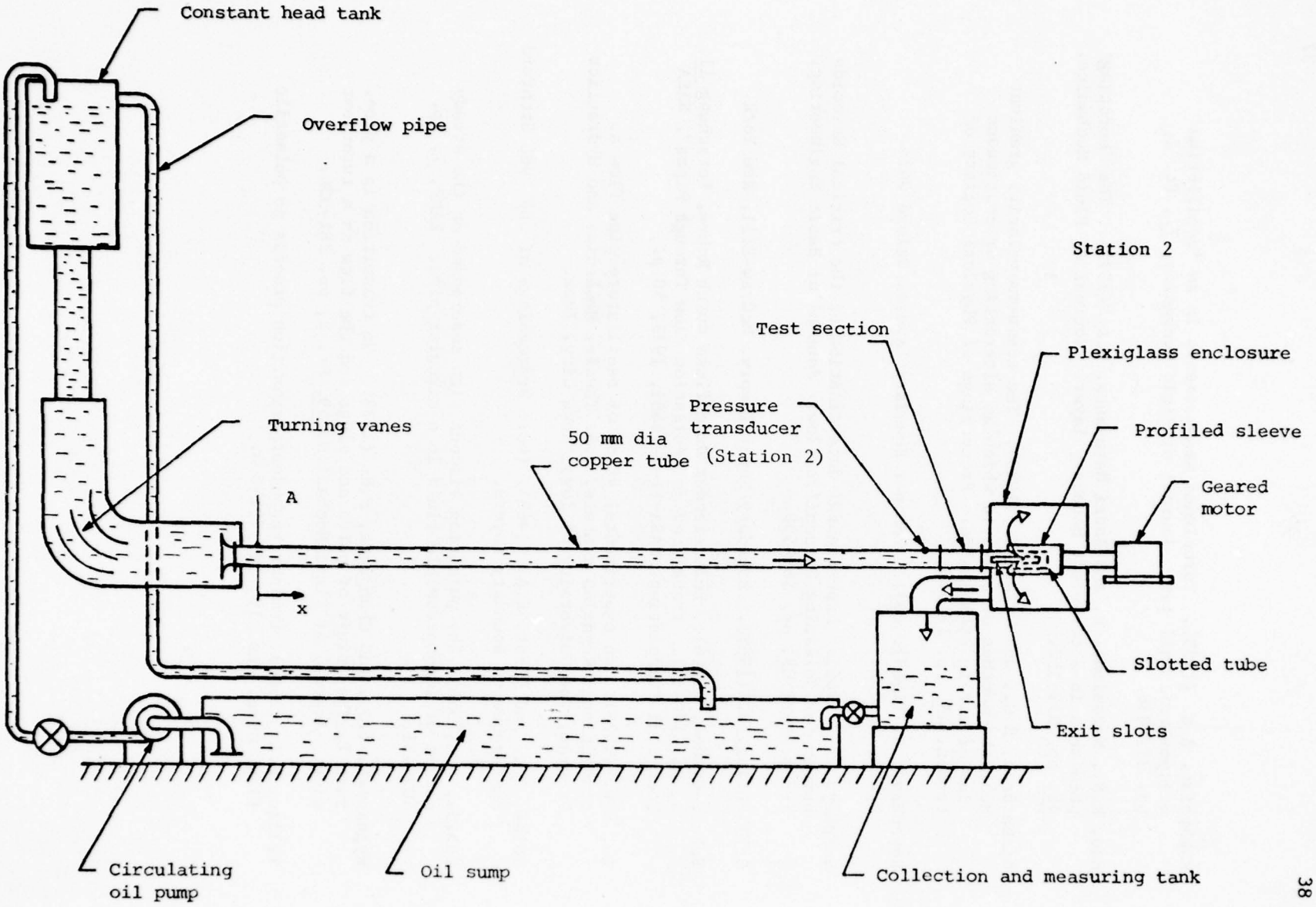

Figure 1. Schematic layout of the experimental apparatus

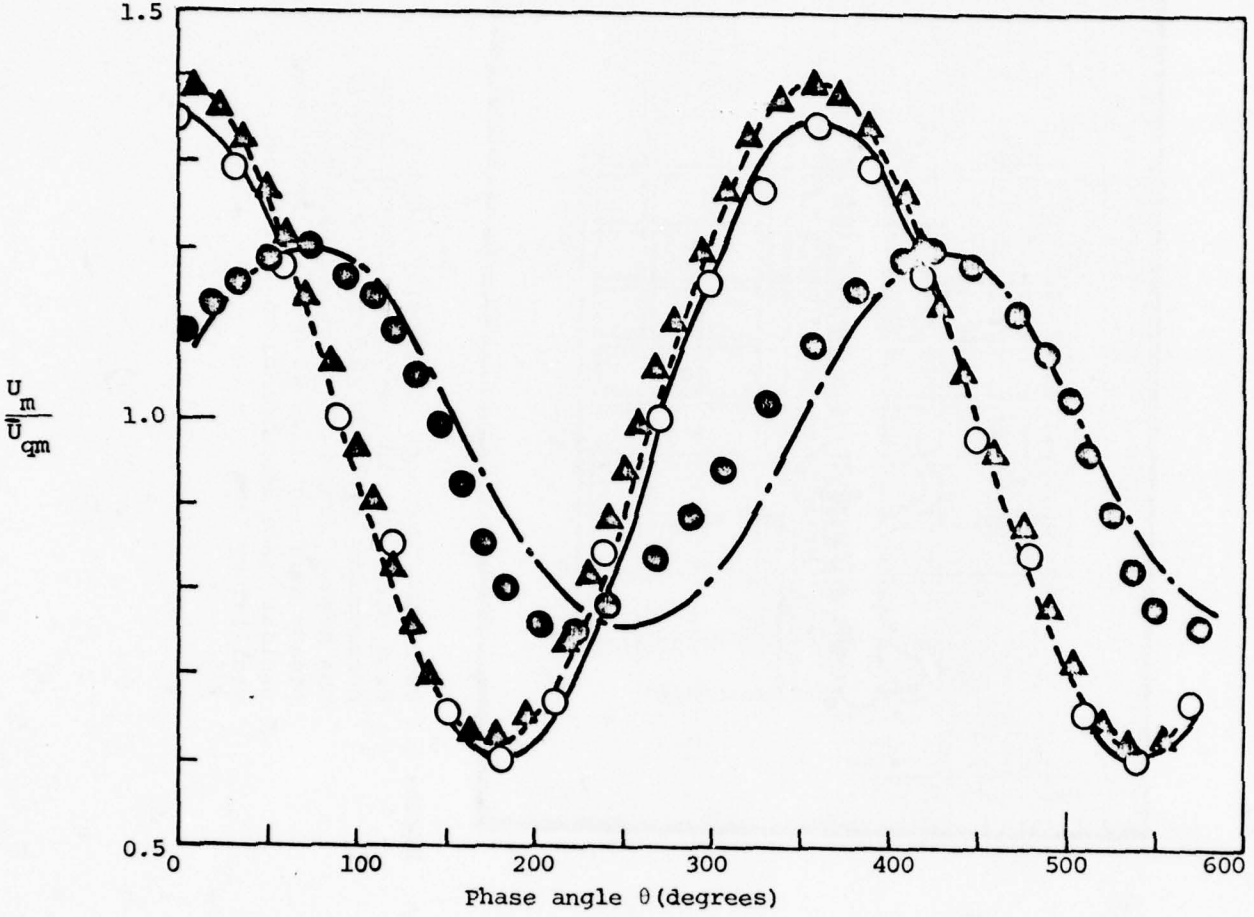

Figure 2. Variation of the cross sectional average velocity during a cycle. O, quasi-steady; ▲, oscillatory flow at0.057 Hz (Run 24); ●, oscillatory flow at 1.75 Hz (Run 13); Lines denote exact sine waves with corresponding amplitude;——, quasi-steady;---, 0.057 Hz; — · —, 1.75 Hz

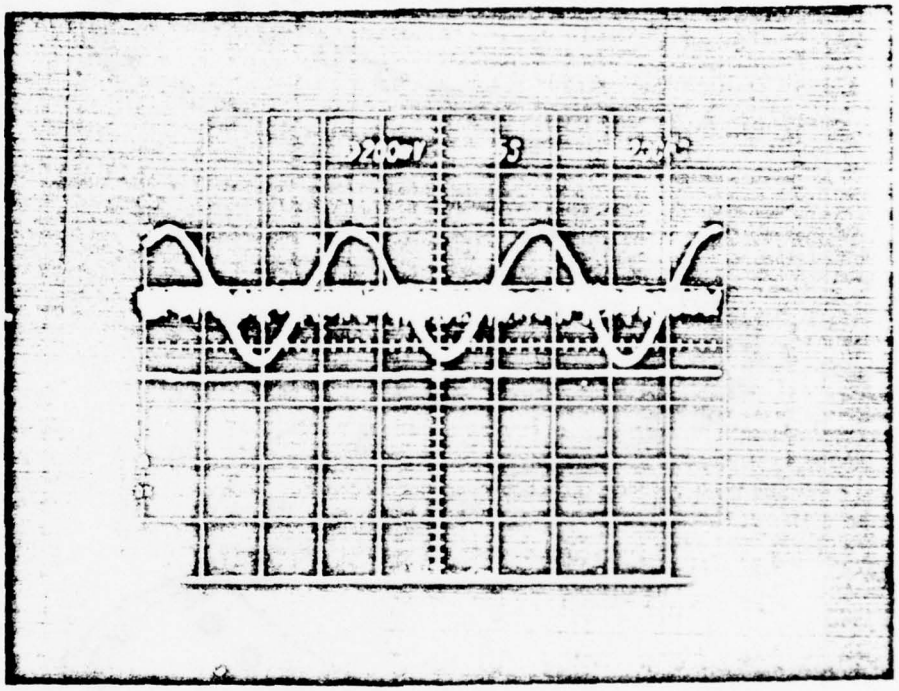

Figure 3. Oscilloscope traces of velocity signals From LDA (r =0). The smooth horizontal trace corresponds to steady laminar flow (θ=180°); the hashed horizontal trace corresponds to steady turbulent flow (θ=0°); the smooth sinusoidal trace corresponds to laminarized oscillatory flow

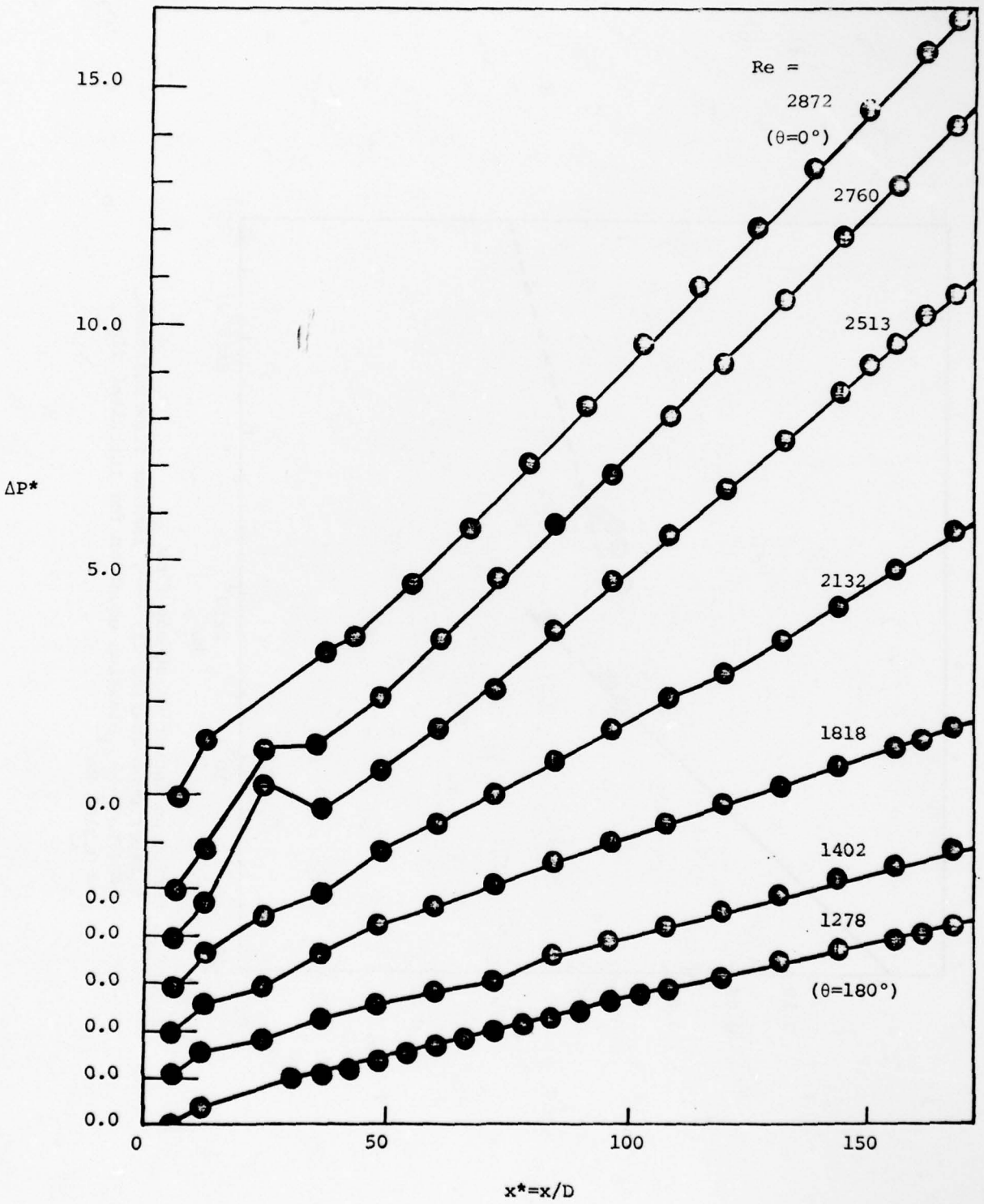

Figure 4. Static pressure drop along the pipe in steady flow; results from experiments of series 2.

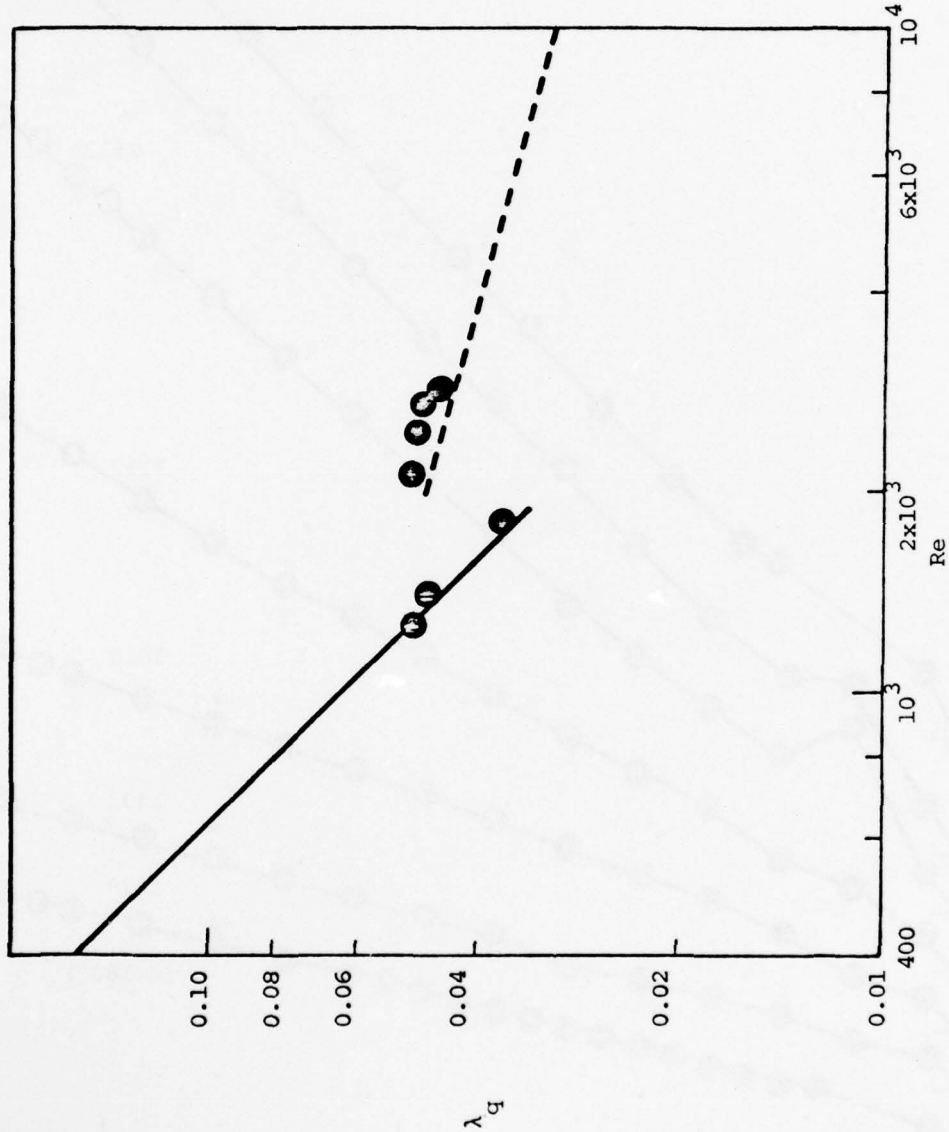

Figure 5. Friction factor in steady flow.
● Experiment (series 2); ——, laminar flow relation $\lambda=64/Re$; ---, Blassius equation for turbulent flow, $\lambda = 0.3165\ Re^{-\frac{1}{4}}$

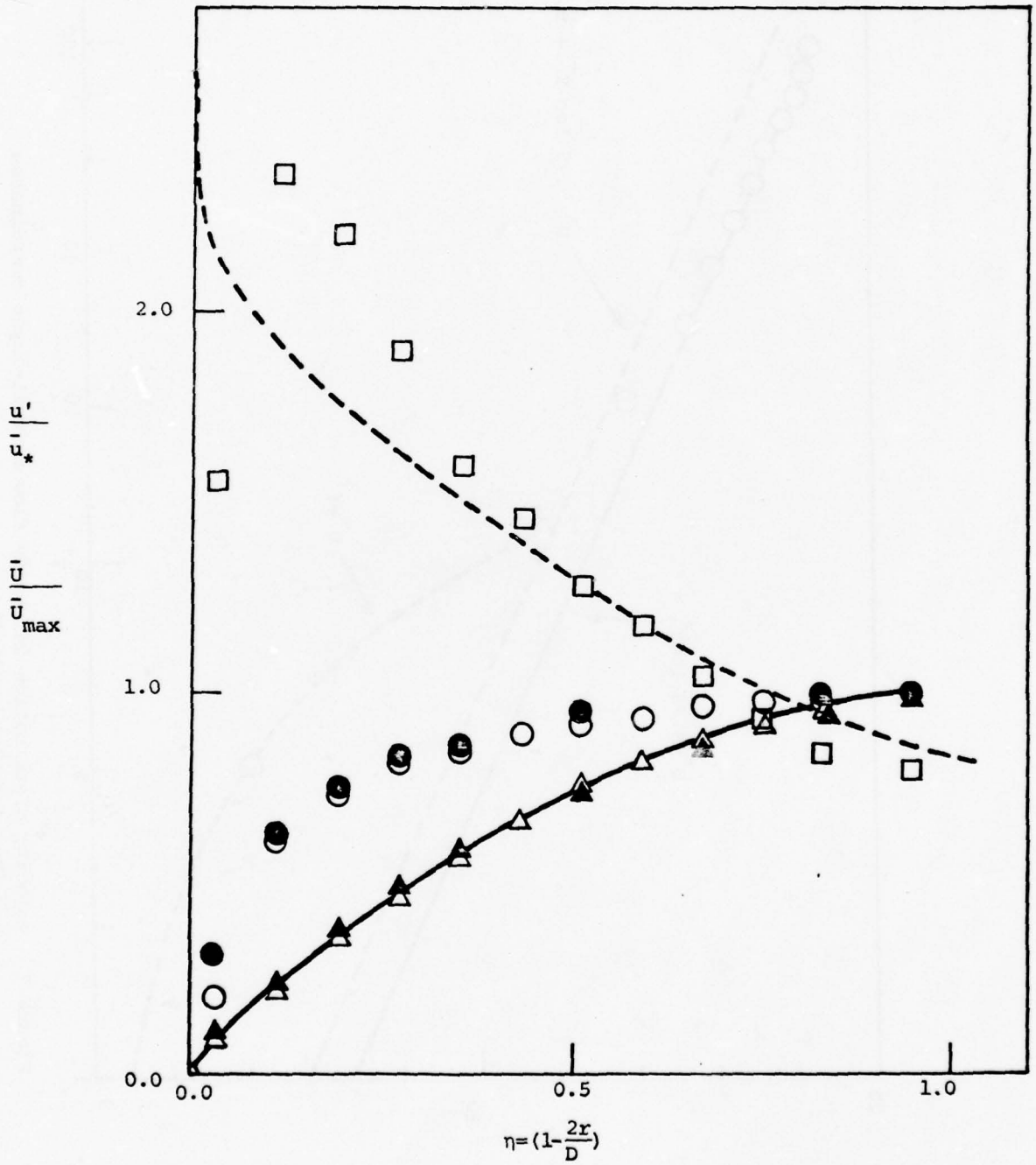

Figure 6. Distributions of mean and turbulent velocities in steady flow.
mean velocity {Δ, Run 11; ▲, Run 21 Laminar flow at θ=180° (Re=1278)
{○, Run 12; ●, Run 22 Turbulent flow at θ=0° (Re=2870
---, theoretical parabolic profile for laminar flow
Turbulent intensity: □, Run 12; ---data from Laufer (1954) for Re=5×10^5

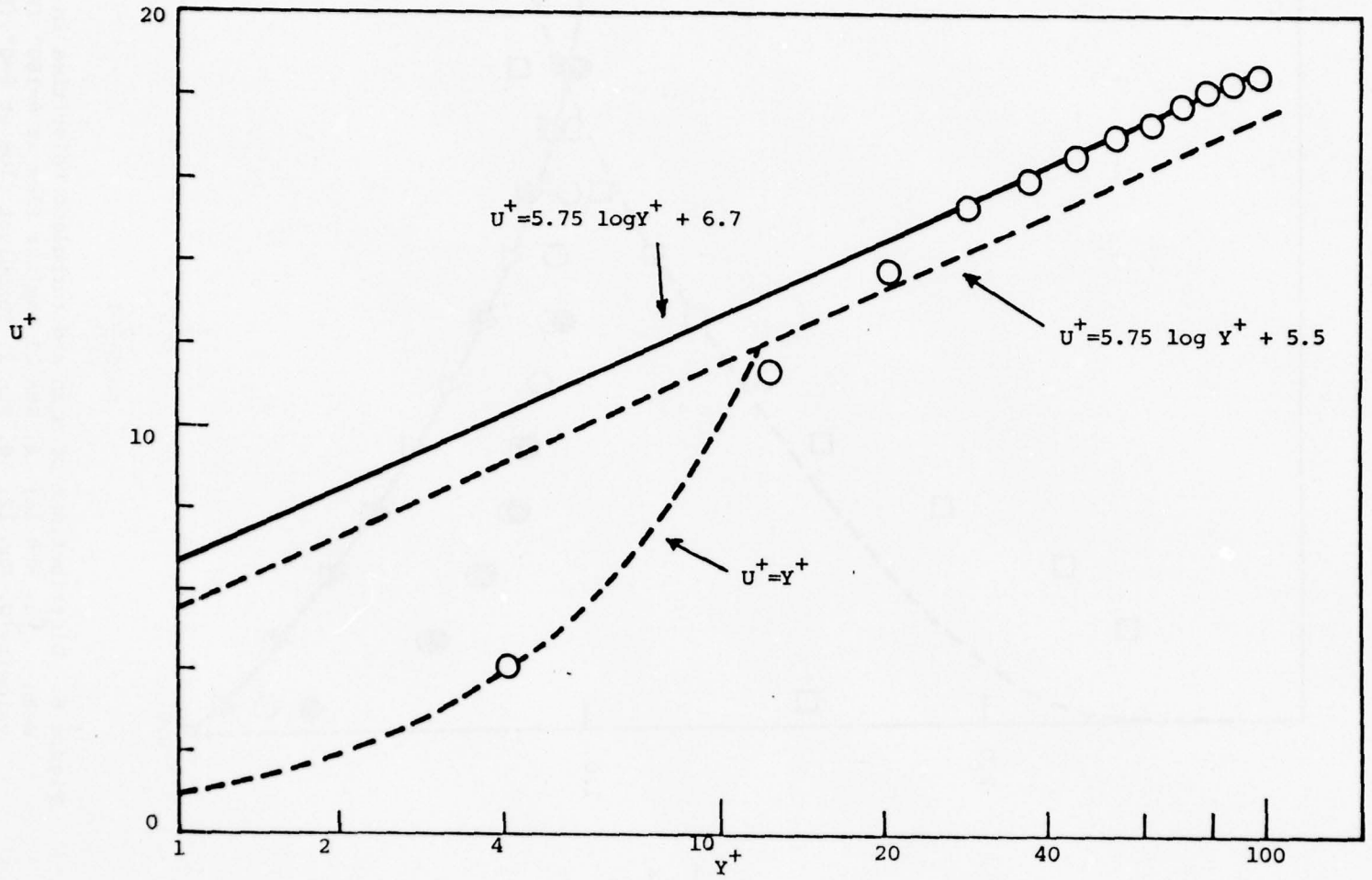

Figure 7. Velocity distribution in steady flow in wall-layer coordinates
$\theta=0$ (Maximum slot opening)

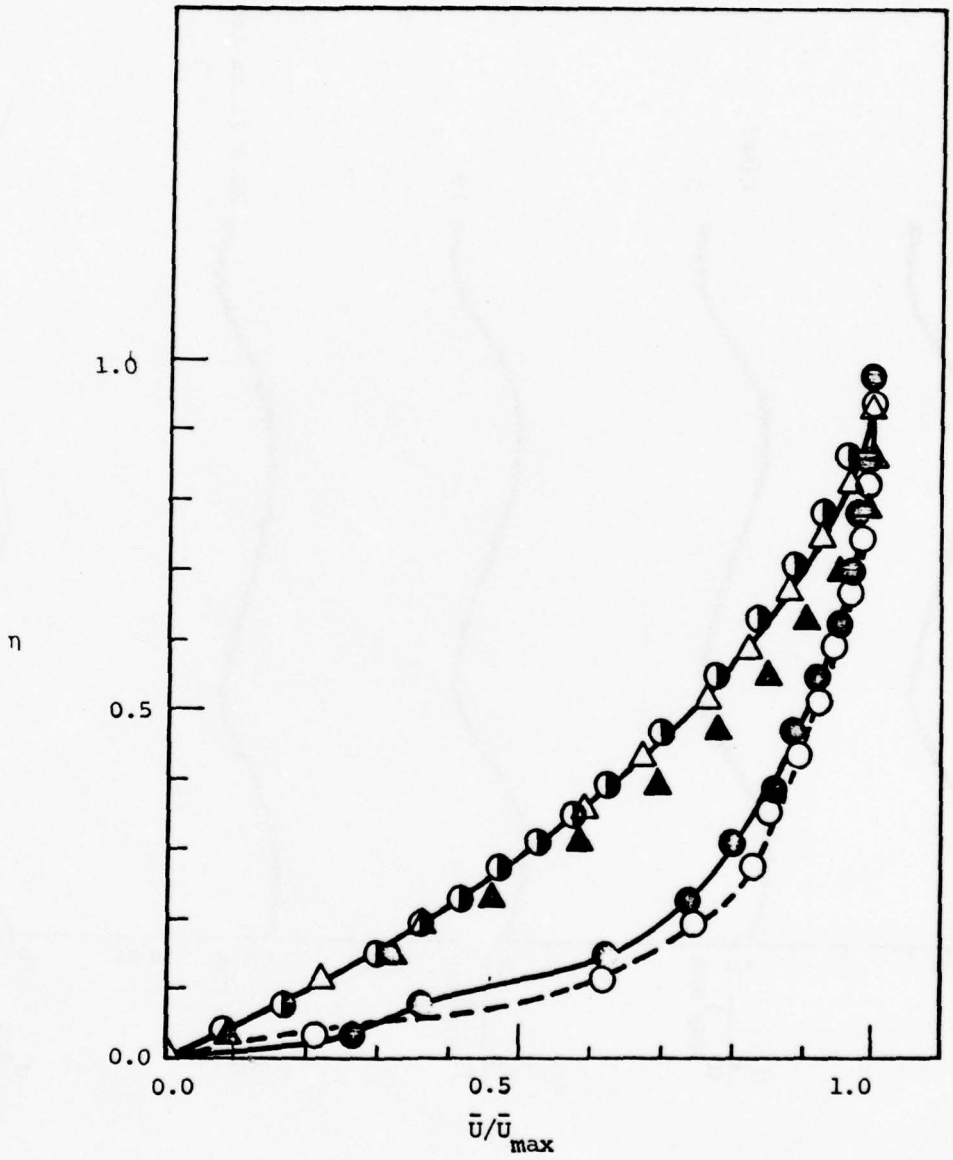

Figure 8. Distribution of the time-mean velocity across the pipe in unsteady flow.

Δ, steady laminar flow (θ=180°); -θ-, steady turbulent flow (θ=0°),
—●—, unsteady turbulent flow at f=1.75 Hz (Run 13);
◐, unsteady laminarized flow at f=1.75 Hz (Run 23),
▲, unsteady laminarized flow at f=0.057 Hz (Run 24);
——, theoretical parabolic profile for laminar flow

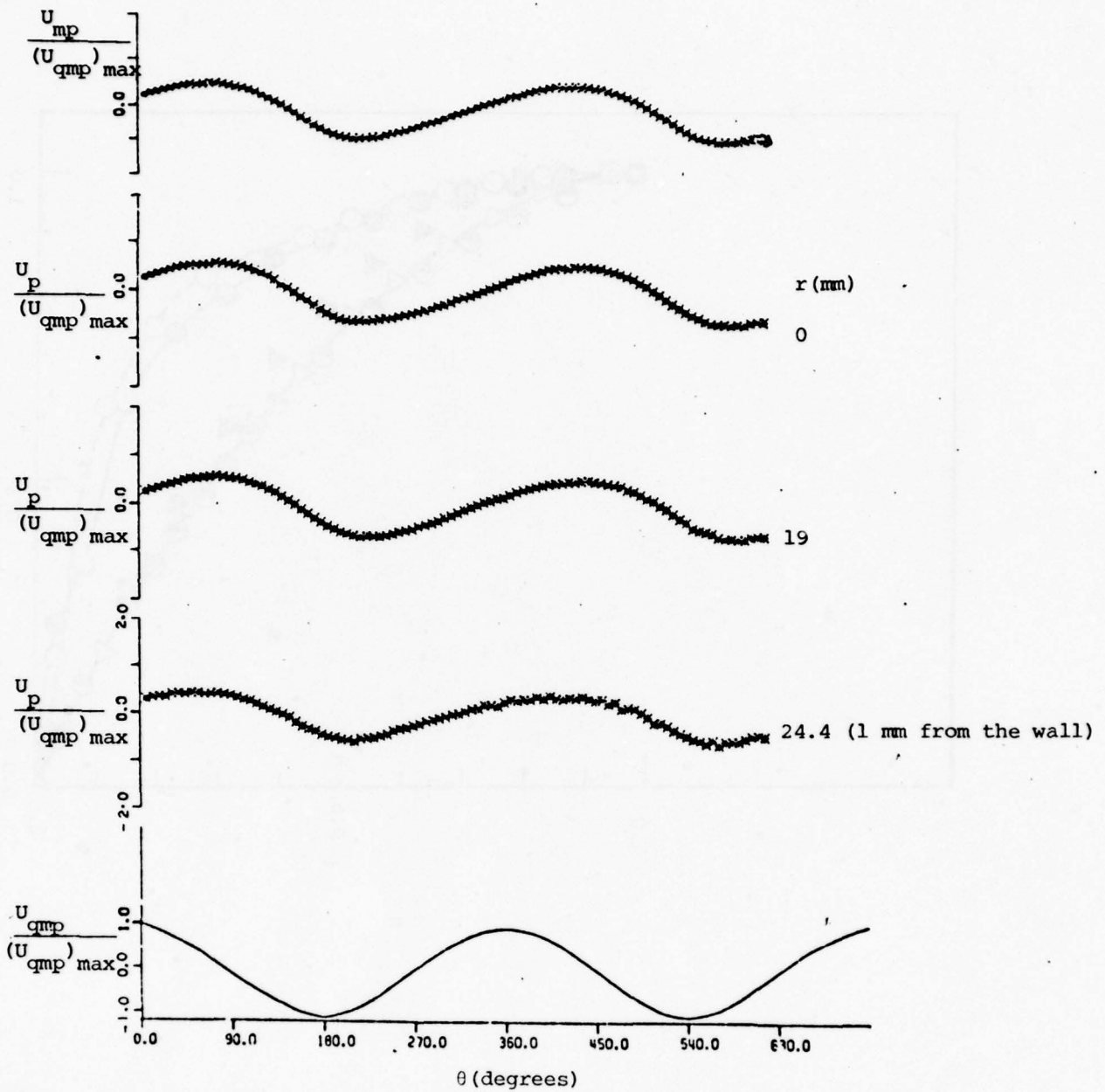

Figure 9(a). Variation of the periodic component of the velocity with phase angle (Run 13).

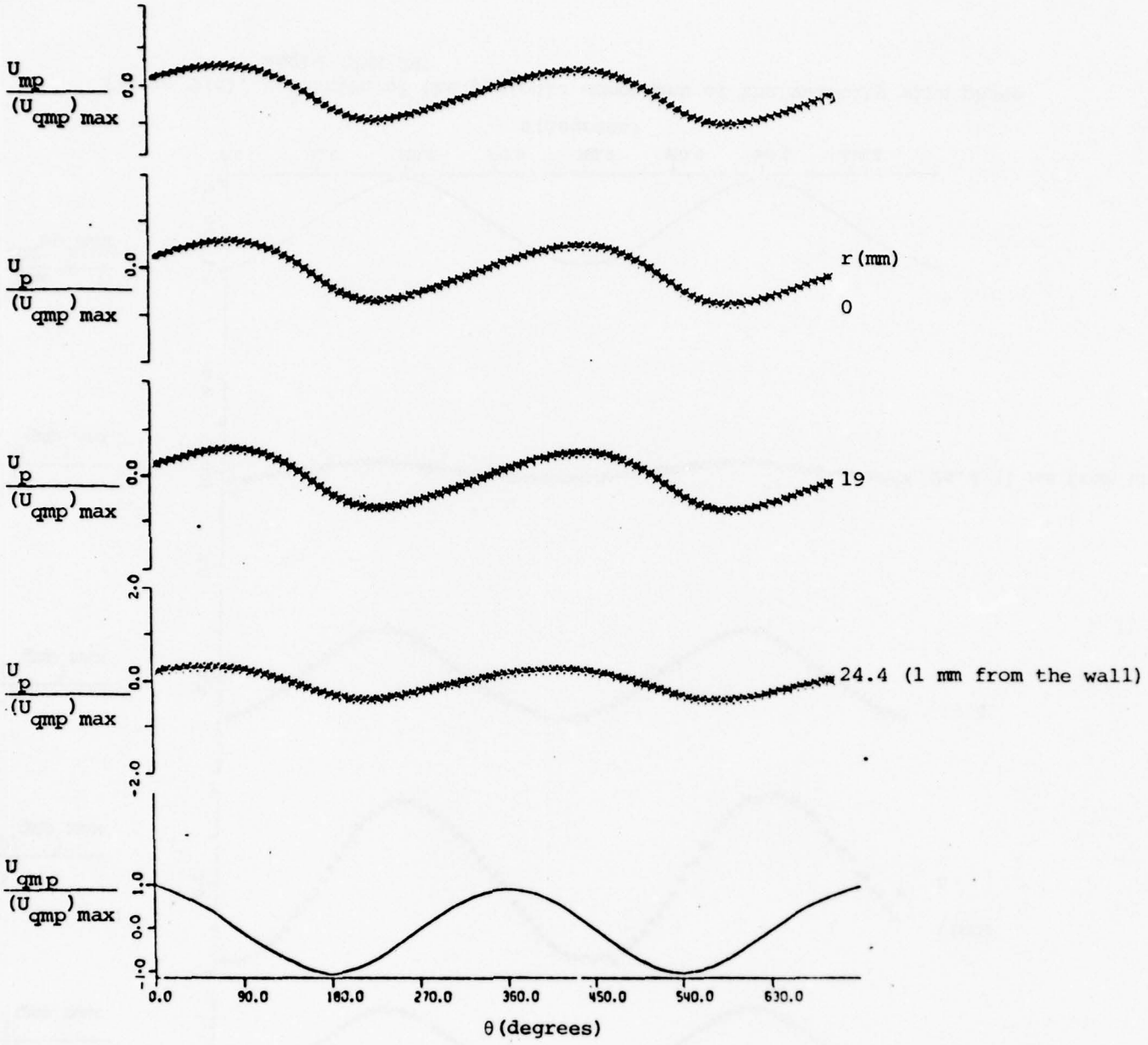

Figure 9(b). Variation of the periodic component of the velocity with phase angle (Run 23).

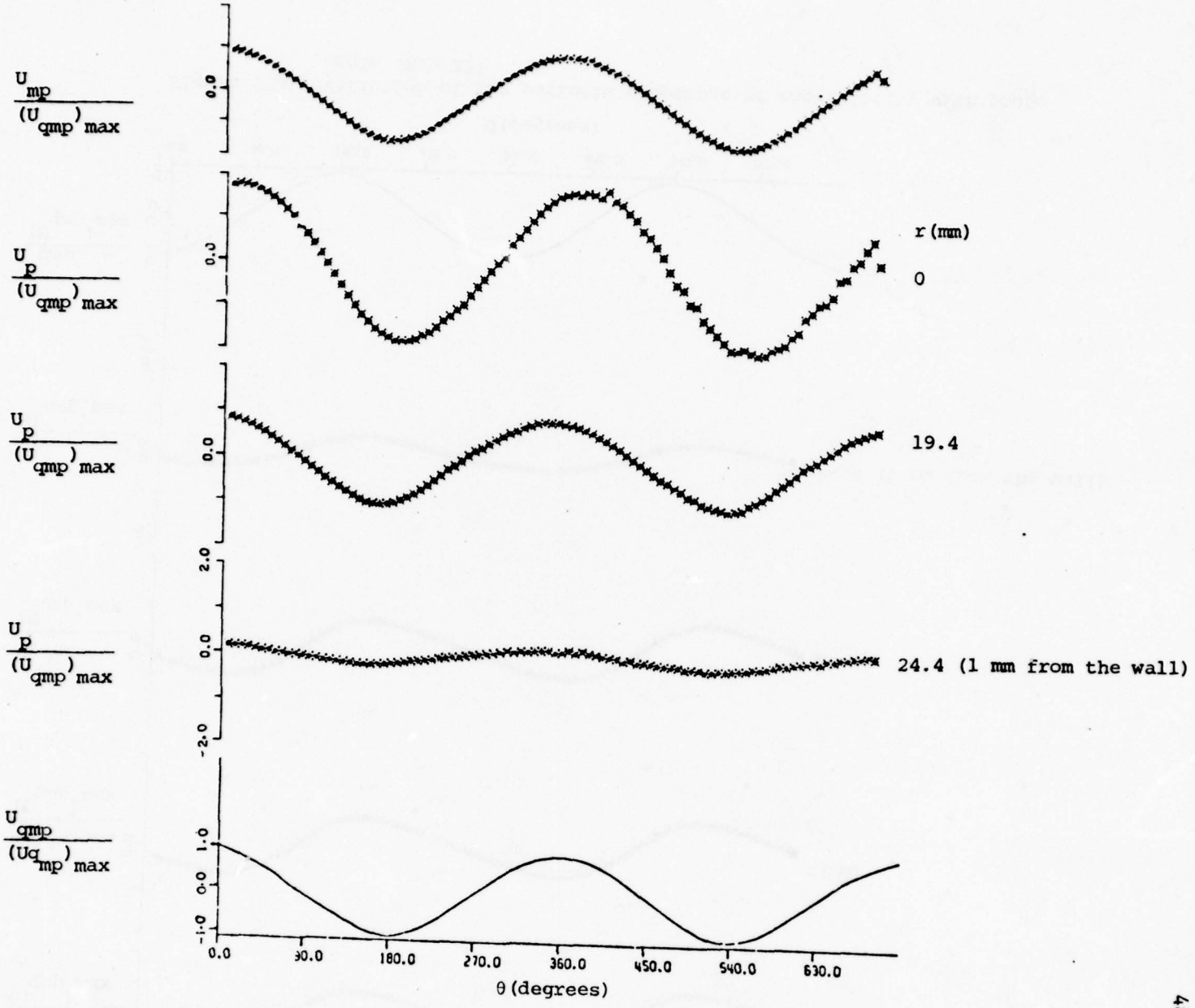

Figure 9(c). Variation of the periodic component of the velocity with phase angle (Run 24)

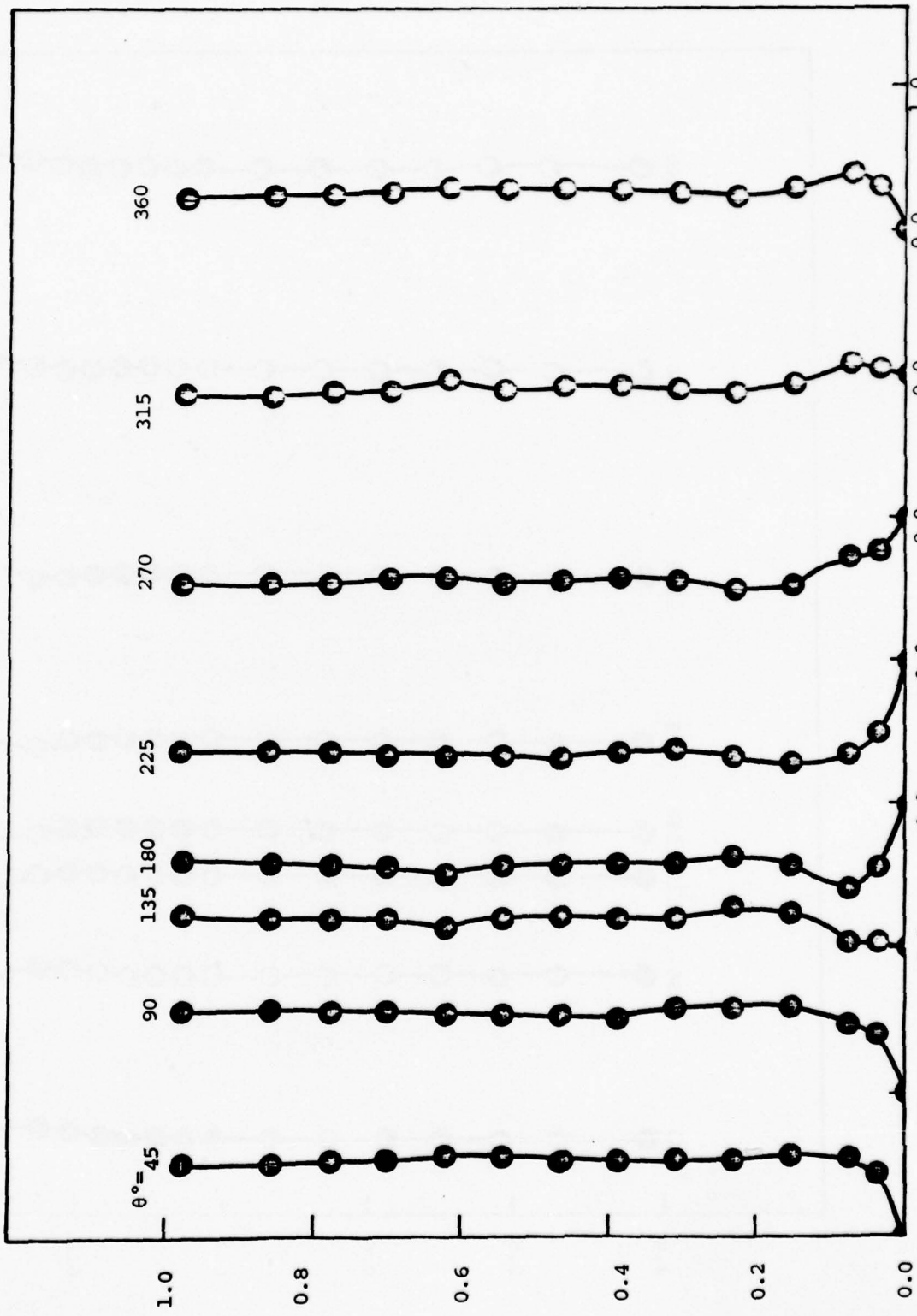

Figure 10(a) Distribution of the periodic component of the velocity across the pipe at fixed phase angle in oscillating turbulent flow; f=1.75 Hz (Run 13).

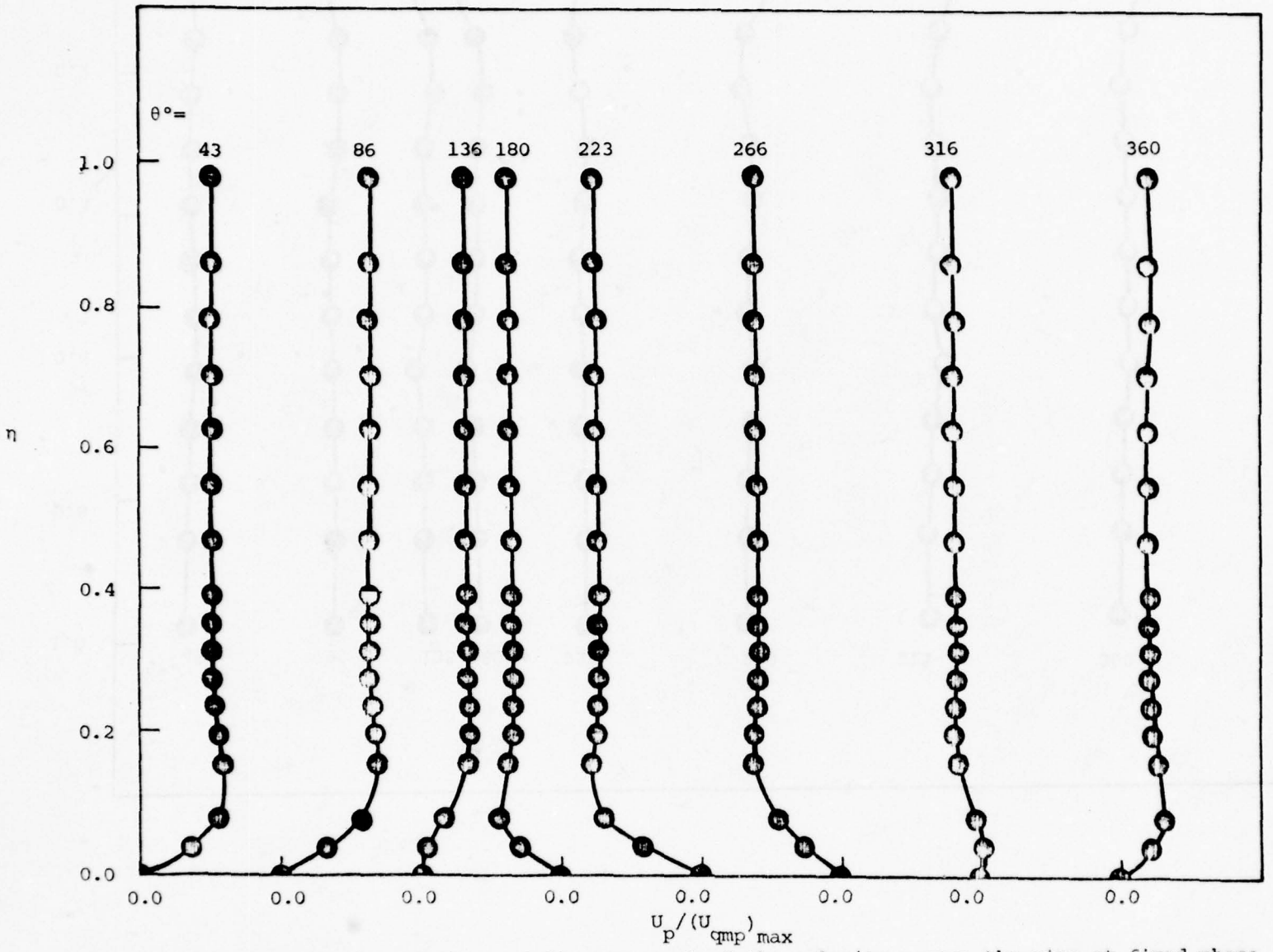

Figure 10(b). Distribution of the periodic component of the velocity across the pipe at fixed phase angle in oscillating laminar flow; f=1.75 Hz (Run 23)

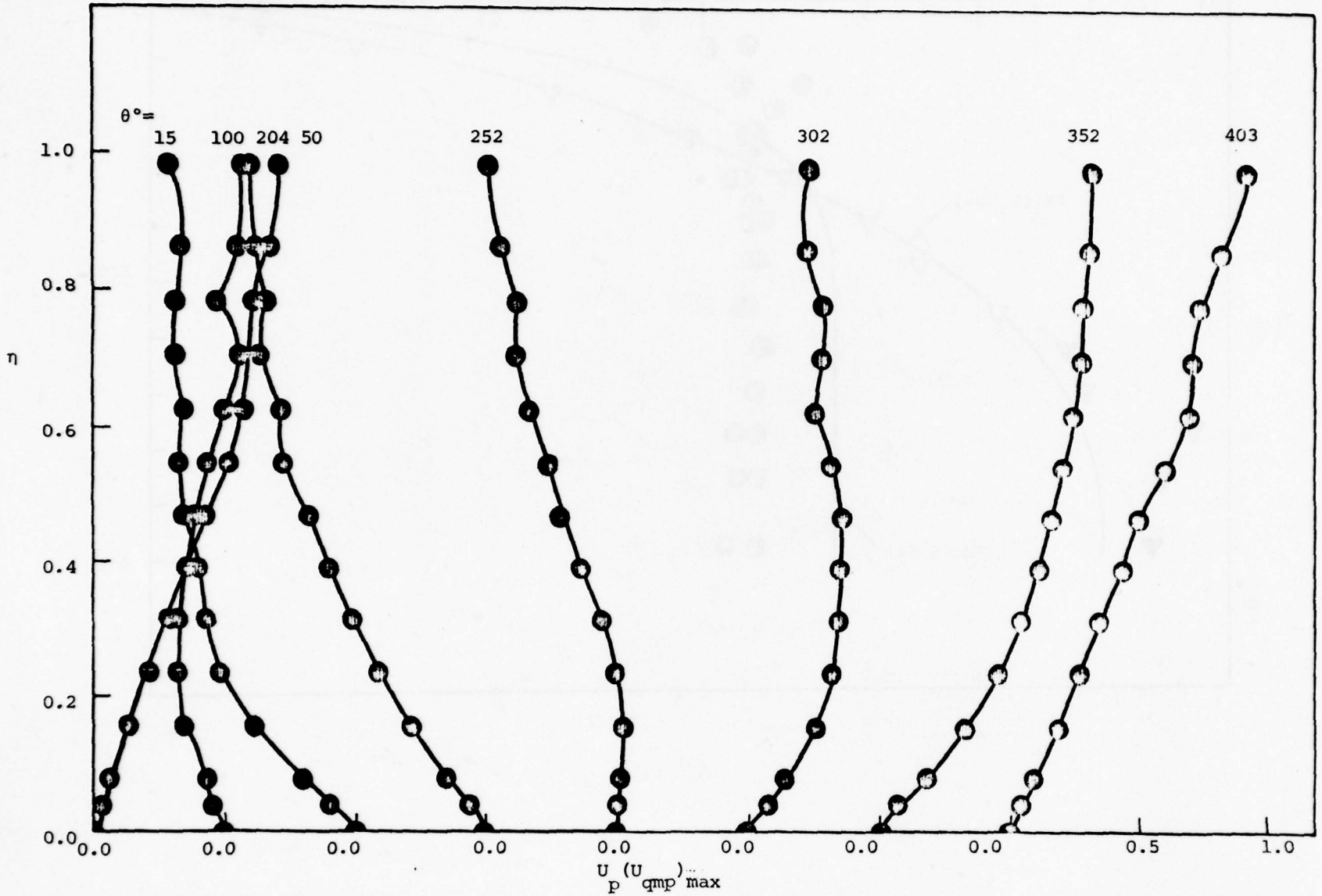

Figure 10(c). Distribution of the periodic component of the velocity across the pipe at fixed phase angle in oscillating laminar flow; f=0.057 Hz (Run 24)

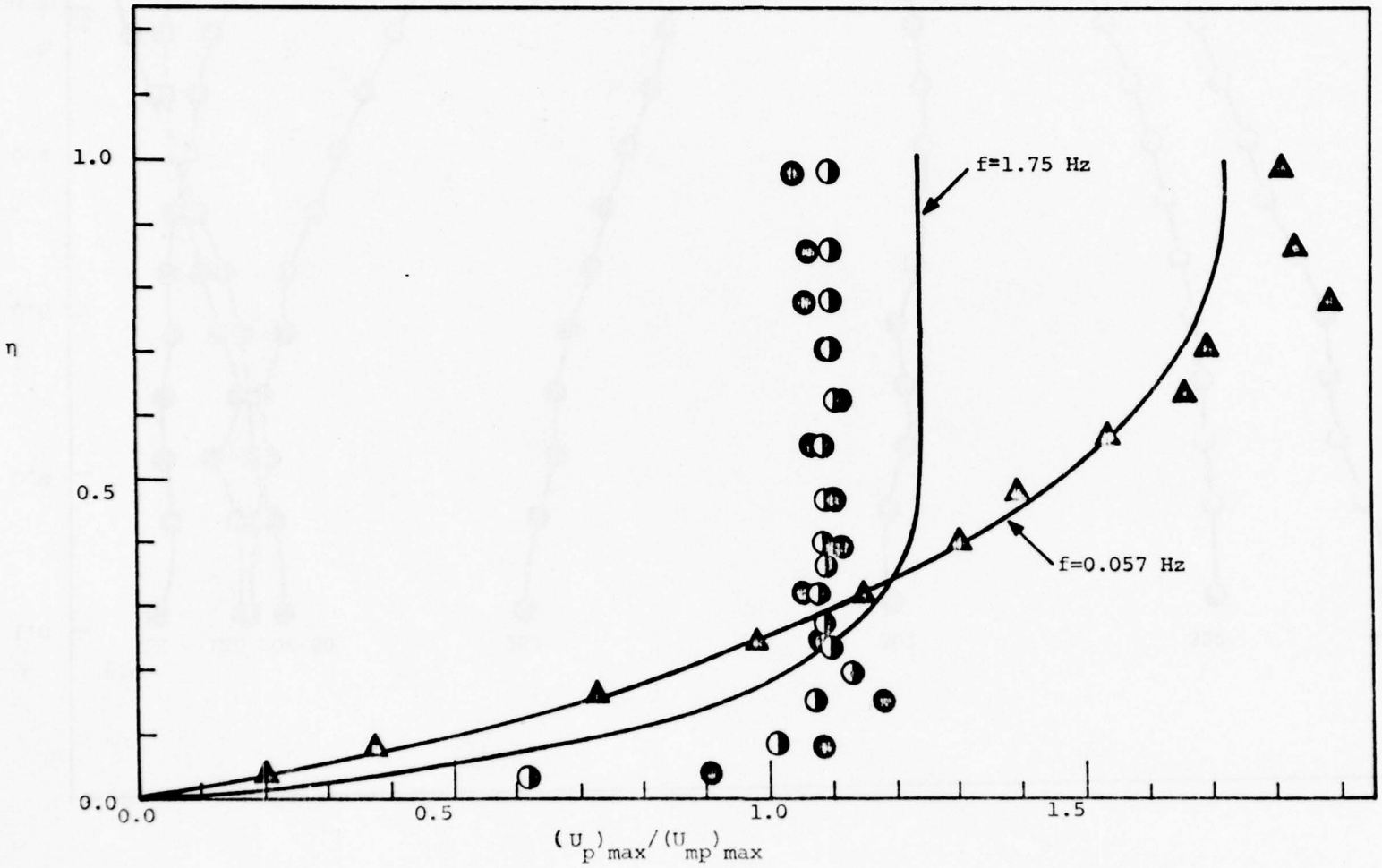

Figure 11. Distribution of the amplitude of the periodic component of velocity across the pipe.
●, Run 13; (f=1.75 Hz) ◑, Run 23; (f=1.75 Hz) ▲, Run 24; (f=0.057 Hz) ——, Laminar theory from Uchida (1956)

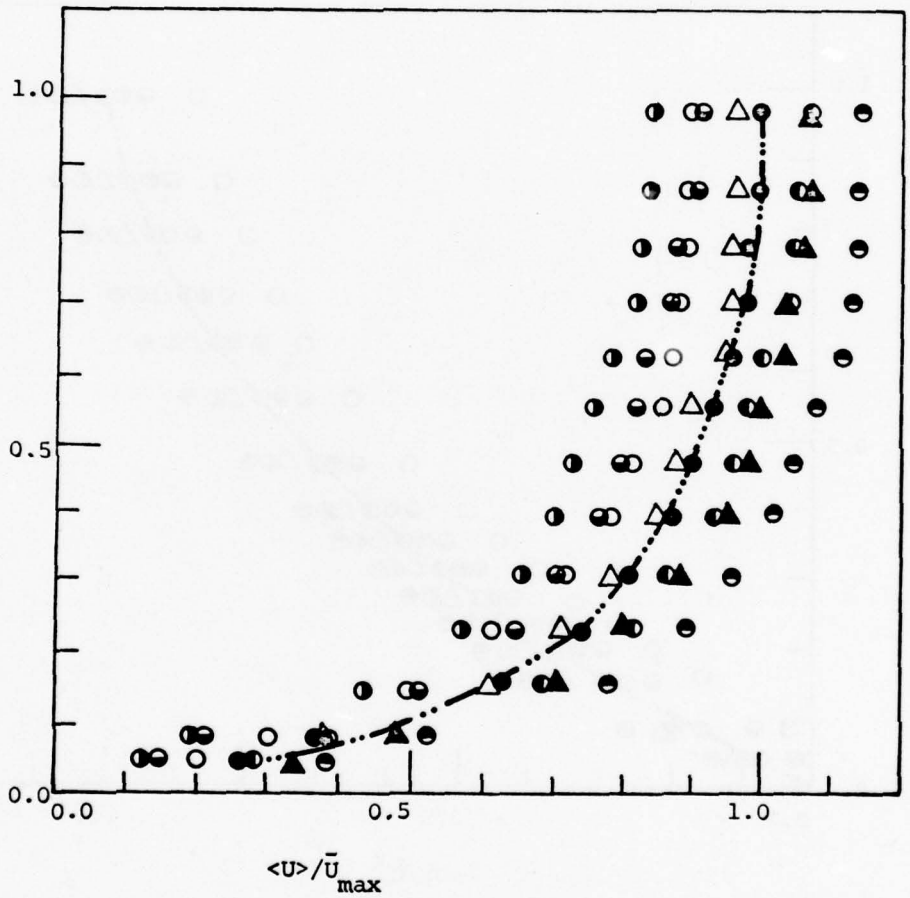

Figure 12(a). Distribution of the ensemble average velocity across the pipe in oscillatory turbulent flow, f=1.75 Hz (Run 13)

symbol, phase angle θ(degrees): ●, 45°; ◐, 135°; ⊖, 180°; ◑, 225°; 0, 270°; Δ, 315°, ▲, 360°; -·-●-·-, time-mean velocity

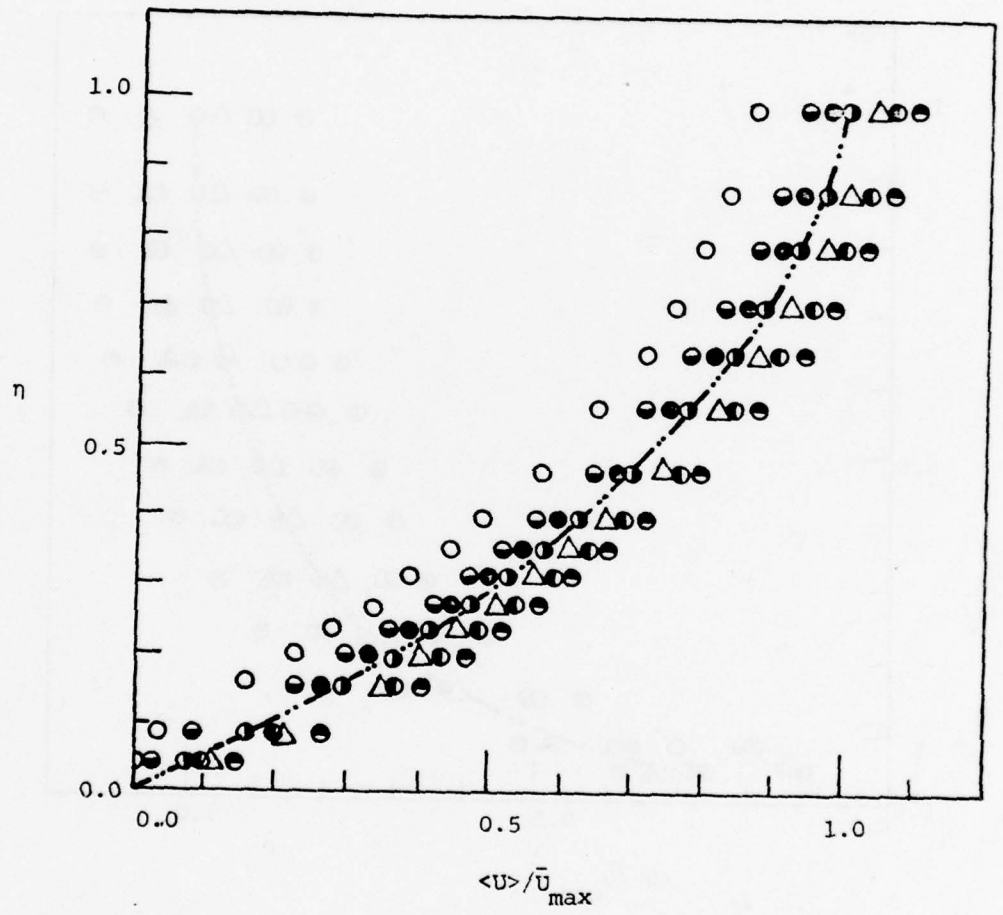

Figure 12(b). Distribution of the ensemble average velocity across the pipe in oscillatory laminarized flow, f=1.75 Hz (Run 23) symbol, phase angle θ(degrees): ⊖, 45°; ◐, 135°; ⊜, 180°; ○, 225°; ●, 315°; △, 360°; —·—○—·— ; time-mean velocity

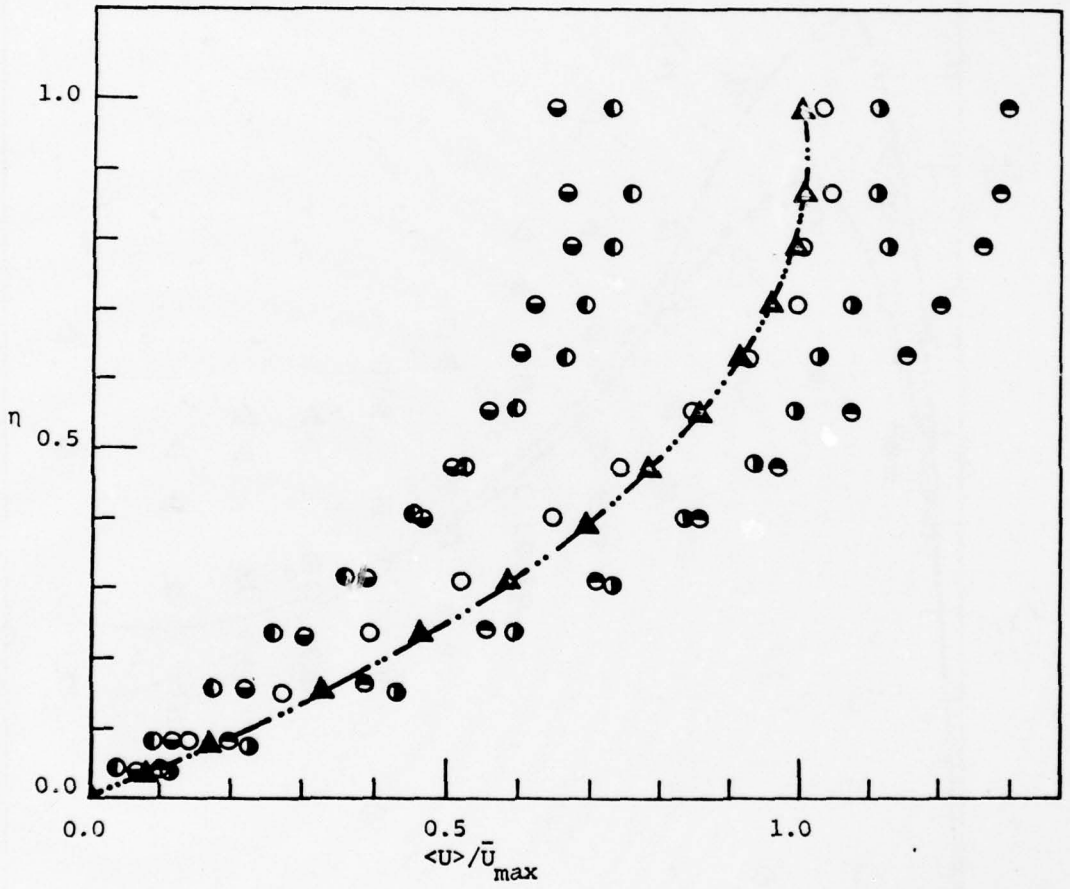

Figure 12(c). Distribution of the ensemble average velocity across the pipe in oscillatory laminarized flow, f=0.057 Hz (Run 24). symbol, phase angle θ(degrees) ◔, 50°; ◑, 100°; ◕, 150°; ●, 200°; ○, 300°; ---▲---, time-mean velocity

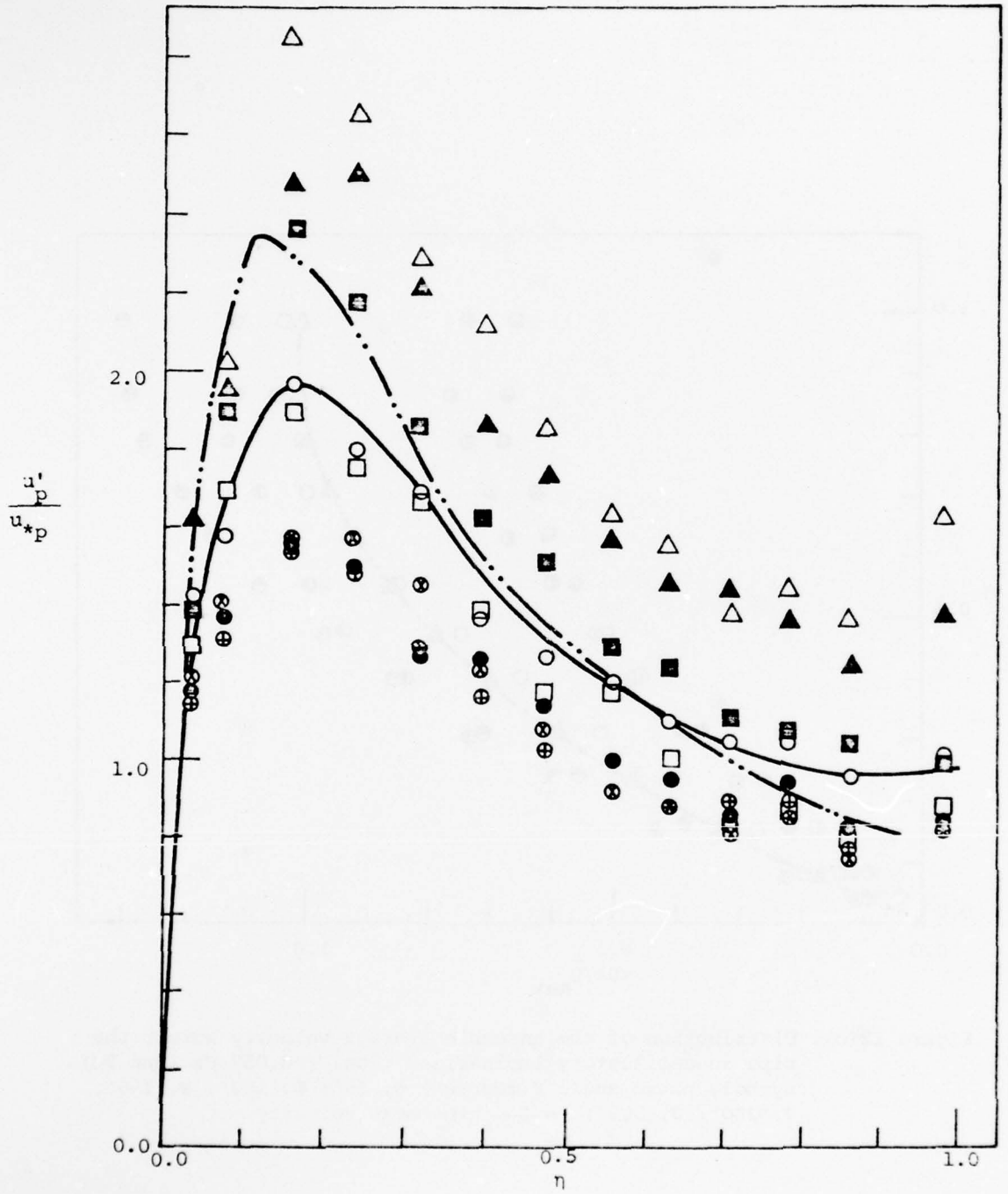

Figure 13. Distribution of the turbulent intensity across the pipe in run 13 (f=1.75 Hz)
——, time averaged turbulent intensity $u'/\bar{u}_*$ in oscillatory flow;
—·—, u'/u_* in quasi-steady flow at $\theta=0°$
Data points denote the ensemble average turbulent intensity u'_p/u_{*p} symbol, phase angle: ⊗, 6°; ⊕, 45°; ●, 90°; ○, 135°; ▲, 180°; △, 225°; ■, 270°; □, 315°

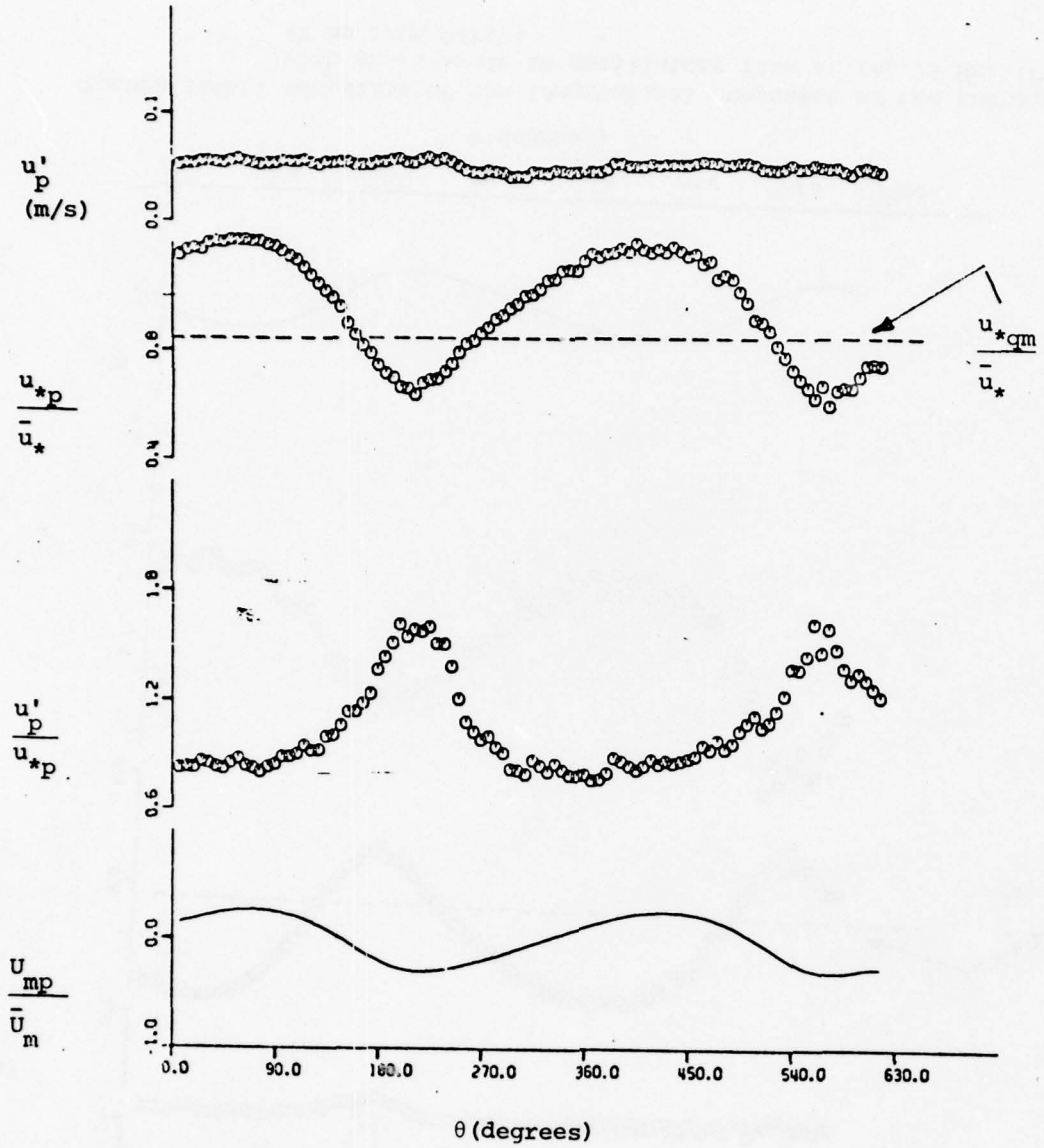

Figure 14 (a). Variation of the longitudinal component of the turbulent velocity with phase angle in oscillatory flow at f=1.75 Hz (r=0)

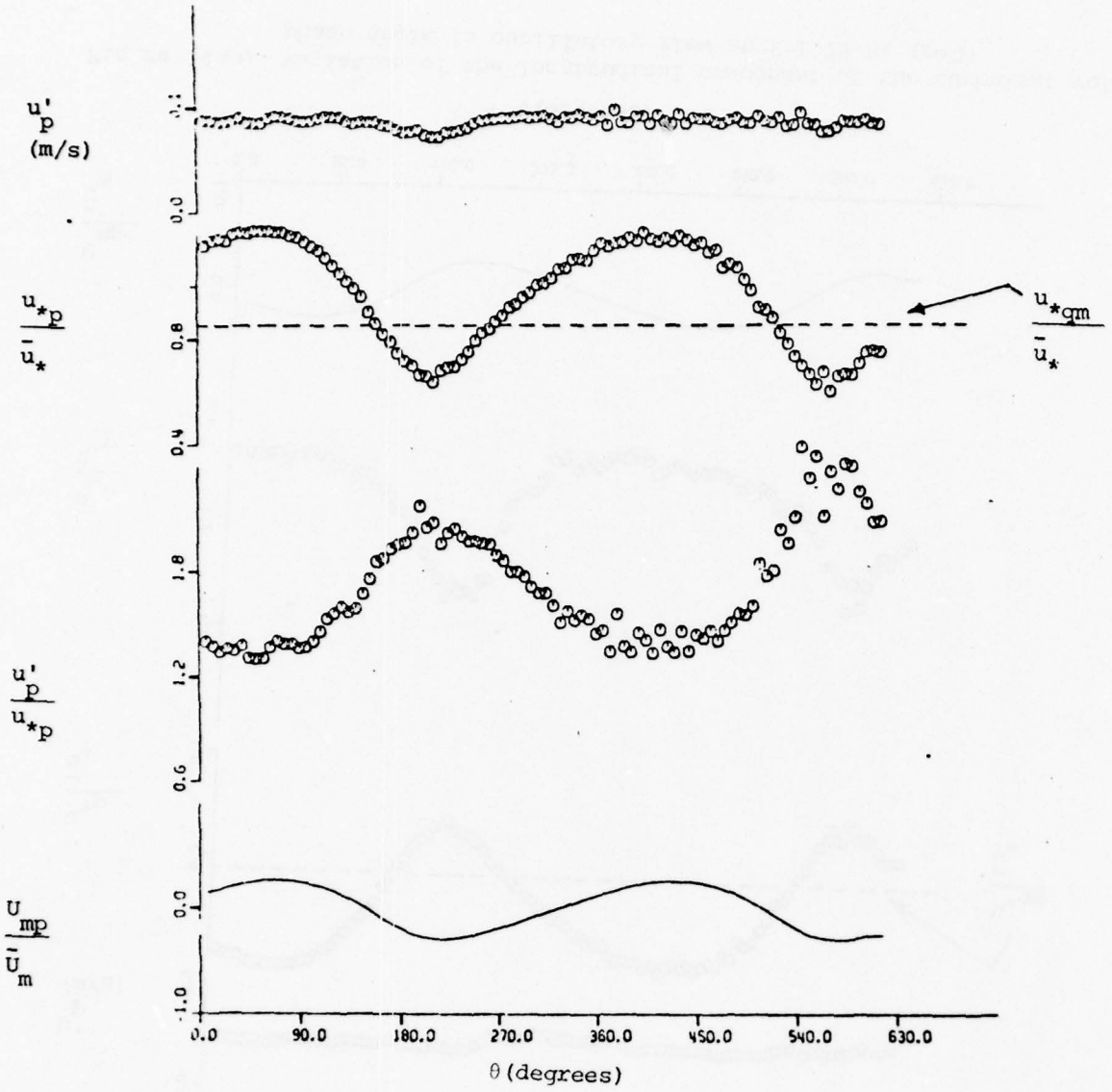

Figure 14(b). Variation of the longitudinal component of the turbulent velocity with phase angle in oscillatory flow at f=1.75 Hz. [r=23.4 mm (2 mm from wall)]

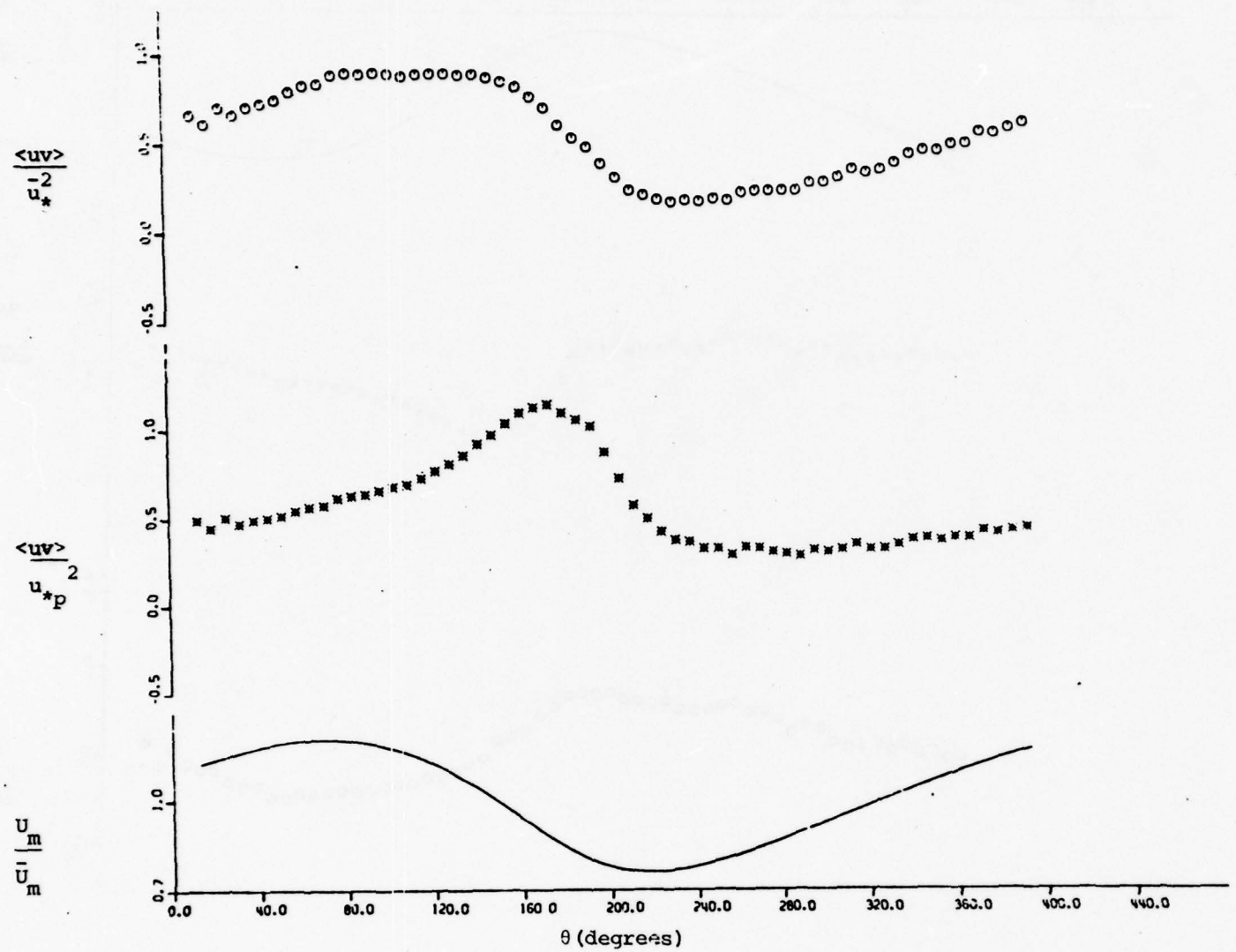

Figure 15(a). Variation of the Reynolds shear stress with phase angle in oscillatory flow. distance: 1 mm from the wall; f=1.75 Hz (Run 13)

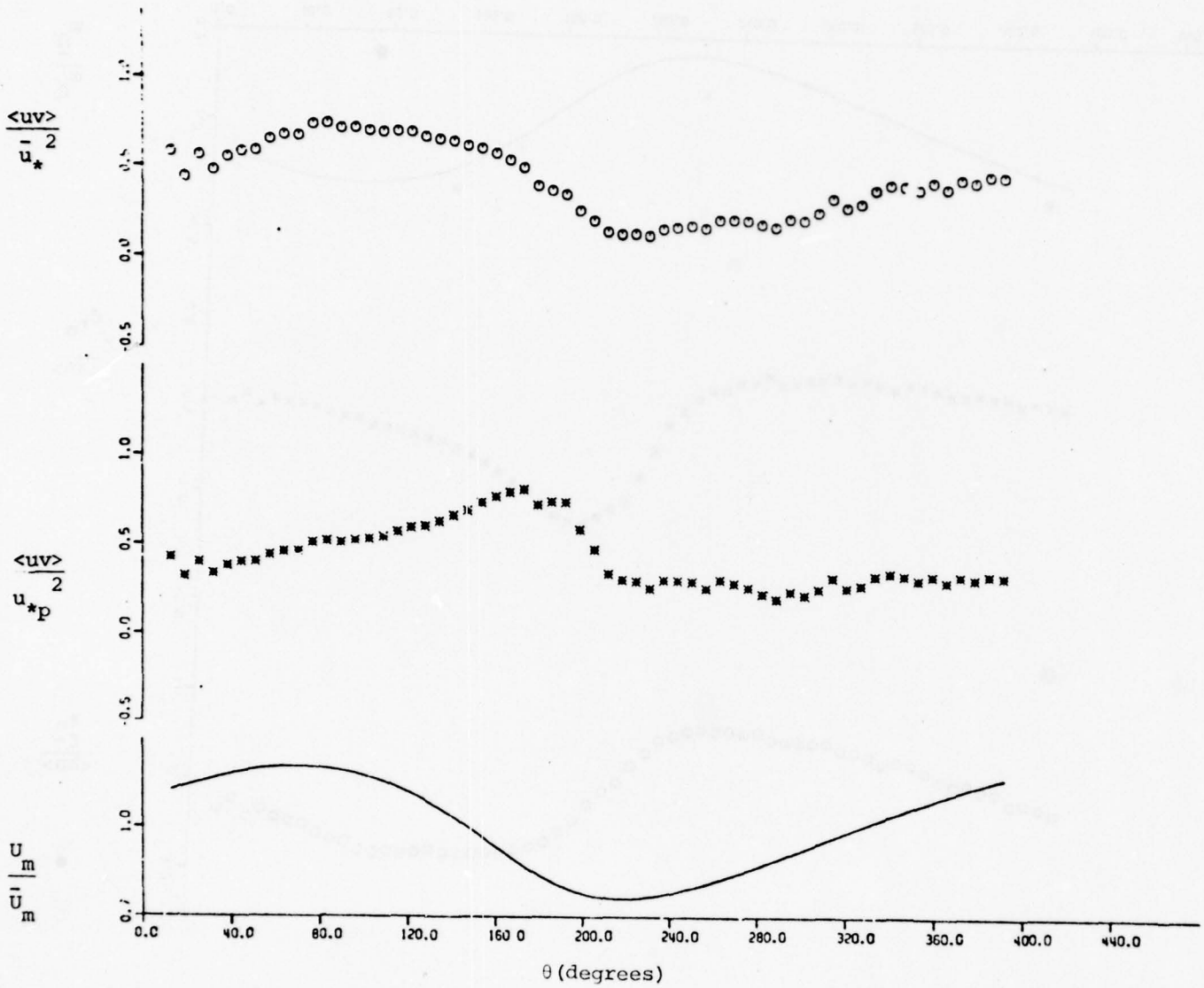

Figure 15(b). Variation of the Reynolds shear stress with phase angle in oscillatory flow. distance: 2 mm from the wall; f=1.75 Hz (Run 13)

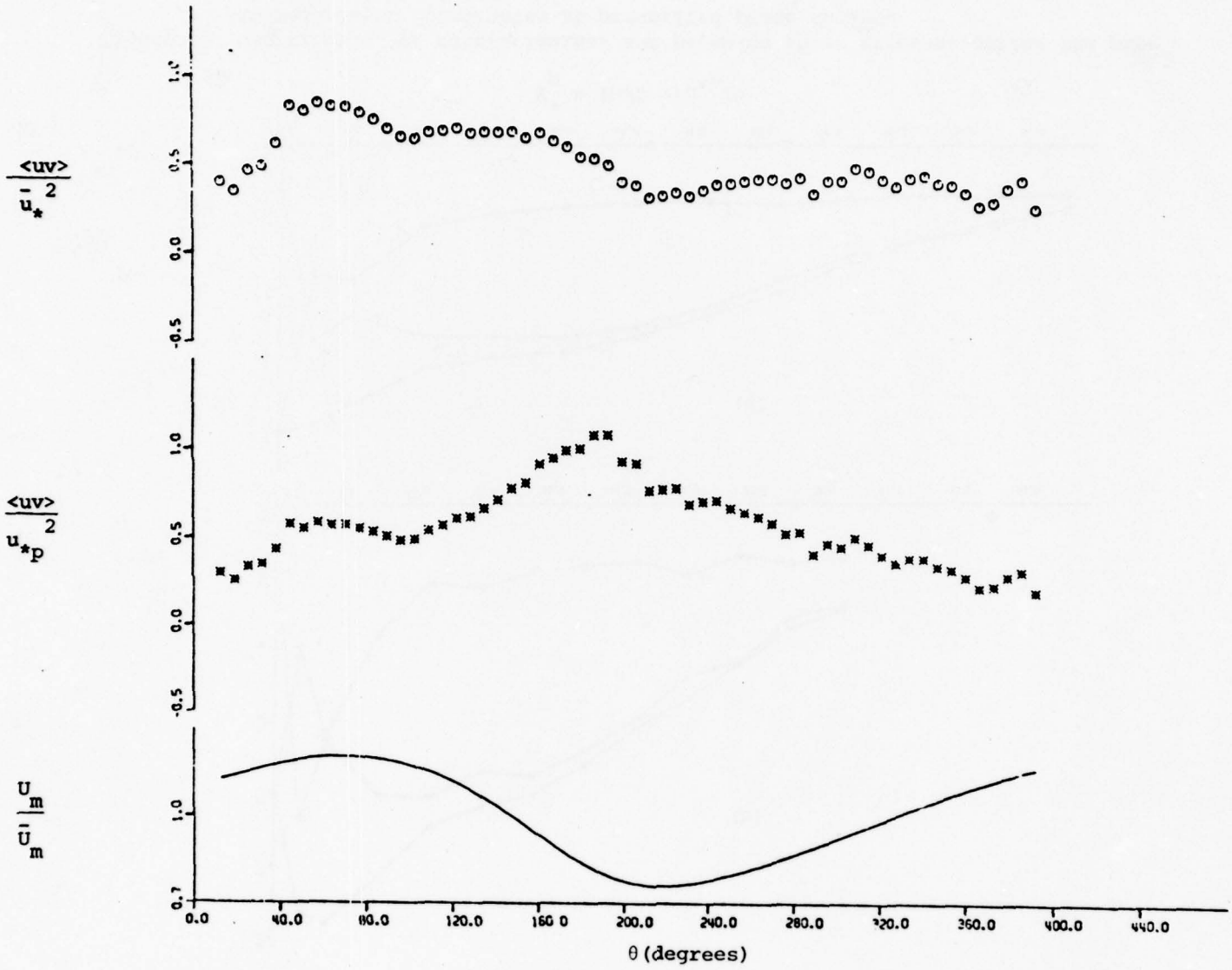

Figure 15(c). Time variation of the Reynolds shear stress with phase angle in oscillatory flow. distance: 10 mm from the wall; f=1.75 Hz (Run 13)

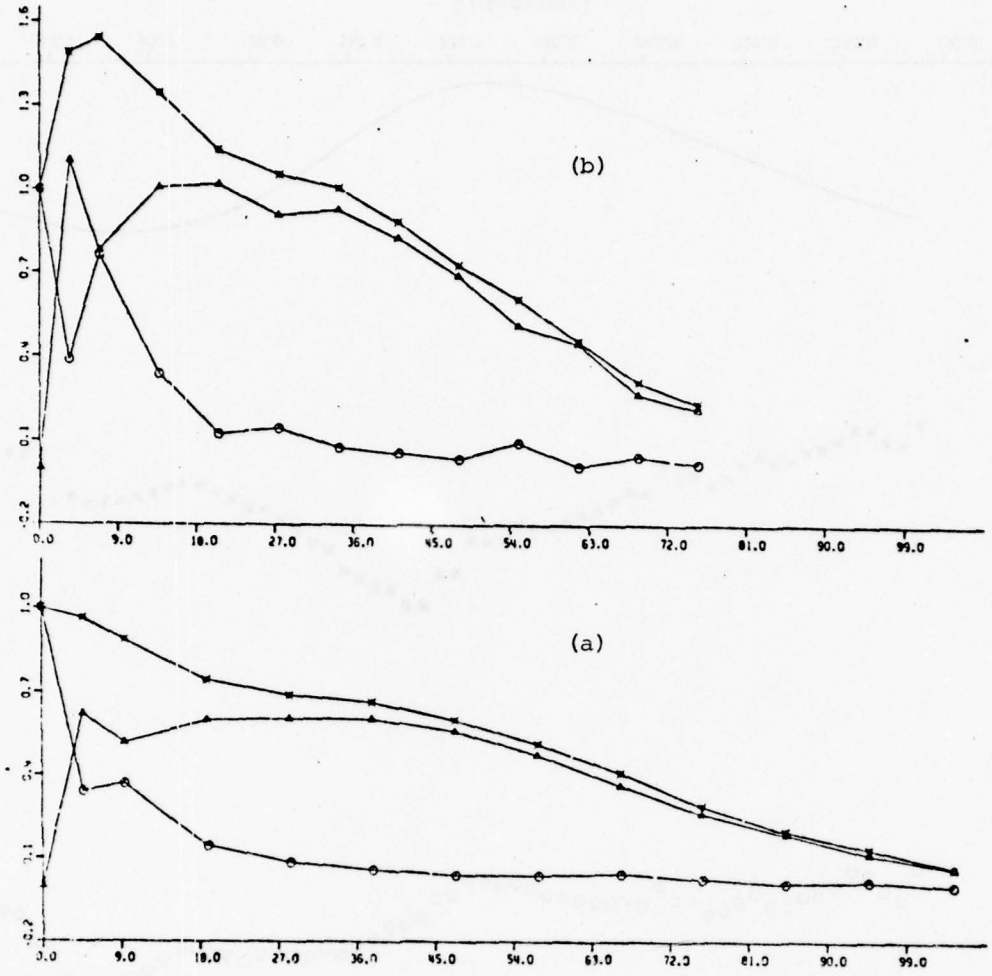

Figure 16. Distribution of total, laminar and Reynolds shear stresses across the pipe in wall-layer coordinates at prescribed phase angles.
(a) $\theta=77°$ (b) $\theta=160°$
—*—, total shear stress; —o—, laminar shear stress; —▲—, Reynolds shear stress. The stresses are normalized with respect to the wall shear stress at the corresponding phase angle.

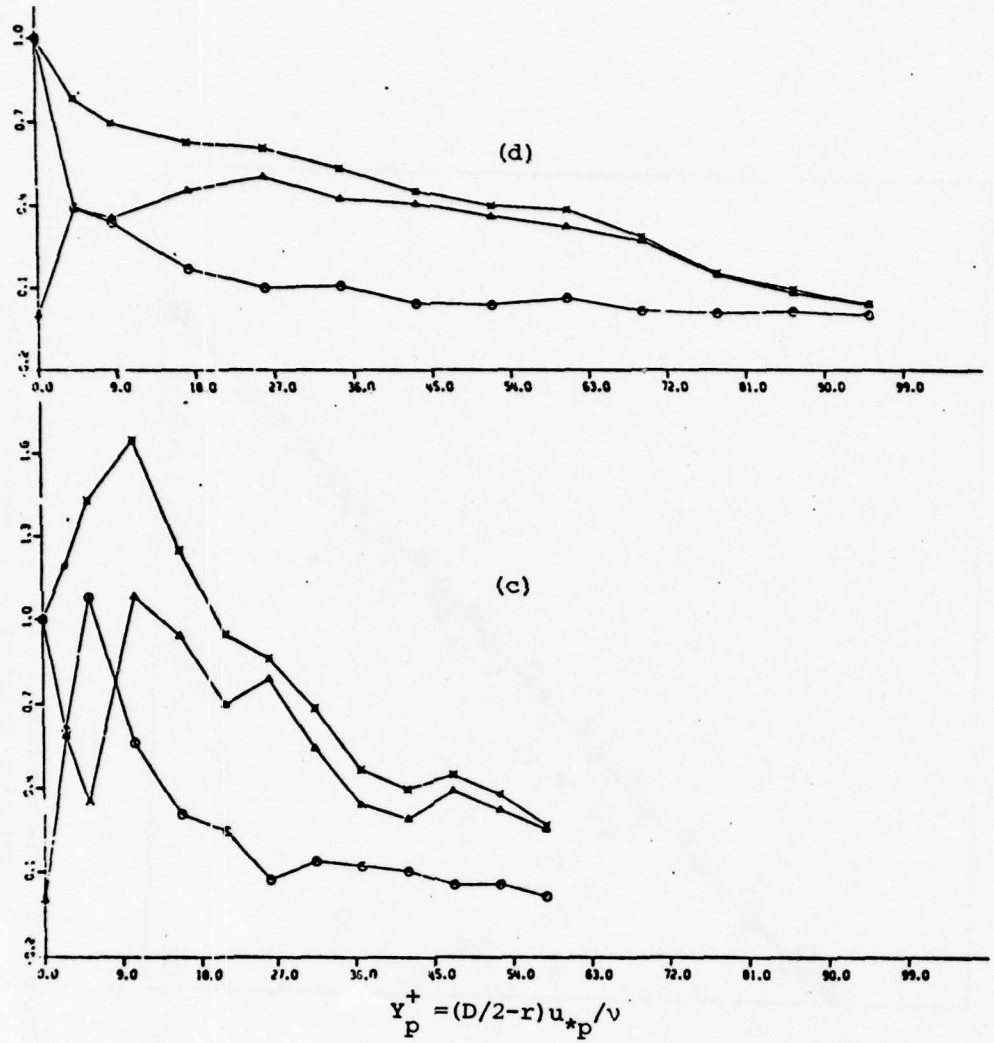

Figure 16. Distribution of total, laminar and Reynolds shear stresses across the pipe in wall-layer coordinates at prescribed phase angles
(c) θ=212° (d) θ=340°
—*—, total shear stress; —0—, laminar shear stress; —▲—, Reynolds shear stress. The stresses are normalized with respect to the wall shear stress at the corresponding phase angle

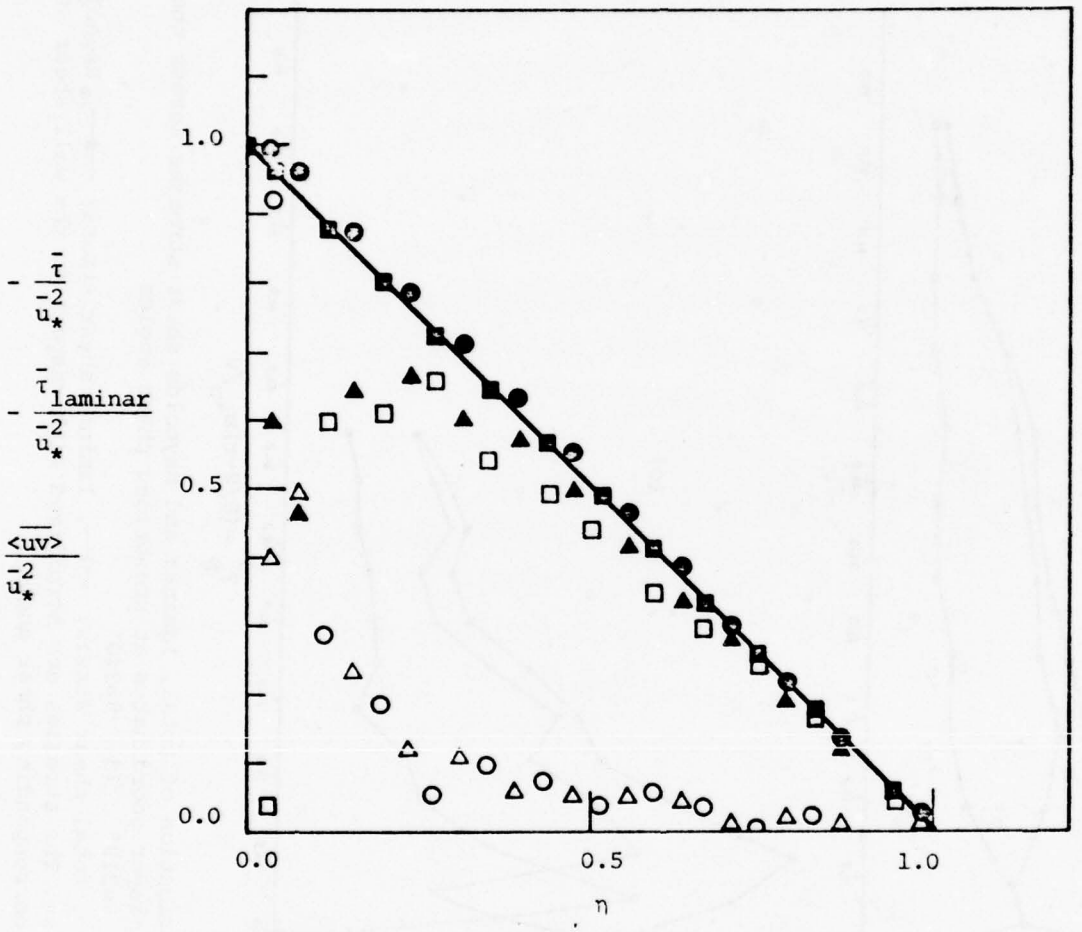

Figure 17. Distribution of the time-averaged total, laminar and Reynolds shear stresses across the pipe.

Steady turbulent flow at a Reynolds number of 2870 (θ=0°)
■ , total shear stress; □ , Reynolds shear stress;
0, laminar shear stress
Unsteady turbulent flow, f=1.75 Hz (Run 13)
●, total shear stress; ▲, Reynolds shear stress;
Δ, laminar shear stress

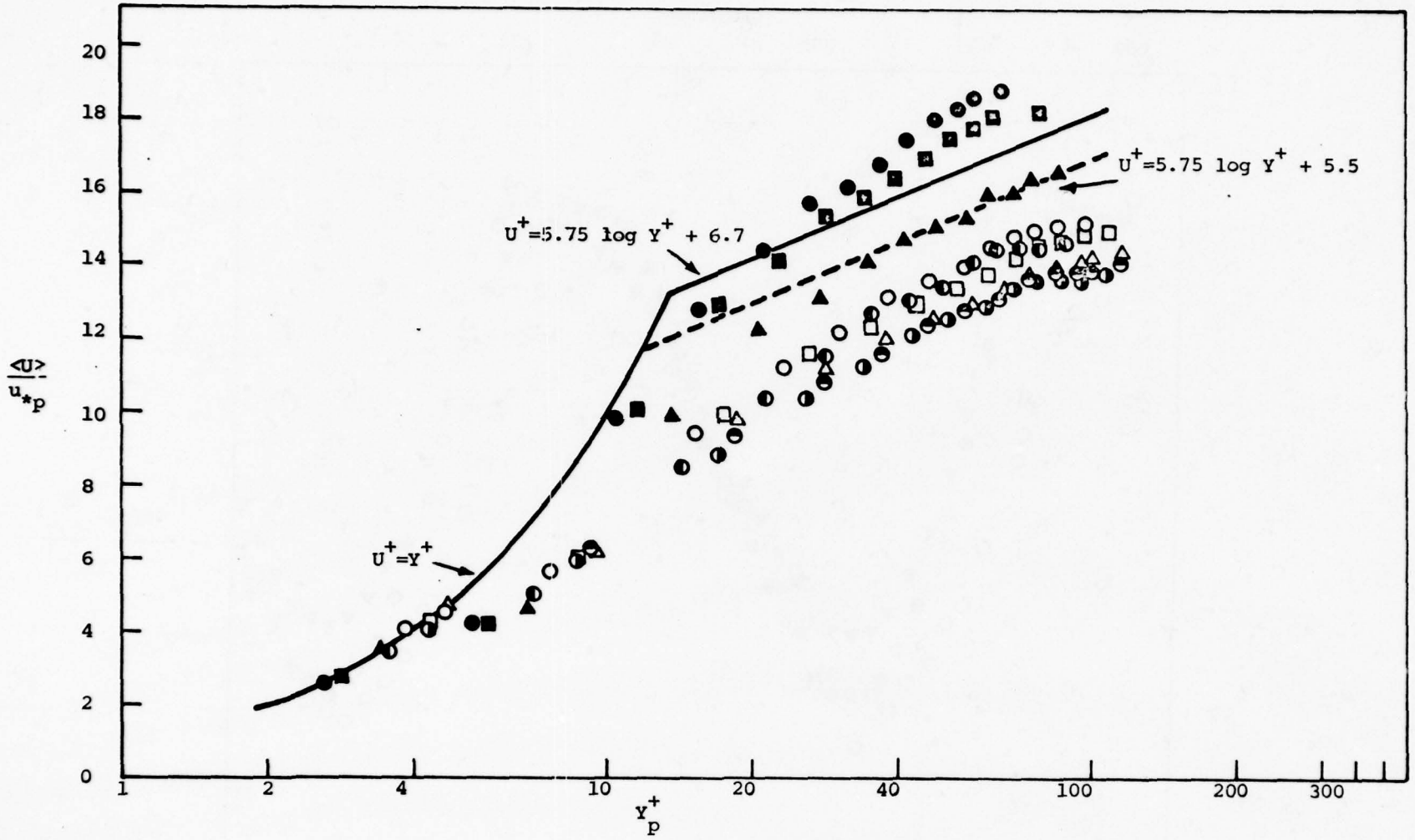

Figure 18. Velocity distribution in unsteady flow in wall-layer coordinates. symbol, phase angle θ(degrees): △, 77°; □, 115°; ▲, 160°; ■, 185°; ●, 212°, ◐, 276°; 0, time-mean distribution $\bar{U}/\bar{u}_*$ Vs $(D/2-r)\bar{u}_*/\nu$; ◑, 340°; ⊖, 385°; ——, steady flow (θ=0°); --- universal log law

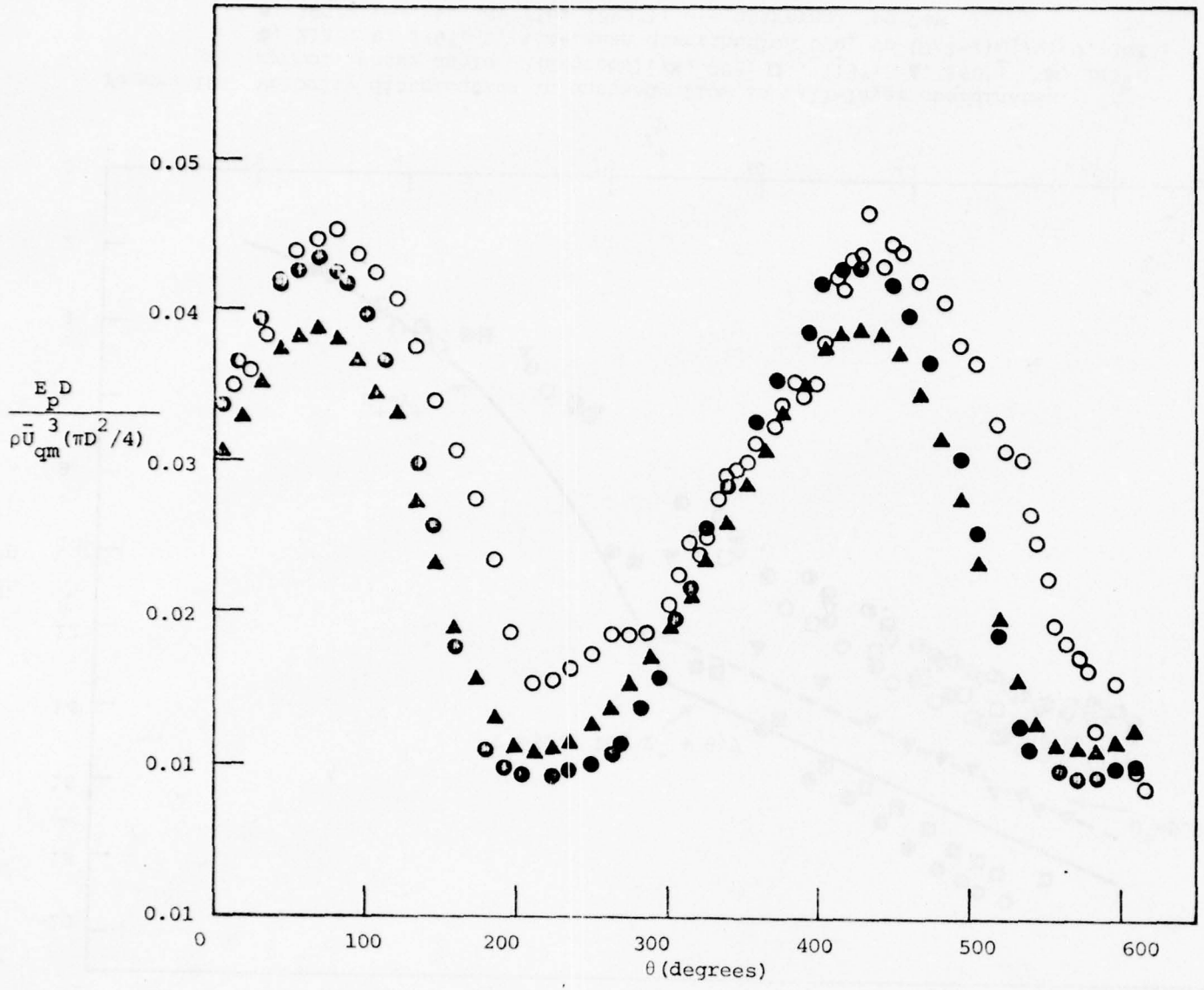

Figure 19. Variation of the rate of shear work with the phase angle. ○, data from unsteady turbulent flow, f=1.75 Hz (Run 13); ▲, based on quasi-steady Blasius relation, $\lambda = 0.3165\ Re^{-\frac{1}{4}}$; ●, based on quasi-steady pressure drop measurements in actual transitional flow

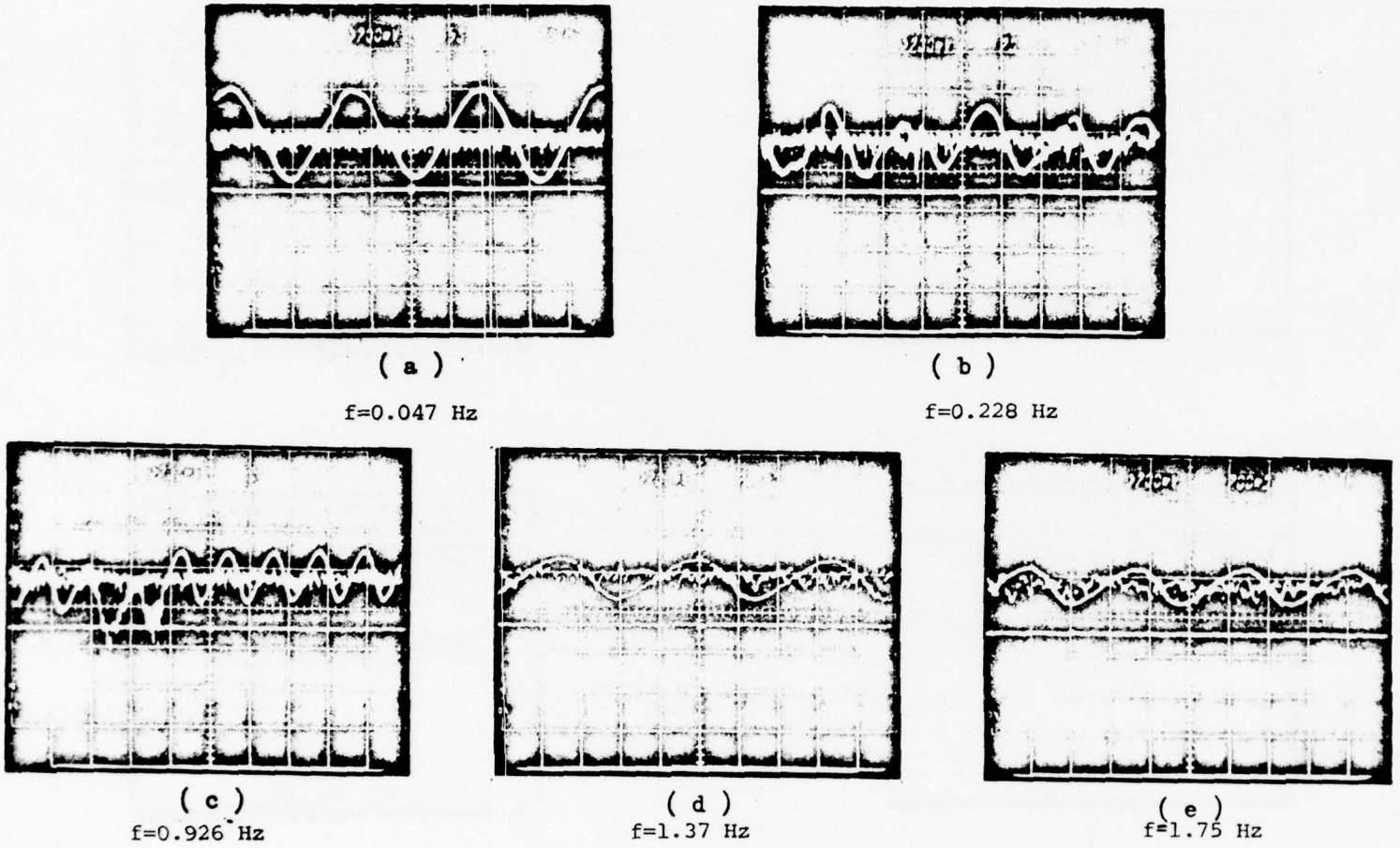

Figure 20. Oscilloscope traces of velocity signals from LDA from experiment series 2. r=0

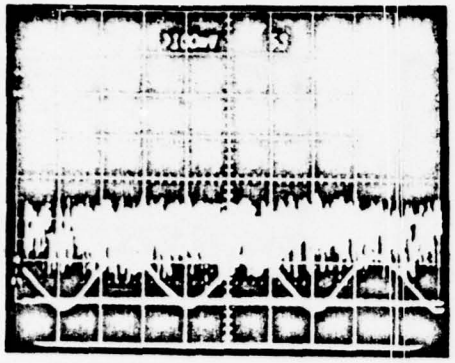

(a)
f=0.047 Hz

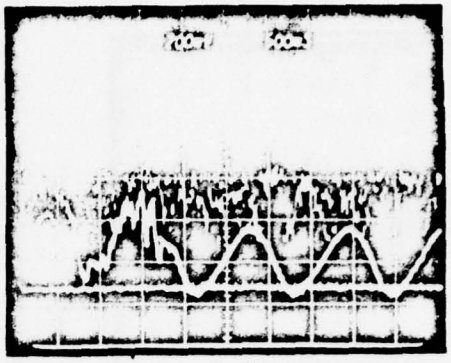

(b)
f= 0.926 Hz

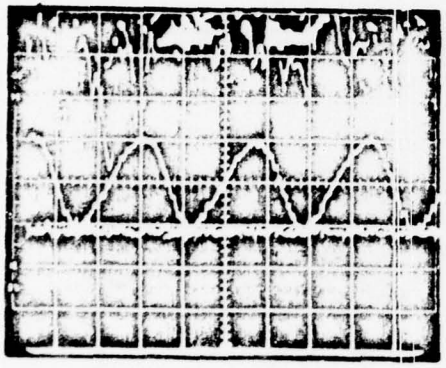

(c)
f=1.37 Hz

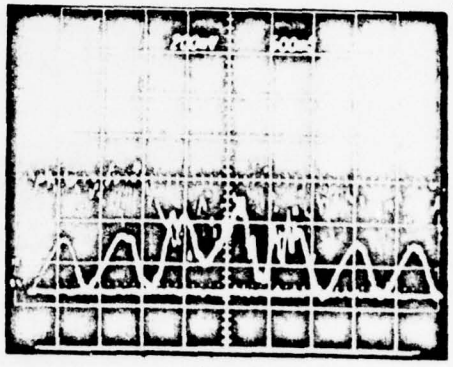

(d)
f=1.75 Hz

Figure 20. Oscilloscope traces of velocity signals from LDA from experiment series 2. r=18.4 mm

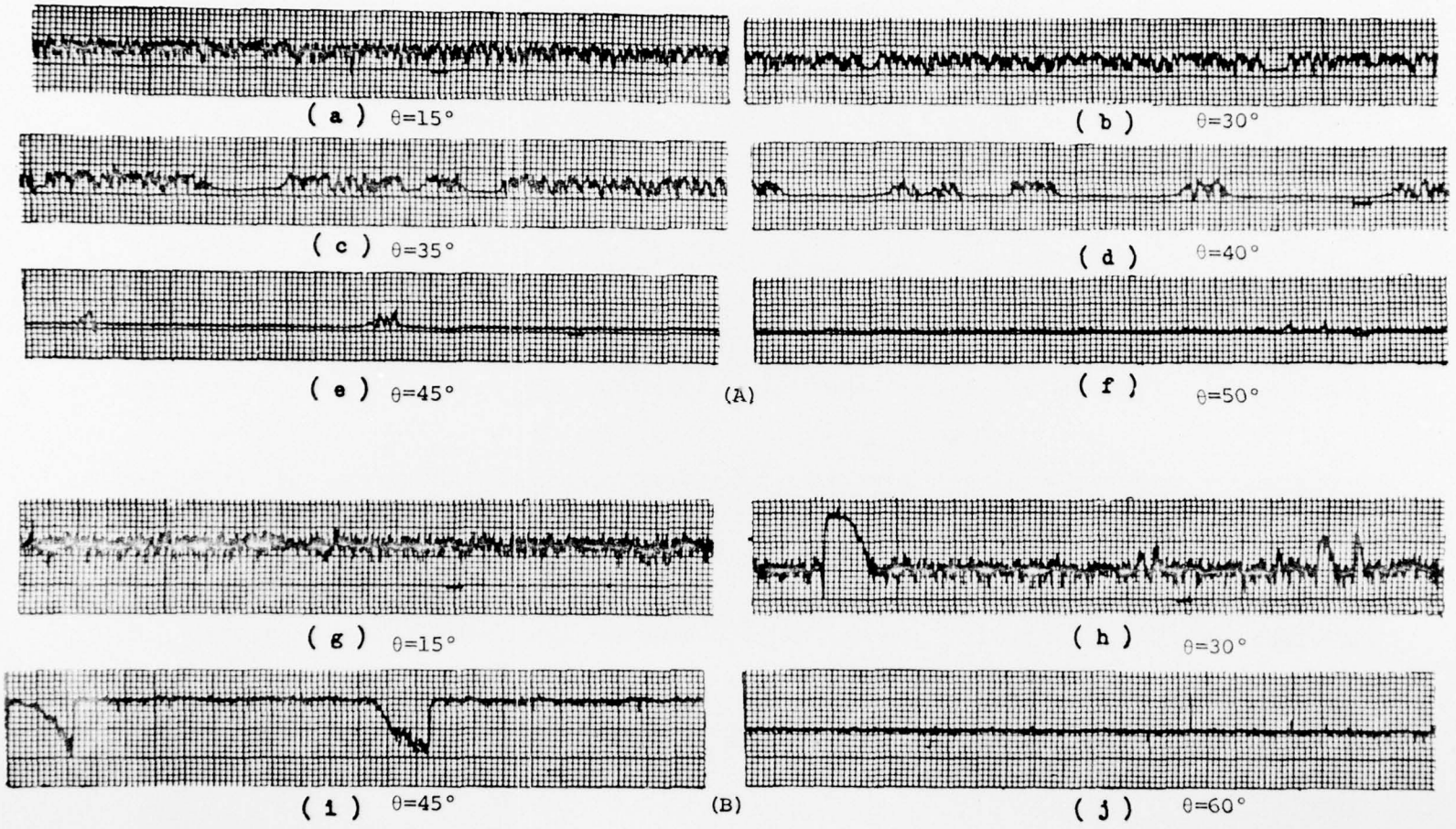

Figure 21. Typical strip chart records of the LDA output signal in steady flow from experimental series 2
(A) r=18.4 mm (B) r=0

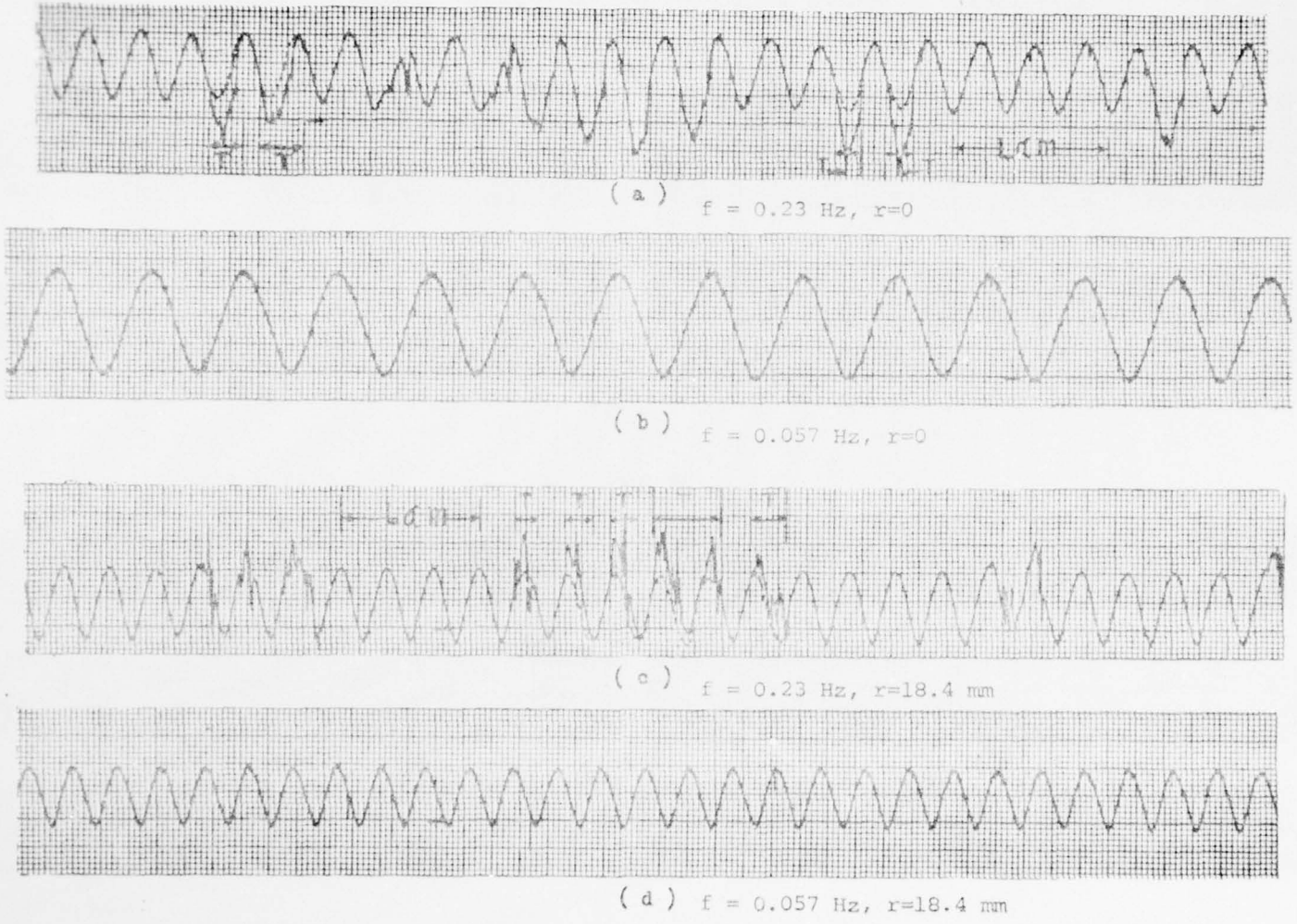

Figure 22. Typical strip chart records of the LDA output signal in oscillatory flow from experiment series 2.
Intervals marked T denotes periods when the velocity trace is distorted from the normal laminar shape (shown by dotted lines) and are hence assumed to represent dutations of turbulent puffs

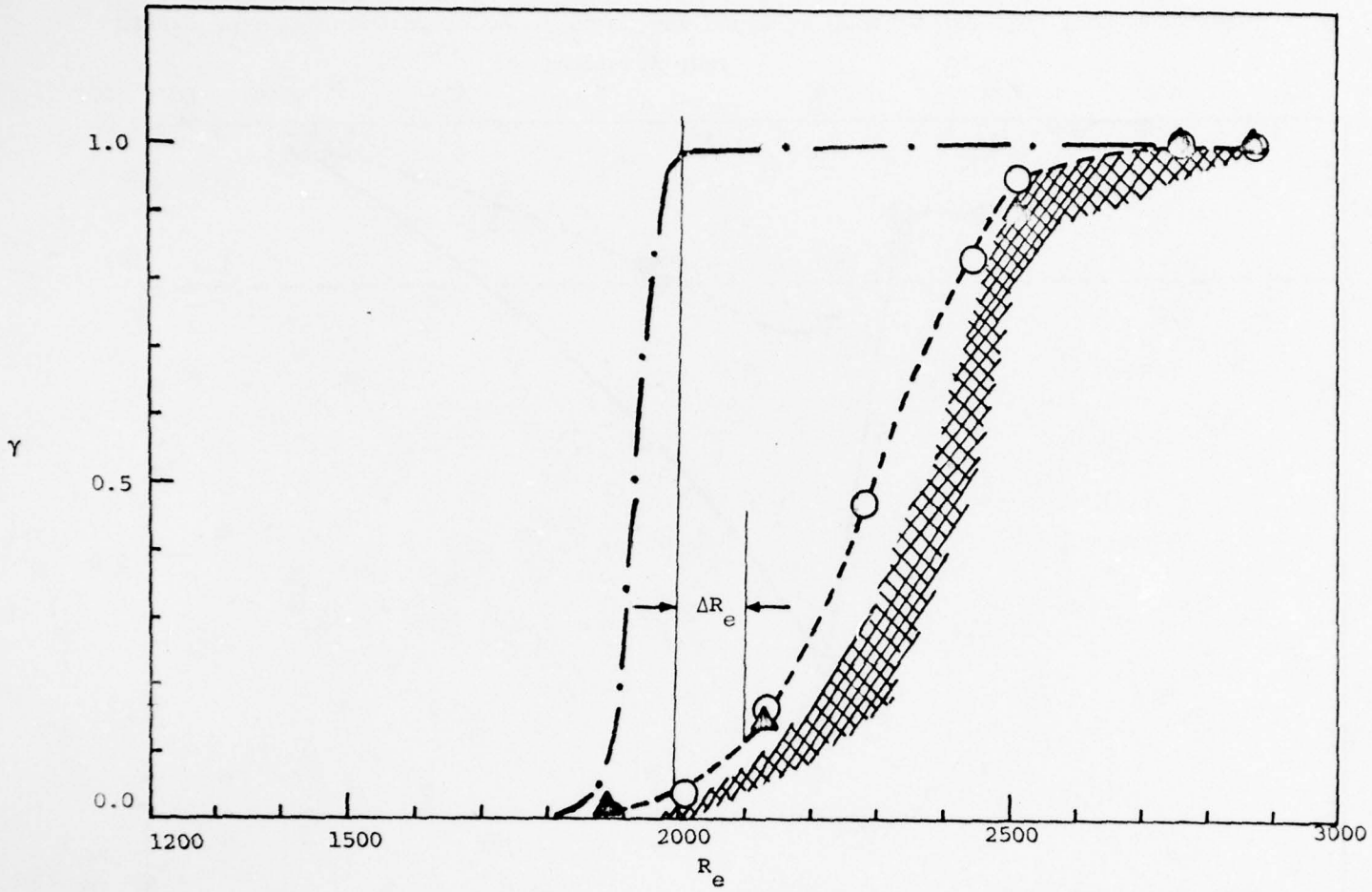

Figure 23. The intermittency of turbulent puffs in steady flow. Data from present series 2 experiments: --▲--, r =0; --0--, r =18.4 mm. —·—, (estimated) intermittency data for steady flow experiments of series 1; ▨, data of Wygnanski and Champagne (1973)

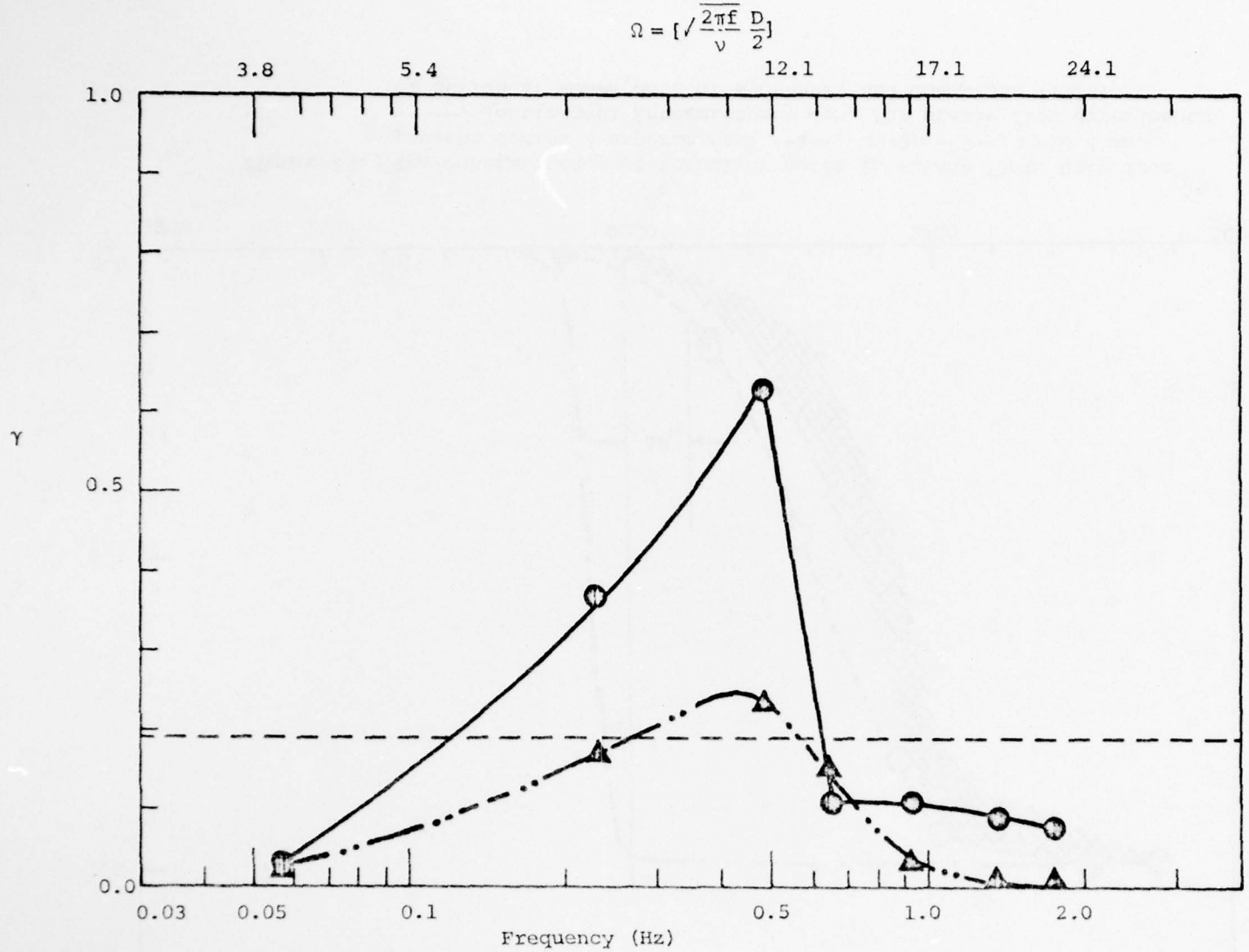

Figure 24. The intermittency of turbulent puffs in oscillatory flow from experiment series 2.
—●—, r=0mm; -·-△-·-, r=18.4 mm; -----, mean quasi-steady flow at Re=2100 (θ=90°)

APPENDIX A

Description of the LDA System at IIHR and sample calculations of velocity from LDA signals

Description of the IIHR LDA System

A. The LDA System

The simple channel LDA system at IIHR is shown schematically in figure A.1. The system consists of a SPECTRAPHYSICS 5 mw He-Ne laser, ill'minating TSI (Thermo System Inc.) optics. The optics consists of a beam splitter which splits the laser beam into two beams each of half the original strength and spaced 50 mm apart. Each of the beams is then passed through an accousto-optic Bragg cell which shifts the frequency of the laser light by a preset amount. The Bragg-cells and the associated electronics were supplied by Opto-Elektronische-Instrumente. It's possible to shift the frequency of each beam independently by 7 selectable discrete frequencies ranging from 38.0 MHz to 44.0 MHz. By shifting the two beams by different frequencies one can obtain a relative frequency shift between the two outcoming beams. In the present case, a relative frequency shift of 0.3 MHz was used. The dual beams from the Bragg cells are focussed by the focussing lens of 104.1 mm focal length at the point (in reality, a finite sampling volume) in the fluid where the velocity is to be measured. The light scattered by a particle which passes through this volume is picked up by the receiving optics shown in the figure. The receiving optics consists of a pair of lenses and a prism that focusses the scattered light on to a photodiode. The photodiode converts the optical signal to an electrical signal which is then amplified.

In this particular arrangement, known as the dual beam system, the scattered light is essentially a mixture of the light scattered by the particle from the two incident beams. Let ν_o be the original laser beam frequency, ν_{B1} and ν_{B2} be the frequency shifts caused by the Bragg cell on the two incident beams, $\vec{n}_{i1}$ and $\vec{n}_{i2}$, the unit vectors in the directions of the incident beams, $\vec{r}$ the unit vector in the direction of collection (see figure A-1). Then, for an idealized case of scattering occurring due to a single particle travelling with a velocity $\vec{V}$ as shown, assuming uniform plane waves, one can write

$$\nu_1 = \nu_o + \nu_{B1} + \{\vec{V} \cdot \frac{\vec{r} - \vec{n}_{i1}}{\lambda_L}\} \qquad (A.1)$$

$$\nu_2 = \nu_o + \nu_{B2} + \{\vec{V}\cdot\frac{\vec{r}-\vec{n}_{i2}}{\lambda_L}\} \qquad (A.2)$$

where ν_1 and ν_2 are the frequencies of scattered light from the two beams, and the bracketed terms represent the Doppler shift frequency in each case. The light picked up by the photodiode is a mixture of the above two. From the principle of hetrodyning, it can be shown that the resulting light will contain the mixture of the sum and difference of the above two frequencies. Of these, the difference equal to

$$(\nu_{B1} - \nu_{B2}) + \vec{V}\cdot[\frac{\vec{n}_{i2}-\vec{n}_{i1}}{\lambda_L}] \qquad (A.3)$$

is the frequency of interest. This frequency is detected in the output signal by a frequency tracker. A TSI model 1090 tracker is used for this purpose. The tracker output, which is a linear function of the instantaneous velocity of the flow is low-pass filtered at 150 Hz to remove unwanted noise and then connected to the IIHR Data Acquisition System. The low-pass filtering frequency of 150 Hz was found to be high enough to include all significant turbulent frequencies in the flow. It is seen from Eq. A.3 that the output signal frequency is independent of the collection direction $\vec{r}$ (through the intensity of the collected light does depend on $\vec{r}$). It is also seen that at zero velocity, the output frequency will be $\nu_{B1} - \nu_{B2}$ i.e., equal to the imposed relative frequency shift.

It is appropriate to mention here briefly some of the problems encountered in LDA measurements. One of them, viz., directional ambiguity has been overcome in the present studies by using frequency shifting technique. Secondly, particle size and distribution introduce complexities, not encountered in the simple single particle analysis. The particle size influences scattered light distribution and intensity, the ability of a particle to follow the flow and the signal to noise ratio. Also, the higher the particle concentration, the more will be the background noise due to phase differences between particles arriving at the sampling volume. Low particle concentrations, on the other hand, limit the velocity versus time information as well as generally increase the complexity of data processing

due to discontinuity in the data, or "signal drop out". Signal drop out can also be caused by large variations in velocity with time as can occur in highly turbulent flows, very low velocities and in oscillatory flows. In these cases, the accompanying frequency changes are too large to be tracked by the tracker. The use of frequency shifting, in fact, has the added advantage of bringing the range of frequency variations into the most efficient region of tracker operation. Ideally, the particles should have a high refractive index, be uniform in size, and be as large as possible (up to 5μ) while still following the flow. The concentration should be low enough to minimize Doppler ambiguity while high enough to obtain adequate time information on flow characteristics. To approach this ideal seeding is generally required. However, naturally occurring particulates in the fluid may often be adequate to give satisfactory results, as in the present study. Thirdly, the spatial resolution of LDA is limited by the requirement of a finite sampling volume. With reference to figure A-1 the dimensions L_m and D_m of the sampling volume depend on the intersection angle ϕ of the beams in the fluid and the diameter of the beam. In the present experiments the dimensions L_m and D_m are 1.1 mm and 0.7 mm respectively. The dimension L_m is very much larger than the diameter of a hot-wire (2.5 μm) but comparable to the diameter of a total head tube. It is, however, to be noted that since oil was used in the present studies, the dimension L_m is still less than the thickness ($\gtrsim$1.5 mm) of the viscous sublayer. The calculations required for obtaining the value of velocity from the LDA output are described in Appendix B.

B. The Traverse Mechanism for LDA

A simple one dimensional traverse mechanism was built for traversing the LDA optics along a horizontal diameter of the test section. The construction of this traverse can be seen from figure A-2. The upper alluminium channel slides over the bottom alluminium channel. The latter rests on a mild steel framework and can be adjusted to be level by using the four levelling screws. The upper channel is moved longitudinally by a spindle and has a travel of 50 mm. A dial indicator of 0.01 mm least count is mounted in such a way as to measure the displacement of

the upper channel. The laser, the entire optics and the photodiode are all mounted on wooden bases fixed to the upper alluminium channel and thus move together as one unit.

Because of the refraction effect, through the tube wall and the liquid, the actual displacement of the focal point (sampling volume) is not equal to the physical displacement of the traverse (apparent displacement). Knowing the thickness of the pipe wall and the refractive indices of the pipe wall and the oil, one can calculate the actual displacement of the focal point for a given apparent displacement. It was, however, felt that a practical calibration would be more desirable, as well as concenient, in the present case. A temporary arrangement consisting of an L-shaped point gage traversed by a precision micrometer (0.025 mm least count) was used for this purpose. The point gage was traversed through a hole in the tube wall, located at such a position that the tip of the gage travelled along the LDA axis. The location of the focal point could be easily determined from observing the light scattered by the tip of the gage as it moved along the axis of the LDA. The focal point was given a series of prescribed apparent displacements as measured by the dial indicator and the corresponding actual displacements as measured by the micrometer were obtained. The resulting calibration curve is shown in A.3 and is seen to be linear (as expected). This result was used in all subsequent experiments to obtain the actual displacement of the focal point. Theoretically, the uncertainty involved in the calibration was equal to the dimension "L_m" of the sampling volume. In practice, however, it was much less than this since it was possible to locate the two "extremes" of this region and set the point gage at the middle of these two positions. The finite length of the sampling volume did present some difficulty in fixing the "zero" distance from the wall during the velocity traverses. This difficulty was overcome by matching the velocity profile in steady laminar flow with the theoretical parabolic distribution. The "zero" so determined was used for the turbulent flow traverse also. In the unsteady flow, the location of the "zero" position was taken to be the point at which the oscillation amplitude (as observed on the oscilloscope) would suddenly go to zero. This was a very well defined point and could be located with

excellent repeatability.

C. Sample Calculation of Velocity from the LDA Signal

If f_D is the Doppler frequency shift, from Eq. (A.3)

$$f_D = \frac{n\vec{V}}{\lambda_L} \cdot (\vec{n}_{i1} - \vec{n}_{i2})$$

From Fig. A.1 $|\vec{n}_{i2} - \vec{n}_{i1}| = 2 \sin \phi/2$

hence, $f_D = \frac{n\vec{V}}{\lambda_L} \cdot \vec{n}_{i2} - \vec{n}_{i1} = 2 \frac{nU}{\lambda_L} \sin \phi/2$

where U is the velocity component normal to the bisector of $\vec{n}_{i1}$ and $\vec{n}_{i2}$. The value of n is taken as unity in air and the angle as $\tan^{-1}$ (d/2L,) where d is the original beam spacing introduced by the beam splitter and L is the focal length of the focussing lens. It can be easily shown that even when the beams pass through media of different refractive indices (in the present experiment, for example, they pass through the plexiglass tube wall and then through the oil), the produce (n · sin $\phi/2$) can still be calculated using the above values for n and ϕ. Hence Eq. (A.3) can be written as

$$f_D = \frac{2U \sin [\text{Tan}^{-1} (d/2L)]}{\lambda_L}$$

or

$$U = f_D \left[\frac{\lambda_L}{2 \sin [\tan^{-1}(d/2L)}\right] = K f_D$$

For the present LDA system, λ_L = 632.8 nm, L = 104.1 mm and d = 50 mm. Hence,

$$K = 1.313 \text{ m/s/MHz}$$

If the relative frequency shift introduced by the Bragg cells is f_s and the measured frequency is f_m

$$U = (f_m - f_s) K$$

As already mentioned, the value of f_s in the present experiments was 0.3 Hz. The tracker output voltage E is proportional to f_m or $E = cf_m$. Hence,

$$U = (\frac{E}{C} - f_s)K \quad (E - Cf_s) \frac{K}{C} = \frac{(E-E_o) K}{C}$$

where E_o is the tracker output voltage at zero velocity. In he present experiments c was 1 volt/MHz ± 0.4%. Thus,

$$U = (E - 0.3) \times 1.313 \text{ m/s}$$

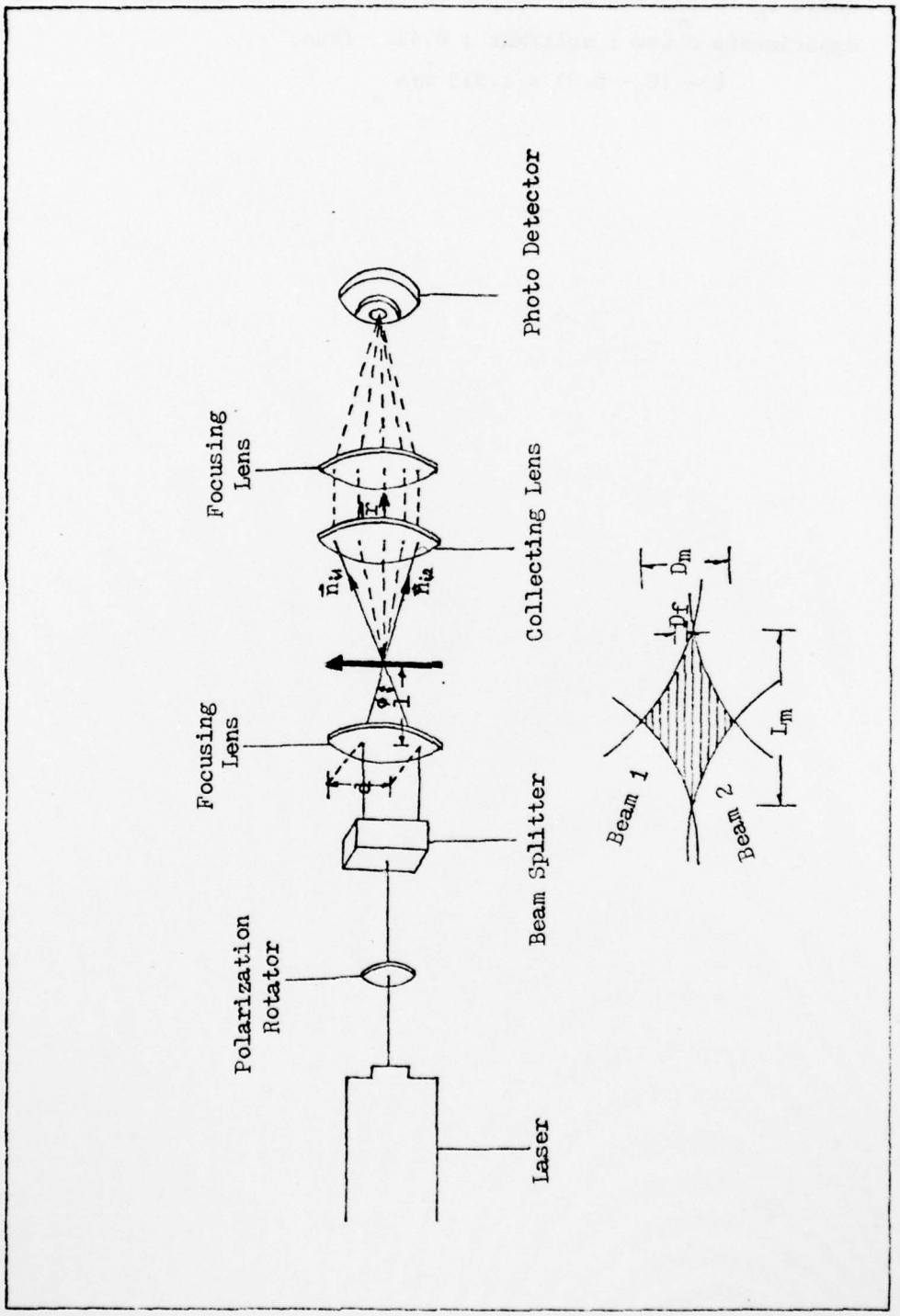

FIG. A1. A DESCRIPTION OF THE IIHR LDA IN DUAL BEAM, FORWARD SCATTER MODE

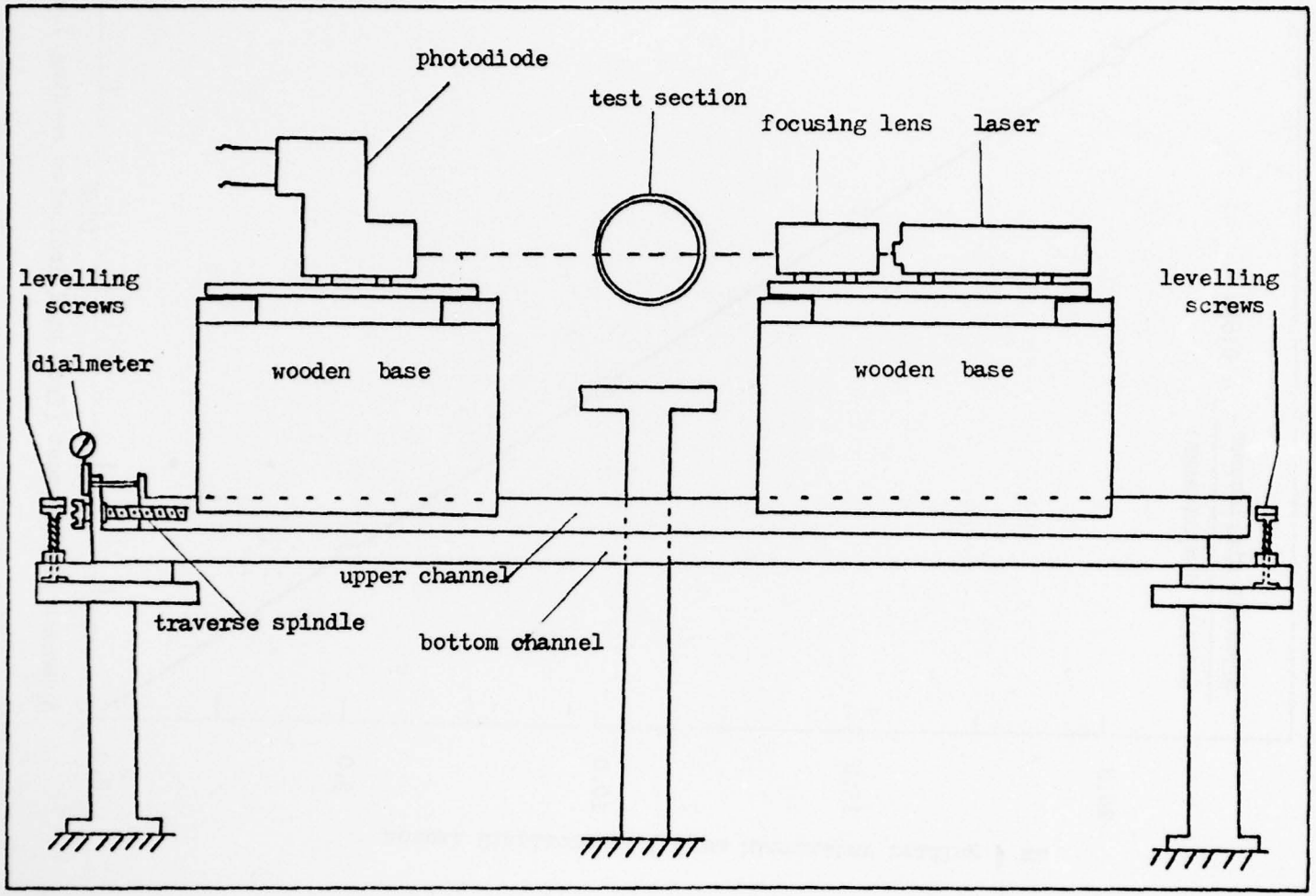

FIG. A2. DETAILS OF THE LDA TRAVERSE

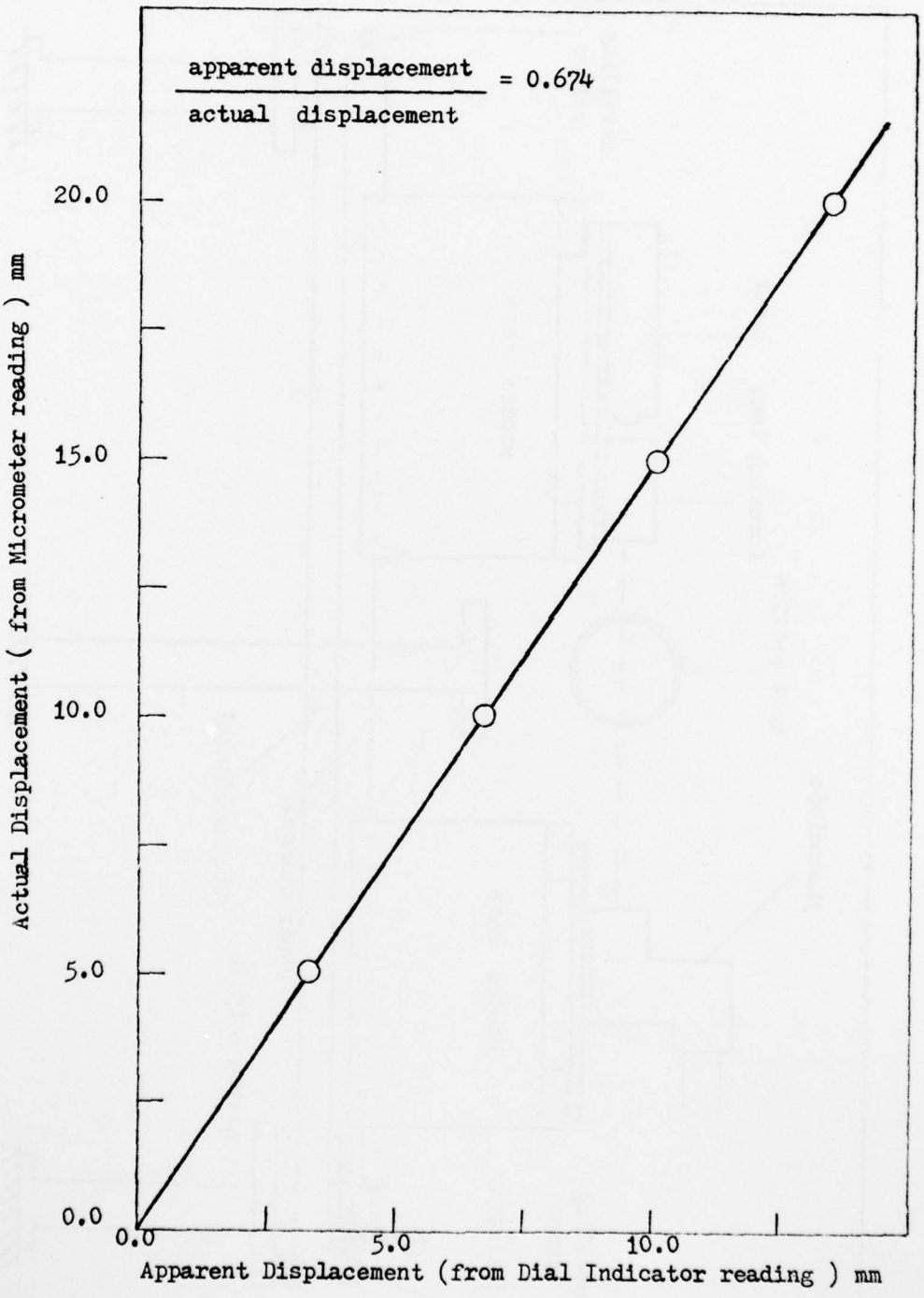

FIG. A3. CALIBRATION OF THE LDA TRAVERSE

APPENDIX B

Experimental Data

AD-A081 180 IOWA INST OF HYDRAULIC RESEARCH IOWA CITY F/G 20/4
EXPERIMENTS ON TRANSITIONAL OSCILLATORY PIPE FLOW,(U)
AUG 79 B R RAMAPRIAN, S W TU DAAG-29-79-G-0017
UNCLASSIFIED IIHR-221 NL

2 OF 2
AD
A081180

END
DATE
FILMED
3-80
DDC

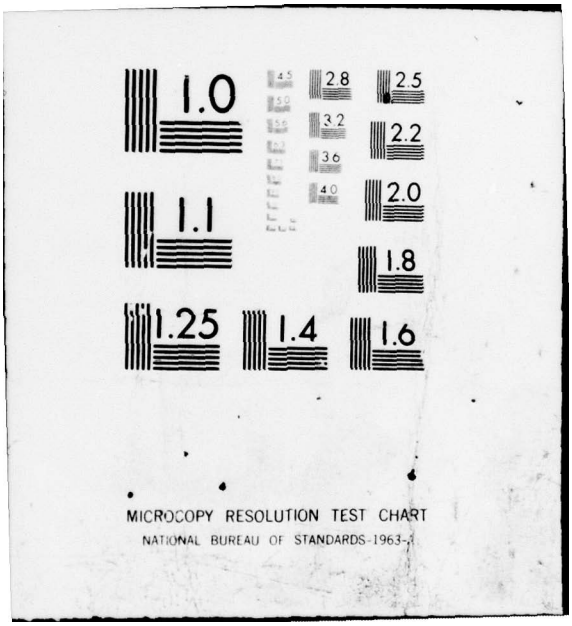
1.0
1.1
1.25
1.4
1.6
1.8
2.0
2.2
2.5
2.8
3.2
3.6
4.0
4.5
5.0
5.6
MICROCOPY RESOLUTION TEST CHART
NATIONAL BUREAU OF STANDARDS-1963-A

TABLE 1.

STEADY PRESSURE DROP

$\nu = 1.384 \times 10^{-5}$ m^2/s

Re / x/D, Δp^*	2872	2760	2513	2132	1818	1402	1278
6	0.0	0.0	0.0	0.0	0.0	0.0	0.0
12	0.561	0.458	0.475	0.589	0.687	1.506	0.941
24	-	1.479	1.989	1.267	1.153	1.442	-
36	1.415	1.532	1.617	1.624	1.914	2.266	2.578
42	1.553	-	-	-	-	-	2.874
48	-	2.022	2.144	2.302	2.552	2.844	3.171
54	2.033	-	-	-	-	-	3.567
60	-	2.628	2.618	2.819	3.018	3.339	3.915
66	2.575	-	-	-	-	-	4.262
72	-	3.246	3.093	3.336	3.558	3.874	4.608
78	3.184	-	-	-	-	-	4.956
84	-	3.788	3.825	3.854	4.098	4.781	5.253
90	3.715	-	-	-	-	-	5.649
96	-	4.299	4.428	4.370	4.540	5.399	5.945
102	4.304	-	-	-	-	-	6.244
108	-	4.863	4.993	4.959	4.982	5.977	6.541
114	4.854	-	-	-	-	-	-
120	-	5.416	5.532	5.405	5.448	6.553	7.186
126	5.395	-	-	-	-	-	-
132	-	6.076	6.186	5.958	5.840	7.172	7.831
138	5.965	-	-	-	-	-	-
144	-	6.726	6.777	6.547	6.282	7.789	8.424
150	6.486	-	7.123	-	-	-	-
156	-	7.236	7.393	7.153	6.649	8.326	8.969
162	7.075	-	7.726	-	6.943	-	9.265
168	7.390	7.864	7.996	7.795	7.189	8.821	9.564

$\bar{U}$ave :(m/s) , dp/dx : (newton/m^2/m)

$\bar{U}$ ave	0.780	0.750	0.683	0.580	0.494	0.381	0.348
-dp/dx	233.73	224.78	191.95	140.59	74.93	57.65	49.95
$\lambda \times 10^{+2}$	4.620	4.850	5.000	5.090	3.730	4.820	5.020

TABLE 2.

MEASUREMENTS IN STEADY FLOW

η	Re= 2872 (θ = 0°)						Re = 1278(θ= 90°)	
	RUN 12				RUN 22		RUN 11	RUN 21
	$\langle\bar{U}\rangle/\langle\bar{U}\rangle_{max}$	$\langle\bar{U}\rangle/\bar{u}_*$	$'y\bar{u}_*/\nu$	$u'/\bar{u}_*$	$\langle\bar{U}\rangle/\langle\bar{U}\rangle_{max}$	$u'/\bar{u}_*$	$\langle\bar{U}\rangle/\langle\bar{U}\rangle_{max}$	$\langle\bar{U}\rangle/\langle\bar{U}\rangle_{max}$
0.0	0.0	0.0	0.0	0.0	0.0	0.0	0.0	0.0
0.039	0.218	4.15	4.14	1.55	0.327	1.70	0.095	0.099
0.118	0.619	11.48	12.42	2.35	0.631	2.39	0.221	0.236
0.197	0.745	13.98	20.71	2.21	0.759	2.23	0.362	0.372
0.276	0.828	15.36	28.99	1.90	0.832	1.91	0.470	0.484
0.354	0.851	16.11	37.28	1.60	0.866	1.65	0.582	0.583
0.433	0.894	16.59	45.56	1.46	-	-	0.675	-
0.512	0.926	17.17	53.84	1.28	0.957	1.12	0.769	0.749
0.591	0.943	17.49	62.13	1.19	-	-	0.826	-
0.670	0.969	17.97	70.41	1.05	-	-	0.880	0.877
0.748	0.983	18.23	78.69	0.92	-	-	0.927	-
0.827	0.986	18.34	86.98	0.85	0.991	0.9	0.964	0.962
0.945	1.0	18.55	99.40	0.80	1.0	0.85	1.0	1.0
$\langle\bar{U}\rangle_{max}$ (m/s)	1.06				1.07		0.709	0.711
$\bar{U}_{ave}$ (m/s)	0.783				*		0.351	*
$\bar{u}_*$ (m/s)	0.057**						-	-

* In RUN 21 and RUN 22, measurements were made at only a few points to check RUN 11 and RUN 12, hence enough points were not available to calculate $\bar{U}$ave. However, $\bar{U}$ave in these experiments can be assumed to be the same as in RUN 11 and RUN 12 respectively.

** Based on pressure drop measurements.

TABLE 3.

MEASUREMENTS IN UNSTEADY FLOW (RUN 23)

$\bar{U}_{max}$=1.086m/s, $(U_{qm})_{pmax}$= 0.43 m/s , $\bar{u}_*$ =0.0344 m/s

η	$\bar{u}/\bar{u}_{max}$	$u_{pmax}/(U_{qm})_{pmax}$	$\bar{u}/\bar{u}_*$	$y\bar{u}_*/\nu$	ϕ_*(degree)
0.0	0.0	0.0	0.0	0.0	-
0.04	0.078	0.365	2.516	2.486	-60.8
0.08	0.163	0.602	5.164	4.972	-72.0
0.158	0.297	0.696	9.380	9.944	-79.2
0.197	0.361	0.672	11.400	12.430	-82.8
0.236	0.414	0.652	13.056	14.916	-86.4
0.276	0.470	0.647	14.827	17.402	-90.0
0.315	0.522	0.640	16.475	19.888	-79.2
0.354	0.572	0.647	18.043	22.374	-86.4
0.394	0.619	0.640	19.531	24.860	-82.8
0.472	0.700	0.640	22.10	29.831	-82.8
0.551	0.775	0.643	24.464	34.803	-82.8
0.630	0.836	0.659	26.404	39.775	-86.4
0.709	0.884	0.656	27.919	44.747	-82.8
0.787	0.929	0.656	29.327	49.719	-82.8
0.866	0.962	0.656	30.381	54.691	-86.4
0.984	1.0	0.656	31.568	62.149	-86.4

TABLE 4.

MEASUREMENTS IN UNSTEADY FLOW (RUN 24)

$\bar{U}_{max}$= 1.11 m/s , $(U_{qm})_{pmax}$= 0.43 m/s , $\bar{u}_*$ =0.036 m/s

η	$\bar{u}/\bar{u}_{max}$	$u_{pmax}/(U_{qm})_{pmax}$	$\bar{u}/\bar{u}_*$	$y\bar{u}_*/\nu$	ϕ_*(degrees)
0.0	0.0	0.0	0.0	0.0	-
0.04	0.082	0.214	2.541	2.583	- 7.2
0.08	0.170	0.395	5.286	5.166	+ 14.4
0.158	0.328	0.769	10.256	10.331	+ 14.4
0.236	0.461	1.029	14.365	15.497	+ 14.4
0.315	0.584	1.205	18.210	20.662	+ 14.4
0.394	0.691	1.367	21.535	25.828	0
0.472	0.780	1.463	24.322	30.994	0
0.551	0.856	1.607	26.667	36.160	- 14.4
0.630	0.910	1.743	28.372	41.325	- 7.2
0.709	0.954	1.771	29.719	46.491	- 7.2
0.787	0.998	1.983	31.117	51.657	- 21.6
0.866	1.007	1.914	31.364	56.822	- 14.4
0.984	1.000	1.897	31.151	64.571	- 21.6

TABLE 5.

MEASUREMENTS IN UNSTEADY FLOW (RUN 13)

$\bar{U}_{max}$=0.818 m/s , $(U_{qm})_{pmax}$=0.43 m/s , $\bar{u}_*$ = 0.0535 m/s

η	$\bar{u}/\bar{u}_{max}$	$u_{pmax}/(U_{qm})_{pmax}$	$\bar{u}/\bar{u}_*$	$y\bar{u}_*/\nu$	ϕ_* (degrees)	$u'/\bar{u}_*$	$u'/\bar{u}_{max}$
0.0	0.0	0.0	0.0	0.0	-	0.0	0.0
0.04	0.266	0.546	4.068	3.864	- 51.4	1.35	0.0883
0.08	0.370	0.652	5.664	7.729	- 64.3	1.66	0.1083
0.158	0.625	0.713	9.556	15.457	- 70.7	1.97	0.1284
0.236	0.741	0.651	11.339	23.186	- 77.1	1.86	0.1213
0.315	0.806	0.634	12.330	30.915	- 77.1	1.70	0.1115
0.394	0.867	0.675	13.265	38.643	- 70.7	1.44	0.0944
0.472	0.894	0.660	13.675	46.372	- 70.7	1.30	0.0850
0.551	0.921	0.643	14.091	54.101	- 64.2	1.19	0.0778
0.630	0.955	0.679	14.604	61.829	- 77.1	1.11	0.0721
0.709	0.975	0.660	14.923	69.558	- 83.6	1.01	0.0662
0.787	0.980	0.634	15.003	77.287	- 70.7	1.03	0.0670
0.866	0.993	0.638	15.197	85.016	- 83.6	0.974	0.0636
0.984	1.000	0.624	15.293	96.609	- 77.1	1.02	0.0667

APPENDIX C

Assembler Language Program for Sampling and Processing Periodic Turbulent Flows on the IIHR IBM/1800 System

```
// JOB   0000011111
// ASM ACSV3
*LIST
                        ********************************************************
                        *                PROCESS PROGRAM ACSV3                 *
                        *  THIS PROGRAM TAKES DATA FROM MPX3 PTS               *
                        *  /1016,/1017,/1018. A SYNCHRONIZING SIGNAL           *
                        *  MUST BE PRESENT FOR EXTERNAL SYNC ON THE ADC.       *
                        *  EXITS AFTER 25 SECOND DELAY IF NO SYNC.             *
                        *  THE NO. OF WAVES, THE NO. OF POINTS PER WAVE,       *
                        *  AND THE DELAY TIME BETWEEN DATA POINTS ARE          *
                        *  OBTAINED FROM FIL20. THE DATA OF THE 3 CHANNEL      *
                        *  ARE TESTED FOR LOCKON OF THE LDA-TRACKER.           *
                        *  THE RAW DATA FROM ALL THREE CHANNEL ARE             *
                        *  STORED ON DISK IN FIL03,FIL04,FIL05.                *
                        *  PROGRAMMED BY MUELLER BASED ON ACSV2                *
                        *  MARCH, 1977                                         *
                        ********************************************************
0000 0  0877        START XIO     LITOM
0001 30 17403003            CALL    PKLPL
0003 20 2FFF3A15            LIDF    UPTYM
0004 0  2002                DC      /2002
0005 1  1FFD                DC      DMTSS-1
0006 0  0800        ON      DC      /0800
0007 20 2FFF3A15            LIDF    UPTYM
0008 0  0002                DC      /0002
0009 0  73F9                MDX     *-3
000A 01 0C000185            XIO   L 10CCA
000C 0  E050                AND     H0200
000D 0  4808                BSC     *
000F 0  700C                MDX     NOGNG
000F 30 22503003            CALL    SPECL
0011 30 03201547            CALL    CHANG
0013 30 24550000            CALL    UNC
0015 30 01162073            CALL    ACSV3
0017 0  0001                DC      1
0018 0  0850                XIO     LITOF
0019 30 25241F00            CALL    VIAO
001B 01 C4000100    NOGNG   LD    L WDCNT     SET UP WORD COUNT TO STORE
001D 01 D4000F09            STO   1 STDT1     DATA IN DISK.
001F 01 D4000FF0            STO   L STDT2
0021 01 D4001300            STO   L STDT3
0023 0  1080                SLT     32        SET ZERO IN A & Q REG.
0024 01 DC000180            STD   L AREAC+308
0026 01 DC0001BE            STD   L AREAC+310
0028 01 DC0001C0            STD   L AREAC+312
002A 01 0C0001B0            XIO   L 10CCF     SHUT OFF TIMER.
002C 00 C4000000            LD    L /0000
002E 01 D4000DDF            STO   L SAVE
0030 00 C4000006            LD    L /0006
0032 01 D4001BBF            STO   L AREAC+314
0034 00 2C400000            STS   L /0000,/40
0036 0  C03F                LD      ADDRT
0037 00 D4000000            STO   L /0000
0039 0  C008                LD      DLY
003A 00 D4000006            STO   L /0006
003C 01 0C000100            XIO   L 10CCF
003E 20 01257DD5            LIDF    AIRTM
003F 0  1010                DC      /1010
0040 1  02F2                DC      DATAW+2
0041 1  02F1                DC      DATAW+1
0042 0  F30C        DLY     DC      -3125     LOOP COUNT FOR DELAY FOR SYNC
0043 20 01257DD5            LIDF    AIRTM
0044 0  0000                DC      /0000
```

```
0045 0  70FD            MDX     *-3
0046 01 0C000160        XIO  L  IOCCD
0048 01 C6000000        LD   L  SAVE
004A 00 04000000        STO  L  /0000
004C 0  7016            MDX     FORVD
004D 20 20003A15    EXIT1 LIBF  WRTYW      TERMINATES IF NO SYNC.SIG.
004F 0  2002            DC      /2002
0050 1  1956            DC      DMES7-1
0051 0  0000            DC      0
0052 20 20003A15        LIBF    WRTYW
0053 0  0002            DC      /0002
0054 0  70FD            MDX     *-3
0055 01 C600015F    EXIT2 LD    L  AREAA+314
0057 00 04000000        STO  L  /0000
0059 01 C600020F        LD   L  SAVE
005B 00 04000000        STO  L  /0000
005D 00 20410000        STS  L  /0000,/41
0060 01 0C000166        XIO  L  IOCCE      START TIMERS
0062 0  0815            XIO     LITOF
0063 30 25241C00        CALL    VIAQ
0065 01 4C00016A    FORVD BSC  L  PAUZ1
0067 0  0200        H0200 DC      /0200
0068 1  0007        ADDRT DC      TIMEW
0069 0  0000        TIMEW DC      *-*
006A 01 0C000160        XIO  L  IOCCB      SHUT OFF TIMERS
006C 01 0C000164        XIO  L  IOCCD      SENSE DEV.
006E 0  4878            BOSC    +Z-
006F 0  1000            NOP
0070 00 67000067        LDX  I3 103
0072 20 01257BD5        LIBF    AIPTW
0074 0  3000            DC      /3000
0075 01 4C000040        BSC  L  EXIT1
0077 0  0000        OFF   DC    0
0078    0000            BSS  E  0          INSURE THAT AREAA IS EVEN ADDRESS
0079 1  0078        LITOF DC    OFF
007A 0  617D            DC      /617D
007B 1  0806        LITON DC    ON
007C 0  617D            DC      /617D
007D 0  0004        AREAA DC    4
007E 31 0C253C00    INFOW DSA   FIL20      INFORMATION STORED ON DISK.
0080 0  0000        DELAY DC    *-*        DELAY TIME.
0081 0  0000        POINTS DC   *-*        NO. OF POINTS ON A WAVE.
0082 0  0000        WAVES DC    *-*        NO. OF WAVES TAKEN.
0083 0  0000        CLICK DC    *-*        LOCATION OF RUN NO.
0084 0  0000        U00   DC    *-*
0085 0  0000        U11   DC    *-*
0086 0  0000        LIMIT DC    *-*
0087    0139        AREAC BSS   313
01BE    0000            BSS  E  0
01BF 0  0000        IOCCA DC    /0000      READ D.E.S INTO A  REG.
01C0 0  0740            DC      /0740
01C1 0  0000        IOCCB DC    /0000      SHUT OFF TIMERS
01C2 0  0420            DC      /0420
01C3 0  8000        IOCCC DC    /8000      TURN ON TIMER A
01C4 0  0420            DC      /0420
01C5 0  0000        IOCCD DC    /0000      SENSE DEV
01C6 0  0721            DC      /0721
01C7 0  2000        IOCCE DC    /2000      START TIMER C
01C8 0  0420            DC      /0420
01C9 0  0780        WDCNT DC    1920
01CA 0  3200        D128W DC    12800      LENGTH OF FILES 03 06 05
01CB 0  C005        PAUZ1 LD    WDCT2      SET UP WORD COUNT.
01CC 01 04000078        STO  L  INFOW
01CE 20 04262B05        LIBF    DISKW      READ INFORMATION FROM THE DISK.
01D0 0  1000            DC      /1000
01D1 1  0078            DC      INFOW
```

THIS DOCUMENT IS BEST QUALITY PRACTICABLE.
THE COPY FURNISHED TO DDC CONTAINED A
SIGNIFICANT NUMBER OF PAGES WHICH DO NOT
REPRODUCE LEGIBLY.

```
01D0 0  0140        UPST2 DC      320
01D1 20 042C2495          LIBF    DISKN
01D3 0  0100              DC      /0100
01D3 1  007B              DC      INFOM
01D4 0  70FC              MDX     *-4
01D5 20 20663A15          LIBF    UPTYN
01D6 0  2002              DC      /2002
01D7 1  1048              DC      DMES6-1
01D8 0  0000              DC      0
01D9 20 20663A15          LIBF    UPTYN
01DA 0  0002              DC      /0002
01DB 0  70FD              MDX     *-3
01DC 20 23A17172          LIBF    TYPE2
01DD 1  007F              DC      DELAY
01DE 0  0003              DC      3
01DF 20 20663A15          LIBF    UPTYN
01E0 0  2002              DC      /2002
01E1 1  1074              DC      DMES9-1
01E2 0  0000              DC      0
01E3 20 20663A15          LIBF    UPTYN
01E4 0  0002              DC      /0002
01E5 0  70FD              MDX     *-3
01E6 20 23A17172          LIBF    TYPE2
01E7 1  0082              DC      U00
01E8 0  0003              DC      3
01E9 01 C4000002          LD    L U00       TRANSFER U0,U1,LIMIT
01EB 01 D4000209          STO   L U0
01ED 01 C4000003          LD    L U11
01EF 01 D400020A          STO   L U1
01F1 01 C4000004          LD    L LIMIT
01F3 01 D400020C          STO   L LIMIT
01F5 01 C4000080          LD    L WAVES
01F7 01 A400007F          M     L POINTS
01F9 0  1020              SLT     16
01FA 0  B00E              CMP     D128N     FILE LENGTH IS 40 SECTORS
01FB 0  7002              MDX     NGOOD
01FC 0  700A              MDX     GOOD
01FD 0  7009              MDX     GOOD
01FE 20 20663A15    NGOOD LIBF    UPTYN
01FF 0  2002              DC      /2002
0200 1  1004              DC      DMES8-1
0201 0  0000              DC      0
0202 20 20663A15          LIBF    UPTYN
0203 0  0002              DC      /0002
0204 0  70FD              MDX     *-3
0205 01 D400004D          DSC   L EXIT1       OUT IF FILES TOO SMALL
0207 01 C4000080    GOOD  LD    L WAVES
0209 01 D4000200          STO   L NUMBR       STORE NO. OF WAVES
020B 01 C400007F          LD    L POINTS
020D 0  1001              SLA     1           MULTIPLY BY TWO
020E 01 D400020D          STO   L TWPTS       TWICE THE NUMBER OF POINTS
0210 0  1040              SLT     32          ZERO A AND Q REG.
0211 01 840002DD          S     L TWPTS
0213 01 D400020D          STO   L TWPTS       MINUS TWICE THE NUMBER
0215 0  1010              SLA     16          ZERO A REG.
0216 01 840000FF          S     L POINTS      OBTAIN  TWICE THE NUMBER
0218 01 D400020F          STO   L NWPTS       OF POINTS NEGATIVE.
021A 01 00300100          XIO   L IOCCB       SHUT OFF TIMER C
021C 00 C4000000          LD    L /0000       SAVE THE ADDRESS OF IOM'S
021E 01 D4000210          STO   L SAVE        LEVEL ZERO INTER. ROUTINE.
0220 00 2040000D          STS   L /0000,64    UNWRITE STOP, PROT. BIT.
0222 01 C40302F8          LD    L ADDRA       SUBSTITUTE OUR INTERRUPT
0224 00 D4000000          STO   L /0000       ROUTINE ADDRESS.
0226 30 14002400          CALL    MASK
0228 1  1AF0              DC      MSK1
0229 1  1AF1              DC      MSK2
```

```
022A 01 C400007F    SYNCH LD    L   DELAY       SET UP DELAY INT TIMER  A
022C 01 D4000004          STO   L   /0004
022E 01 D5000000          LDX   I1  TWOTS       LOOP FOR DATA
0230 20 01257805          LIBF      AIRTH       TAKE FIRST PT. ONLY AFTER THE
0231 0  1010              DC        /1010       SYNC. SIGNAL IS RECEIVED.
0232 1  02F2              DC        DATAW+2
0233 1  02F1              DC        DATAW+1
0234 0  0000              DC        /0000
0235 20 01257805          LIBF      AIRTH
0236 0  0000              DC        /0000
0237 0  70F0              MDX       *-3
0238 0  0889              XIO       IOCCC       START TIMER A
0239 0  3000              WAIT                  WAIT FOR TIMER INTERRUPT
023A 0  70FF              MDX       *-2
023B 0  0000    TIMER     DC        *-*         TIMER INTERRUPT ROUTINE
023C 0  0887              XIO       IOCCD       SENSE DEV
023D 0  4878              BOSC      +Z-         RESET INDICATORS
023E 0  1000              NOP
023F 01 C400007F          LD    L   DELAY
0241 00 D4000004          STO   L   /0004       RESET TIMER A
0243 20 01262615          LIBF      AISQN       OBTAIN DATA SEQUENTIALLY.
0244 0  2000              DC        /2000
0245 1  02E0              DC        DATAW
0246 1  02E8              DC        ERROR
0247 20 01262615          LIBF      AISQN       TEST FOR COMPLETION.
0248 0  0030              DC        /0000
0249 0  70F0              MDX       *-3
024A 01 C40002E2          LD    L   DATAW+2
024C 01 D4000400  DKST1   STO   L   STDT1+2     FOR CHANNEL1.
024E 01 74010250          MDX   L   DKST1+1,1
0250 01 C40002E3          LD    L   DATAW+3
0252 01 D4000EE0  DKST2   STO   L   STDT2+2     STORE CHAN.2 DATA IN DISK AREA.
0254 01 74010253          MDX   L   DKST2+1,1   SET UP FOR NEXT DSL STORE.
                  *                             TEST FOR TRACKER
0256 01 C40002E4          LD    L   DATAW+4     TEST IF U1>U0
0258 0  8010              A         U0
0259 0  4810              BSC       -
025A 0  7015              MDX       OK
0258 01 C40002E4          LD    L   DATAW+4     TEST /W1-W1-1/>U1
025D 0  9000              S         LAST
025E 0  4810              BSC       -
025F 0  7003              MDX       LIMTE
0260 0  9007              STO       MEMO
0261 0  1010              SLA       16
0262 0  9005              S         MEMO
0263 0  B006    LIMTE     CMP       U1
0264 0  7000              MDX       OK
0265 0  7008              MDX       NOK
0266 0  7007              MDX       NOK
0267 0  0000    LAST      DC        *-*
0268 0  0000    MEMO      DC        *-*
0269 0  0640    U0        DC        1600        U0=100MVOLT
026A 0  0020    U1        DC        32          U1=2MVOLT
026B 0  0000    COUNT     DC        *-*
026C 0  000A    LIMIT     DC        10
026D 0  0000    ZERO      DC        0
026E 01 74010260  NOK     MDX   L   COUNT,1
0270 01 C40002E4  OK      LD    L   DATAW+4
0272 0  D0F4              STO       LAST
0273 01 D400136E  DKST3   STO   L   STDT3+2     STORE CHAN .3 DATA ON DISK.
0275 01 74010274          MDX   L   DKST3+1,1   SET UP FOR NEXT DSL STORE.
0277 0  7102              MDX     1 +2          DECREMENT INDEX REGISTER.
0278 0  7001              MDX       TIMEX       RETURN FOR NEXT SAMPLE ON THIS WAVE
0279 0  7002              MDX       MWAVE       END SAMPLING , NEXT WAVE.
027A 01 4C800238  TIMEX   BSC   I   TIMER       END OF TIMER INTER. ROUTINE.
027C 01 9C0001C0  MWAVE   XIO   L   IOCCP       SHUT OFF TIMERS.
```

THIS DOCUMENT IS BEST QUALITY PRACTICABLE.
THE COPY FURNISHED TO DDC CONTAINED A
SIGNIFICANT NUMBER OF PAGES WHICH DO NOT
REPRODUCE LEGIBLY.

```
027F 0  00FC            LD      COUNT     TEST NO OF BAD POINTS
0280 0  00FC            S       LIMIT
0281 0  4008            BSC     +
0282 0  7012            MDX     GOON
0283 20 23A17172        LIBF    TYPE2
0284 1  026F            DC      COUNT
-------------------------------------------------------------------
0285 0  0001            DC      1
0286 0  00C7            LD      DKST1+1   RESTORES ADDRESS CH.1
0287 01 9400007F        S   L   POINTS
0289 0  00C4            STO     DKST1+1
028A 0  00C9            LD      DKST2+1   RESTORES ADDRSS CH.2
028B 01 9400007F        S   L   POINTS
028D 0  00C6            STO     DKST2+1
028E 0  00CE            LD      DKST3+1   RESTORES ADDRESS CH.3
028F 01 9400007F        S   L   POINTS
0291 0  00F3            STO     DKST3+1
0292 0  00DF            LD      ZERO      RESET COUNT
0293 0  0008            STO     COUNT
-------------------------------------------------------------------
0294 0  700E            MDX     SYNCH
0295 0  00D8    GOON    LD      ZERO
0296 0  0005            STO     COUNT
0297 0  00C6            LD      DKST1+1
0298 01 9400046B        S   L   ADD07
0299 01 9400016B        CMP L   WRCNT     CHECK TO SEE IF THE DISK
-------------------------------------------------------------------
029B 0  7001            MDX     OUT       AREA IS FULL.
029C 0  7002            MDX     RCCNT
029D 01 440004A9    OUT BSI L   GDISK     GO TO DISK OUTPUT SUBROUTINE.
029F 01 74FF03DC    RCCNT MDX L WWORD,-1  DECREMENT NUMBER OF WORDS.
02A1 0  7008            MDX     SYNCH     GO BACK TO SYNCH LOOP.
02A2 01 440004A9        BSI L   GDISK
-------------------------------------------------------------------
02A4 0  003C    EXITS LD        SAVE      RESTORE IRQ1, IRQ2, ZERO
02A5 00 9400000F        STO L   /000F     INTER. ROUTINE ADDRESS.
02A7 00 20410000        STS L   /0000,05  WRITE STORAGE PROT. BIT.
02A9 30 24554A80        CALL    WAIT
02AB 1  1AF0            DC      MSK1
02AC 1  1AF1            DC      MSK2
-------------------------------------------------------------------
02AD 01 00000108        XIO L   IRQCF     TURN OFF TIMER C.
02AF 30 034D0002        CALL    CLOCK     OBTAIN RUN NUMBER.
02B1 1  0081            DC      CLICK
02B2 0  C03A            LD      DF320
02B3 01 04000078        STO L   INFOM
02B5 20 04262405        LIBF    DISKW     WRITE OUT THE DATA ON DISK.
-------------------------------------------------------------------
02B6 0  3000            DC      /3000     DATA MAY BE USED FOR PLOTTING.
02B7 1  0078            DC      INFOM
02B8 0  0000            DC      /0000
02B9 20 04262405        LIBF    DISKW
02BA 0  0100            DC      /0100
02BB 1  0078            DC      INFOM
-------------------------------------------------------------------
02BC 0  70FC            MDX     *-4
02BD 01 04000081        LD  L   CLICK
02BF 20 02255103        LIBF    BINDC     CONVERT RUN NUMBER FOR
02C0 1  1C07            DC      INPUT     PRINTOUT.
02C1 20 08503500        LIBF    HOLLR
02C2 0  0000            DC      /0000
-------------------------------------------------------------------
02C3 1  1C07            DC      INPUT
02C4 1  1AFA            DC      OTPUT
02C5 0  0006            DC      6
02C6 20 23A17155        LIBF    TYPEH     PRINT RUN NUMBER.
02C7 0  2002            DC      /2002
02C8 1  1AF2            DC      BUFF3-1
-------------------------------------------------------------------
02C9 0  0000            DC      0
02CA 20 23A17155        LIBF    TYPEH     TEST OP. COMPLETE.
02CB 0  0000            DC      0
02CC 0  70FD            MDX     *-3
02CD 30 24550000        CALL    UNC
02CF 30 011F2073        CALL    AGSV3
```

```
02D1 1  0435            DC      UNK
02D2 30 18005005        CALL    QUEUE
02D4 30 00342DF3        CALL    CHART
02D6 0  0001            DC      1
02D7 0  0000            DC      0
02D8 01 0C000070        XIO  L  LITOF
02DA 30 952A1C00        CALL    XIAD
02DC 0  0000    NUMBR   DC      *-*     NUMBER OF WAVES TO BE SAMPLED
02DD 0  0000    TWPTS   DC      *-*     TWICE NO. OF POINTS.
02DE 0  0000    MNPTS   DC      *-*     MINUS TWICE NO. OF PTS.
02DF 0  0000    SAVE    DC      *-*     SAVED ADDRESS IN /000F
02E0 0  0004    DATAW   DC      4
02E1 0  1010            DC      /1010
02E2 1  02E2            DC      DATAW+2
02E3 1  02E3            DC      DATAW+3
02E4 1  02E4            DC      DATAW+4
02E5    0003            BSS     3
02E8 0  0000    ERROR   DC      *-*
02E9 01 4C7002E8        BSC  I  ERROR
02EB 1  023B    ADDRA   DC      TIMER   ADDRESS OF TIMER ROUTINE
02EC 0  2717    SCALE   DC      10007   SCALING COEF.
02ED 0  0140    DC320   DC      320     CONSTANT USED FOR DISKN
02EE    0000            BSS  E  0
02EF    0138    AREAR   BSS     315     DISKN AREA
0429 0  0000    OUTSK   DC      *-*     DISK OUTPUT SUBROUTINE.
042A 20 04262495        LIBF    DISKN   RUN RAW DATA INTO DISK
042B 0  3000            DC      /3000   FOR CHAN1.
042C 1  0469    ADC01   DC      STDT1
042D 0  0000            DC      0
042E 20 04262495        LIBF    DISKN
042F 0  0100            DC      /0100
0430 1  0469            DC      STDT1
0431 0  70FC            MDX     *-4
0432 20 04262495        LIBF    DISKN   RUN RAW DATA INTO DISK
0433 0  3000            DC      /3000   FOR CHAN.2.
0434 1  0FFF    ADC02   DC      STDT2
0435 0  0001    UNK     DC      1
0436 20 04262495        LIBF    DISKN
0437 0  0100            DC      /0100
0438 1  0FFF            DC      STDT2
0439 0  70FC            MDX     *-4
043A 20 04262495        LIBF    DISKN   RUN RAW DATA INTO DISK
043B 0  3000            DC      /3000   FOR CHAN.3.
043C 1  13FF    ADC03   DC      STDT3
043D 0  0000            DC      0
043E 20 04262495        LIBF    DISKN
043F 0  0100            DC      /0100
0440 1  13FF            DC      STDT3
0441 0  70FC            MDX     *-4
0442 01 04000FFC        LD   L  STDT2+1
0444 0  8022            A       DEC6    CHANGE OF SECTOR ADDRESS.
0445 01 04000FFC        STO  L  STDT2+1
0447 01 0400136F        LD   L  STDT3+1
0449 0  8019            A       DEC6    CHANGE OF SECTOR ADDRESS.
044A 01 0400136F        STO  L  STDT3+1
044C 0  C01D            LD      STDT1+1
044D 0  8019            A       DEC6    CHANGE OF SECTOR ADDRESS.
044E 0  D01D            STO     STDT1+1
044F 01 74010400        MDX  L  STCNT,1
0451 0  C010            LD      ADC04
0452 01 04000240        STO  L  DKST1+1 RESTORE STORE ADDRESS.
0454 0  C00F            LD      ADC05
0455 01 04000253        STO  L  DKST2+1
0457 0  C00C            LD      ADC06
0458 01 04000274        STO  L  DKST3+1
045A 0  C00B            LD      STCNT
```

THIS DOCUMENT IS BEST QUALITY PRACTICABLE.
THE COPY FURNISHED TO DDC CONTAINED A
SIGNIFICANT NUMBER OF PAGES WHICH DO NOT
REPRODUCE LEGIBLY.

```
0458 0  8009            CMP     DEC12
0459 0  7003            MRX     EXDIT
0450 0  7000            MRX     OUT2
045F 01 4C000A20  OUT2  BSC  L  ODISK
0460 01 4C0002A4  EXDIT BSC  L  EXITS
0462 1  046E      ADCC4 DC      STDT1+2
0463 1  0472      ADCC5 DC      STDT2+2
0464 1  137E      ADCC6 DC      STDT3+2
0465 0  000C      DEC12 DC      12
0466 0  0000      STCNT DC      *-*
0467 0  0006      DEC6  DC      6
0468 1  046A      ADCC7 DC      STDT1+1
0469 31 00253C33  STDT1 DSA     FIL03     SEDIMENT CONCENTRATION.
046C    077E            BSS     1919
0472 31 00253C34  STDT2 DSA     FIL04     HORIZONTAL VELOCITY COMPONENT.
0475    077E            BSS     1919
137D 31 00253C35  STDT3 DSA     FIL05     VERTICAL VELOCITY COMPONENT.
1380    077E            BSS     1919
1AFF 0  FE3F      PIPES DC      /FE3F
1AF0 0  0FFC      MSK1  DC      /0FFC     MASKING CONSTANT
1AF1 0  FFFF      MSK2  DC      /FFFF     MASKING CONSTANT
1AF2 0  000A            DC      DMESX-DMES3
1AF3    000F      DMES3 DMES    '2PRUN NUMBER 'E
1AFA    0003      OTPUT BSS     3
1AFD    0000      DMESX BES     0
1AFD 0  000C            DC      DMESR-DMES4+2
1AFF    0012      DMES4 DMES    'PAVERAGE VALUE = 'E
1B07    0000      DMESR BSS     0
1B07    0006      INPUT BSS     6
1B00 0  003A            DC      DMESC-DMES5
1B0F    001F      DMES5 DMES    '2PDATA CORRECTION FOR SEDIMENT '
1B1D    001F            DMES    CONCENTRATION AND TWO VELOCITY '
1B2D    001F            DMES    COMPONENTS.'DTO CHANGE PROGRAM '
1B3C    001B            DMES    CONSTANTS, SET D.E.S. E.'E
1B48    0000      DMESC BES     0
1B4B 0  000D            DC      DMESD-DMES6
1B59    001A      DMES6 DMES    '2P   DELAY POINTS   LAYES'E
1B66    0000      DMESD BES     0
1B6F 0  000D            DC      DMESP-DMES7
1B67    001A      DMES7 DMES    'R'AEXIT1, NO SYNC SIGNAL.'D'E
1B84    0000      DMESP BES     0
1B84 0  000F            DC      DMESQ-DMES8
1B85    001F      DMES8 DMES    'PFILES 03 04 05 ARE TOO SMALL'P
1B74    0000      DMESQ BES     0
1B74 0  0
104 14.F18 02          1442 NOT DEFCY 00D              DC      DMES"-DMES9
1B75    001A      DMES9 DMES    'R    H0      U1      LIMIT'E
1B92    0000      DMES" BES     0
1B92    0000            END     START
    NO ERRORS IN ABOVE ASSEMBLY.
ASSY3
DUP FUNCTION COMPLETED
```

```
// JOB   0000011111
// ASM COMPT
*LIST
                    ********************************************************
                    *                  PROGRAM : COMPT                     *
                    *  THIS PROGRAM COMPUTES THE PERIODIC MEAN             *
                    *  AND THE RMS OF THE RANDOM COMPONENT                 *
                    *  OF THE SIGNALS FOR 3 CHANNELS FROM THE DATA         *
                    *  STORED ON DISK BY THE PROCESS PROGRAM AGSV3.        *
                    *  PROGRAMMED BY A.MUELLER, APRIL 1977                 *
                    ********************************************************
0000 01 0C000152  START XIO   L   LITON
0002 01 C40006F9        LD    L   STDT1+1     SAVE SECTOR ADDRESS.
0004 01 D400007A        STO   L   SECSV
0006 01 C4000370        LD    L   DE320       SET UP WORD COUNT TO OBTAIN
0008 01 D4000163        STO   L   INFOM       EXPERIMENTAL PARAMETERS.
000A 20 04262495        LIBF      DISKN       READ FIL20 FROM DISK
000B 0  1000            DC        /1000       WHICH CONTAINS THE
000C 1  0163            DC        INFOM       NUMBER OF POINTS PER WAVE,
000D 0  0000            DC        /0000       THE NUMBER OF WAVES SAMPL-
000E 20 04262495        LIBF      DISKN       ED AND THE RUN NUMBER.
000F 0  0100            DC        /0100
0010 1  0163            DC        INFOM
0011 0  70FC            MDX       *-4
0012 01 C4000168  LOOP1 LD    L   WAVES       SET UP COUNTER FOR NUMBER
0014 01 D400015A        STO   L   NUMBR       OF AVERAGES COMPUTED.
0016 01 C4000167        LD    L   PONTS       COMPUTE TWICE THE NUMBER
0018 0  1001            SLA       1           OF POINTS.
0019 01 D4000158        STO   L   TNPTS
001B 0  10A0            SLT       32          CLEAR STORAGE FOR
001C 01 65800158        LDX   I1  TNPTS       ACCUMULATION OF SUMS.
001E 01 DD0002A6  CLEAR STD   L1  AREAC-2      AREAC : USED FOR ACCUMULA-
0020 0  71FE            MDX   1  -2            TION OF SUMS.
0021 0  70FC            MDX       CLEAR
0022 00 6500FDC0        LDX   L1  -576        CLEAR AREAD.
0024 01 D5000585  CLER2 STO   L1  AREAD+576
0026 0  7101            MDX   1  1
0027 0  70FC            MDX       CLER2
0028 01 94000158        S     L   TNPTS       OBTAIN MINUS TWICE THE
002A 01 D4000158        STO   L   TNPTS       NUMBER OF POINTS. TNPTS
002C 01 C400007C        LD    L   XR4         CONTAINS -2*PONTS.
002E 01 D400007D        CMP   L   TWO         CHECK FOR LOOP, SET UP OF
0030 0  7002            MDX       NSKIP       ADDRESSES.
0031 0  7016            MDX       SKIP
0032 0  701A            MDX       SKIP
0033 0  C02F      NSKIP LD        ADDD1+1
0034 01 94000158        S     L   TNPTS       MODIFY ADDRESSES FOR
0036 0  D02C            STO       ADDD1+1     ACCUMULATION AND
0037 0  D02D            STO       ADDD1+3     MANIPULATION OF DATA.
0038 01 D4000099        STO   L   LDDD1+1
003A 01 C400011C        LD    L   ADDD2+1     SET UP ADDRESSES.
003C 01 94000158        S     L   TNPTS       DO FOR FIRST LOOP ONLY.
003E 01 D400011C        STO   L   ADDD2+1
0040 01 D400011E        STO   L   ADDD2+3
0042 0  1010            SLA       16          ZERO A REG.
0043 01 94000167        S     L   PONTS       COMPUTE MINUS THE
0045 01 D4000159        STO   L   MNPTS       NUMBER OF POINTS.
0047 01 C4000167        LD    L   PONTS
0049 01 84000114        A     L   SUBCP+1
004B 01 D4000114        STO   L   SUBCP+1
004D 01 C4000157  SKIP  LD    L   WDCNT       SET UP WORD COUNT FOR
004F 01 D40006F8        STO   L   STDT1       DISK READ.
0051 20 04262495  READD LIBF      DISKN       READ IN THE FIRST SET OF
0052 0  1000            DC        /1000       DATA STORED ON DISK IN
```

THIS DOCUMENT IS BEST QUALITY PRACTICABLE.
THE COPY FURNISHED TO DDC CONTAINED A
SIGNIFICANT NUMBER OF PAGES WHICH DO NOT
REPRODUCE LEGIBLY.

```
0053 1  06F8                DC      STDT1
0054 0  0000                DC      /0000
0055 20 04262495            LIBF    DISKN
0056 0  0100                DC      /0100
0057 1  06F8                DC      STDT1
0058 0  70FC                MDX     *-4
0059 01 65800158    AGAIN   LDX     I1 TNPTS        LOAD INDEX REGISTERS TO
005B 01 66800159            LDX     I2 MNPTS        BEGIN SIGNAL AVERAGING.
005D 01 C40006FA    LOAD1   LD      L  STDT1+2
005F 0  D019                STO     SAVE1
0060 0  C018                LD      SAVE1
0061 0  1890                SRT     16              COMPUTE SIGNAL AVERAGED
0062 01 8D0002A8    ADDD1   AD      L1 AREAC        RESULTS.
0064 01 DD0002A8            STD     L1 AREAC
0066 01 7401005E            MDX     L  LOAD1+1,1    MODIFY ADDRESS.
0068 0  C0F5                LD      LOAD1+1         CHECK FOR END OF DATA BLOCK.
0069 01 94000158            S       L  ADCO1
006B 01 B4000157            CMP     L  WDCNT
006D 0  400F                BSI     MORDT           MORE DATA REQUIRED.
006E 0  7001                MDX     MCOMP           COMPUTATIONS CONTINUE.
006F 0  400D                BSI     MORDT           MORE DATA REQUIRED.
0070 0  7201        MCOMP   MDX     2 1             DECREMENT XR2.
0071 0  1000                NOP
0072 0  7102                MDX     1 +2            DECREMENT XR1.
0073 0  70E9                MDX     LOAD1           GO BACK FOR MORE DATA.
0074 01 74FF015A            MDX     L  NUMBR,-1     DECREMENT NUMBER OF WAVES.
0076 0  70E2                MDX     AGAIN           GET ANOTHER WAVE SET.
0077 0  701C                MDX     COMPT           GO TO COMPUTATION SCHEME.
0078 0  0000        TEMP    DC      *-A*            TEMPORARY STORAGE.
0079 0  0000        SAVE1   DC      *-*             TEMPORARY STORAGE.
007A 0  0000        SECSV   DC      *-*             SAVE SECTOR ADDRESS FOR
0078 0  0002        TWO     DC      2               RAW DATA.
007C 0  0003        XR4     DC      3               INDEX REGISTER FOR LOOP.
                    ********************************************************
                    * DISK DATA SUBROUTINE TO OBTAIN MORE DATA.            *
                    ********************************************************
007D 0  0000        MORDT   DC      *-*             SUBROUTINE TO GET
007E 01 C4000158            LD      L  ADCO1        MORE DATA FROM DISK.
0080 01 D400005E            STO     L  LOAD1+1      RESET ADDRESSES OF LOADING
0082 01 D4000112            STO     L  LOAD2+1      OPERATION.
0084 01 C40006F9            LD      L  STDT1+1      UPDATE SECTOR ADDRESS.
0086 01 84000162            A       L  DEC6
0088 01 D40006F9            STO     L  STDT1+1
008A 20 04262495            LIBF    DISKN           CALL TO DISK FOR
008B 0  1000                DC      /1000           MORE DATA.
008C 1  06F8                DC      STDT1
008D 0  0000                DC      /0000
008E 20 04262495            LIBF    DISKN
008F 0  0100                DC      /0100
0090 1  06F8                DC      STDT1
0091 0  70FC                MDX     *-4
0092 01 4C80007D            BSC     I  MORDT        END SUBROUTINE.
                    ********************************************************
0094 01 65800158    COMPT   LDX     I1 TNPTS        LOAD INDEX REGISTERS
0096 01 66800159            LDX     I2 MNPTS        TO SCALE THE DATA.
0098 01 CD0002A8    LDDD1   LDD     L1 AREAC
009A 01 AC000168            D       L  WAVES
009C 01 D40005D8    STOR2   STO     L  CBCCD+2      UNSCALED SIGNAL AVERAGED
009E 01 7401009D            MDX     L  STOR2+1,1    RESULT STORED IN FIL27
00A0 0  7102                MDX     1 +2            RESULT STORED BACK INTO
00A1 0  1000                NOP                     AREAC.
00A2 0  7201                MDX     2 +1
00A3 0  70F4                MDX     LDDD1
00A4 01 74FF007C            MDX     L  XR4,-1       DECREMENT OF INDEX REG.
00A6 0  7001                MDX     LUCKY           FOR LOOP COUNTER.
00A7 0  7018                MDX     LOOP4
```

```
00A8 01 C4000070     LUCKY LD    L  XR4
00AA 01 84000078           CMP   L  TWO
00AC 0  7010               MDX      LOOP4
00AD 0  7008               MDX      LOOP3
00AE 0  7000               MDX      LOOP2
00AF 01 C4000E78   LOOP2  LD    L  STDT2+1   SET UP SECTOR ADDRESS FOR
00B1 01 D40006F9           STO   L  STDT1+1   CHANNEL 2.
00B3 01 C400015B           LD    L  ADC01     CHANNEL2 & RESET LOAD
00B5 01 D400005E           STO   L  LOAD1+1   INSTRUCTION.
00B7 01 4C000012           BSC   L  LOOP1     GO BACK TO OPERATE ON
00B9 01 C4000E7E   LOOP3  LD    L  STDT3+1   CHANNEL 2 & GET SUM. OF CHAN.3.
00BB 01 D40006F9           STO   L  STDT1+1
00BD 01 C400015B           LD    L  ADC01
00BF 01 D400005E           STO   L  LOAD1+1
00C1 01 4C000012           BSC   L  LOOP1     GO BACK TO OPERATE ON
00C3 01 C400007A   LOOP4  LD    L  SECSV     CHANNEL 3.
00C5 01 D40006F9           STO   L  STDT1+1   SAVE SECTOR ADDRESS FOR
00C7 01 7403007C           MDX   L  XR4,3     CHANNEL1.
00C9 0  C005               LD         CONST   SAVE SECTOR ADDRESS FOR
00CA 01 D40005B6           STO   L  CBQCD     CBQCD.
00CC 20 04262495           LIBF       DISKN   STORE UNSCALED SIGNAL
00CD 0  3000               DC         /3000   AVERAGED DATA (AREAE)
00CE 1  05B6               DC         CBQCD   INTO DISK.
00CF 0  0140       CONST   DC         320
00D0 20 04262495           LIBF       DISKN
00D1 0  0100               DC         /0100
00D2 1  05B6               DC         CBQCD
00D3 0  70FC               MDX        *-4
00D4 01 C4000168   INDEX  LD    L  WAVES
00D6 01 D400015A           STO   L  NUMBR
00D8 01 C400007C           LD    L  XR4       LOAD INDEX REGISTER TO
00DA 01 84000078           CMP   L  TWO       CHECK THE LOOP STEP.
00DC 0  7028               MDX        READF
00DD 0  7014               MDX        LOOPB
00DE 01 C4000E7B   LOOPA  LD    L  STDT2+1   LOAD & STORE THE DATA OF
00E0 01 D40006F9           STO   L  STDT1+1   CHANNEL 2 &.CHANGE ADDRESS
00E2 01 C4000114           LD    L  SUBCP+1
00E4 01 84000167           A     L  PONTS
00E6 01 D4000114           STO   L  SUBCP+1
00E8 01 C400015B           LD    L  ADC01
00EA 01 D4000112           STO   L  LOAD2+1
00EC 0  C02F               LD         ADDD2+1  MODIFY ADDRESS FOR
00ED 01 94000158           S     L  TNPTS     ACCUMULATION & MANIPULATION
00EF 0  D02C               STO        ADDD2+1  OF DATA.
00F0 0  D02D               STO        ADDD2+3
00F1 0  7013               MDX        READF
00F2 01 C4000E7E   LOOPB  LD    L  STDT3+1   LOAD & STORE THE DATA OF
00F4 01 D40006F9           STO   L  STDT1+1   CHANNEL 3 & CHANGE ADDRESS.
00F6 01 C4000114           LD    L  SUBCP+1
00F8 01 84000167           A     L  PONTS
00FA 01 D4000114           STO   L  SUBCP+1
00FC 01 C400015B           LD    L  ADC01
00FE 01 D4000112           STO   L  LOAD2+1
0100 0  C018               LD         ADDD2+1  MODIFY ADDRESS FOR
0101 01 94000158           S     L  TNPTS     ACCUMULATION & MANIPULATION
0103 0  D018               STO        ADDD2+1  OF DATA.
0104 0  D019               STO        ADDD2+3
0105 20 04262495   READF  LIBF       DISKN    READ OUT THE SET OF DATA
0106 0  1000               DC         /1000    STORED ON DISK.
0107 1  06F8               DC         STDT1
0108 0  0000               DC         /0000
0109 20 04262495           LIBF       DISKN
010A 0  0100               DC         /0100
010B 1  06F8               DC         STDT1
010C 0  70FC               MDX        *-4
010D 01 65800158   AGAN1  LDX   I1 TNPTS      LOAD INDEX REGISTER TO
```

```
010F 01 66800159            LDX   I2 MNPTS      BEGIN SIGNAL AVERAGING.
0111 01 C40006FA  LOAD2 LD    L  STDT1+2    LOAD FROM DISK AREA.
0113 01 9600058B  SUBCP S     L2 AREAE-1    SUBTRACT UNSCALED MEAN
0115 01 A400015C            M     L  SCALE      RAW DATA & MEAN VALUE.
0117 01 D4000078            STO   L  TEMP
0119 01 A4000078            M     L  TEMP
011B 01 8D000374  ADDD2 AD    L1 AREAD-1
011D 01 DD000374            STD   L1 AREAD-1
011F 01 74010112            MDX   L  LOAD2+1,1  MODIFY ADDRESS.
0121 0  C0F0                LD       LOAD2+1    CHECK FOR END OF DATA BLOCK
0122 01 9400015B            S     L  ADCO1
0124 01 B4000157            CMP   L  WDCNT
0126 0  7001                MDX      DATA1      MORE DATA REQUIRED.
0127 0  7002                MDX      MCMP1      MORE COMPUTATIONS.
0128 01 4400007D  DATA1 BSI   L  MORDT
012A 0  7201      MCMP1 MDX     2 1            DECREMENT XR2.
012B 0  1000                NOP
012C 0  7102                MDX    1 +2         DECREMENT XR1.
012D 0  70E3                MDX      LOAD2      GO BACK FOR MORE DATA.
012E 01 74FF015A            MDX   L  NUMBR,-1   DECREMENT NO. OF WAVES.
0130 0  70DC                MDX      AGAN1      GET ANOTHER WAVE SET.
0131 01 74FF007C            MDX   L  XR4,-1
0133 0  7001                MDX      LOOPZ
0134 0  7002                MDX      LAST
0135 01 4C0000D4  LOOPZ BSC   L  INDEX
0137 01 C400013E  LAST  LD    L  WORDC
0139 01 D4000372            STO   L  CPVST      RANDOM COMPONENT OF THE
013B 20 04262495            LIBF     DISKN      CONC. FLUCTL TO DISK.
013C 0  3000                DC       /3000
013D 1  0372                DC       CPVST
013E 0  0240      WORDC DC       576
013F 20 04262495            LIBF     DISKN
0140 0  0100                DC       /0100
0141 1  0372                DC       CPVST
0142 0  70FC                MDX      *-4
0143 20 04262495            LIBF     DISKN      READ IN ALL INFORMATIONS
0144 0  3000                DC       /3000      OF CONSTANTS ONTO INFOM.
0145 1  0163                DC       INFOM
0146 0  0000                DC       /0000
0147 20 04262495            LIBF     DISKN
0148 0  0100                DC       /0100
0149 1  0163                DC       INFOM
014A 0  70FC                MDX      *-4
014B 01 0C000150            XIO   L  LITOF
014D 30 25241600            CALL     VIAQ
0150    0000                BSS   E  0
0150 1  0155      LITOF DC       OFF
0151 0  617D                DC       /617D
0152 1  0154      LITON DC       ON
0153 0  617D                DC       /617D
0154 0  0200      ON    DC       /0200
0155 0  0000      OFF   DC       /0000
0156 0  0008      EIGHT DC       8
0157 0  0780      WDCNT DC       1920       WORD COUNT - READ IN DATA.
0158 0  0000      TNPTS DC       *-*        MINUS TWICE NO. OF PTS.
0159 0  0000      MNPTS DC       *-A*        MINUS NO. OF PTS.
015A 0  0000      NUMBR DC       *-*        NBR. OF WAVES.
015B 1  06FA      ADCO1 DC       STDT1+2    ADDR. CHECK ON ENOUGH DATA.
015C 0  2717      SCALE DC       10007      SCALING COEF.
015D    0003      DVSER BSS      3
0160 0  0000      AVRGE DC       *-*
0162    0000                BSS   E  0
0162 0  0006      DEC6  DC       6
0163 31 06253CB0  INFOM DSA      FIL20      INFORMATION STORED ON DISK.
0166 0  FFB0      DELAY DC       -80        DELAY TIME.
0167 0  0060      PONTS DC       96         NUMBER OF POINTS ON A WAVE.
```

```
                                                                    .
0168 0  0064        WAVES  DC      100         NUMBER OF WAVES.
0169 0  0000        CLICK  DC      *-*         LOCATION OF RUN NUMBER.
016A    0060        AREAB  BSS     96         DISKN AREA.
01CA    0003        AREAF  BSS     3
01CD    0003        AREAG  BSS     3
01D0    00D8        AREAH  BSS     216
02A8    00C8        AREAC  BSS  E  200        SCALED.
0370 0  0140        DE320  DC      320        CONSTANT.
0372    0000               BSS  E  0
0372 31 06253CB2    CPVST  DSA     FIL22      USES FIL22 AND FIL23
0375    0240        AREAD  BSS     576
05B6    0000               BSS  E  0
05B6 31 06253CB7    CB3CD  DSA     FIL27      STORAGE OF UNSCALED SIGNAL
05B9    013F        AREAE  BSS     319        AVERAGED RESULT.
06F8 31 06253C33    STDT1  DSA     FIL03      SEDIMENT CONCENTRATION.
06FB    077F               BSS     1919
0E7A 31 06253C34    STDT2  DSA     FIL04      HORIZONTAL VELOCITY COMPONENT.
0E7D 31 06253C35    STDT3  DSA     FIL05      VERTICAL VELOCITY COMPONENT.
0E80 0  0009        DEC9   DC      9
0E81 0  0019        DEC25  DC      25
0E82    0006        INPUT  BSS     6
0E88    0000               END     START
    NO ERRORS IN ABOVE ASSEMBLY.
COMPT
DUP FUNCTION COMPLETED
 // JOB   0000011111
 // END OF ALL JOBS
```

THIS DOCUMENT IS BEST QUALITY PRACTICABLE.
THE COPY FURNISHED TO DDC CONTAINED A
SIGNIFICANT NUMBER OF PAGES WHICH DO NOT
REPRODUCE LEGIBLY.

```
// JOB   0000011111
// ASM CHANG
*LIST
                        ****************************************************
                        *                    CHANG                         *
                        *  THIS PROGESS PROGRAM IS CALLED BY A CALL SPECL  *
                        *  FROM THE SIGNAL AVERAGING PROGRAM ASSM3         *
                        *  AND ALLOWS THE USER TO CHANGE PROGRAM           *
                        *  CONSTANTS, THESE CONSTANTS ARE THE NUMBER OF    *
                        *  WAVES TO BE SAMPLED, THE NUMBER OF POINTS       *
                        *  PER WAVE, THE DELAY TIME IN BE BETWEEN DATA     *
                        *  POINTS, THE MIN.VALUE WO IN MM, THE MAX.        *
                        *  DIFFERENCE W1 IN MM AND THE NUMBER LIMIT OF     *
                        *  ALLOWED BAD POINTS TO TEST THE LDA-TRACKER. ALL *
                        *  ENTRYS ARE MADE THROUGH THE DATA ENTRY          *
                        *  SWITCHES AND AN ECHO CHECK IS PRINTED.          *
                        ****************************************************
0000 20 23A17155    START LIBF    TYPEN     INTRODUCTORY MESSAGE.
0001 0  2002            DC        /2002
0002 1  02F0            DC        DMES0-1
0003 0  0000            DC        0
0004 20 23A17155        LIBF      TYPEN
0005 0  0002            DC        /0002
0006 0  70FD            MDX       *-3
0007 20 23A17155        LIBF      TYPEN
0008 0  2002            DC        /2002     AT PAUSE ENTER THE NUMBER
0009 1  01FF            DC        DMES1-1   OF WAVES TO BE SAMPLED.
000A 0  0000            DC        0
000B 20 23A17155        LIBF      TYPEN
000C 0  0002            DC        /0002
000D 0  70FD            MDX       *-3
000E 01 C8000008        LD    L   AREAA
0010 01 D8000000        STO   L   INFOR
0012 20 0A262A95        LIBF      DISKN     READ IN THE AREA FROM DISK
0013 0  1000            DC        /1000
0014 1  0000            DC        INFOR
0015 0  0000            DC        0
0016 20 0A2E2A95        LIBF      DISKN     ONLY THE FIRST 3 WORDS
0017 0  0100            DC        /0100     IN THE AREA WILL BE CHANGED.
0018 1  0000            DC        INFOR
0019 0  70FD            MDX       *-6
001A 20 17064885        LIBF      PAUSE     PROGRAMMED WAIT
001B 1  02F3            DC        ONE
001C 01 0000000A        XIO   L   IOCCA     READ CONTENTS OF DES. TO VA VES
001E 20 23A17155        LIBF      TYPEN     ECHO CHECK ON THE NUMBER
001F 0  2002            DC        /2002     OF WAVES ENTERED.
0020 1  022A            DC        DMES2-1
0021 0  0000            DC        0
0022 20 23A17155        LIBF      TYPEN
0023 0  0002            DC        /0002
0024 0  70FD            MDX       *-3
0025 01 C8000001        LD    L   WAVES
0027 01 44000200        BSI   L   PRINT
0029 20 23A17155        LIBF      TYPEN     MESSAGE TO ENTER THE
002A 0  2002            DC        /2002     NUMBER OF DATA POINTS
002B 1  0237            DC        DMES3-1
002C 0  0000            DC        0
002D 20 23A17155        LIBF      TYPEN
002E 0  0002            DC        /0002
002F 0  70FD            MDX       *-3
0030 20 17064885        LIBF      PAUSE     WAIT TO ENTER VIA DES.
0031 1  02F3            DC        TWO
0032 0  0B79            XIO       IOCCB     READ DES TO POINTS
0033 20 23A17155        LIBF      TYPEN     ECHO CHECK ON THE NUMBER
```

```
0034 0  2002            DC      /2002       OF POINTS ENTERED.
0035 1  0248            DC      DMES4-1
0036 0  0000            DC      0
0037 20 23A17155        LIBF    TYPEM
0038 0  0002            DC      /0002
0039 0  70FD            MDX     *-3
003A 01 C4000000        LD   L  POINTS
003C 01 44000200        BSI  L  PRINT
003E 20 23A17155        LIBF    TYPEM       MESSAGE TO ENTER  THE DELAY
003F 0  2002            DC      /2002       TIME VIA DES.
0040 1  0258            DC      DMES5-1
0041 0  0000            DC      0
0042 20 23A17155        LIBF    TYPEM
0043 0  0002            DC      /0002
0044 0  70FD            MDX     *-3
0045 20 17064885        LIBF    PAUSE       WAIT TO ENTER INFORMATION.
0046 1  0254            DC      THREE
0047 0  0866            XIO     IOCCC       READ DES. TO DELAY
0048 20 23A17155        LIBF    TYPEM       ECHO CHECK ON THE NUMBER
0049 0  2002            DC      /2002       OF MILLISECONDS DELAY TIME.
004A 1  0269            DC      DMES6-1
004B 0  0000            DC      0
004C 20 23A17155        LIBF    TYPEM
004D 0  0002            DC      /0002
004E 0  70FD            MDX     *-3
004F 0  00FF            LD      DELAY
0050 01 44000200        BSI  L  PRINT
0052 0  1010            SLA     16          ZERO A REG.
0053 0  00FF            S       DELAY       A REG. CONTAINS MINUS DELAY
0054 0  1003            SLA     3           MULTIPLY BY  8
0055 0  00FD            STO     DELAY       STORE IN DELAY
0056 20 23A17155        LIBF    TYPEM       READ IN IO
0057 0  2002            DC      /2002
0058 1  0275            DC      DME10-1
0059 0  0000            DC      0
005A 20 23A17155        LIBF    TYPEM
005B 0  0002            DC      /0002
005C 0  70FD            MDX     *-3
005D 20 17064885        LIBF    PAUSE
005E 1  0255            DC      FOUR
005F 0  0850            XIO     IOCCD
0060 20 23A17155        LIBF    TYPEM
0061 0  2002            DC      /2002
0062 1  0285            DC      DME13-1
0063 0  0000            DC      0
0064 20 23A17155        LIBF    TYPEM
0065 0  0002            DC      /0002
0066 0  70FD            MDX     *-3
0067 01 C4000003        LD   L  IO
0069 01 44000200        BSI  L  PRINT
006B 01 C4000003        LD   L  IO
006D 0  1004            SLA     4           MULTIPLY BY 16
006E 01 D4000003        STO  L  IO
0070 20 23A17155        LIBF    TYPEM       READ IN M1
0071 0  2002            DC      /2002
0072 1  0295            DC      DME11-1
0073 0  0000            DC      0
0074 20 23A17155        LIBF    TYPEM
0075 0  0002            DC      /0002
0076 0  70FD            MDX     *-3
0077 20 17064885        LIBF    PAUSE
0078 1  0256            DC      FIVE
0079 0  0838            XIO     IOCCE
007A 20 23A17155        LIBF    TYPEM
007B 0  2002            DC      /2002
007C 1  0291            DC      DME14-1
```

THIS DOCUMENT IS BEST QUALITY PRACTICABLE.
THE COPY FURNISHED TO DDC CONTAINED A
SIGNIFICANT NUMBER OF PAGES WHICH DO NOT
REPRODUCE LEGIBLY.

```
007D 0  0000                    DC      0
007E 20 23A17155                LIBF    TYPEN
007F 0  0002                    DC      /0002
0080 0  70FD                    MDX     *-3
0081 01 C4000004                LD   L  U1
0083 01 44000208                BSI  L  PRINT
0085 01 C4000004                LD   L  U1
0087 0  1004                    SLA     4           MULTIPLY BY 16
0088 01 D4000004                STO  L  U1
008A 20 23A17155                LIBF    TYPEN       READ IN LIMIT
008C 0  2002                    DC      /2002
008D 1  020F                    DC      DMF12-1
008F 0  0020                    DC      0
0090 20 23A17155                LIBF    TYPEN
0092 0  0002                    DC      /0002
0093 0  70FD                    MDX     *-3
0094 20 17204005                LIBF    PAUSE
0096 1  0257                    DC      SIX
0097 0  6820                    XIO     IOCCF
0098 20 23A17155                LIBF    TYPEN
009A 0  2002                    DC      /2002
009B 1  020D                    DC      DMF15-1
009D 0  0000                    DC      0
009E 20 23A17155                LIBF    TYPEN
00A0 0  0002                    DC      /0002
00A1 0  70FD                    MDX     *-3
00A3 01 C4000005                LD   L  LIMIT
00A5 01 44000208                BSI  L  PRINT
00A7 20 04262405                LIBF    DISKN       READ OUT ONTO DISK
00A9 0  3001                    DC      /3000
00AA 1  00BC                    DC      IMFOR
00AC 0  0000                    DC      /0000
00AD 20 04262405                LIBF    DISKN
00AF 0  0100                    DC      /0100
00B0 1  00BC                    DC      IMFOR
00B2 0  70FC                    MDX     *-4
00B3 30 02063400                CALL    BACK
00B5    0000                    BSS  F  0
00B6 1  0001            IOCCA   DC      WAVES       READ DES TO LOC. WAVES
00B8 0  0240                    DC      /0240
00B9 1  0000            IOCCB   DC      PONTS       READ DES. TO NO. OF PTS.
00BB 0  0240                    DC      /0240
00BC 1  00BF            IOCCC   DC      DELAY       READ DES. DELAY TIME.
00BE 0  0240                    DC      /0240
00BF 1  0003            IOCCD   DC      U0          READ DES TO LOC. U0
00C1 0  0240                    DC      /0240
00C2 1  0004            IOCCE   DC      U1          READ DES TO LOC. U1
00C3 0  0240                    DC      /0240
00C4 1  0005            IOCCF   DC      LIMIT       READ DES TO LOC. LIMIT
00C5 0  0240                    DC      /0240
00C6 0  0000            DATSW   DC      /0000
00C7 0  0740                    DC      /0740
00C8 0  0140            AREAA   DC      320
00C9 31 06253006        FILE    DSA     FILE6
00CC 31 06253000        IMFOR   DSA     FILE0
00CF 0  0000            DELAY   DC      *-*
00D0 0  0000            PONTS   DC      *-*         NUMBER OF POINTS
00D1 0  0000            WAVES   DC      *-*         NO. OF WAVES
00D2 0  0000            CLICK   DC      *-*
00D3 0  0000            U0      DC      *-*
00D4 0  0000            U1      DC      *-*
00D5 0  0000            LIMIT   DC      *-*
00D6    0139                    BSS     313
01FF 0  002A                    DC      DMFSZ-DMFS1
0200    0020            DMFS1   DMFS    '20ENTRY OF CONSTANTS FOR SIGNAL '
0210    0012                    DMFS    AVERAGING PROGRAM.'F
```

```
0210     0022              DMES    '2ENTER NUMBER OF WAVES AT PAUSE 1.'E
0232     0000    DMES2     BSS     0
0232 0   0018              DC      DMESX-DMES2
0233     0018    DMES2     DMES    '2RTHE NO. OF WAVES IS   'E
0237     0000    DMESX     BSS     0
0237 0   0010              DC      DMESX-DMES3
0238     0020    DMES3     DMES    '2RNOW ENTER NO. OF DATA POINTS.'E
0248     0000    DMESX     BSS     0
0248 0   000F              DC      DMESX-DMES4
0249     001F    DMES4     DMES    '2RTHE NO. OF DATA POINTS IS   'E
0258     0000    DMESX     BSS     0
0258 0   0010              DC      DMESX-DMES5
0259     0020    DMES5     DMES    '2RNOW ENTER DELAY TIME IN MSEC.'E
0269     0000    DMESX     BSS     0
0269 0   000F              DC      DMESX-DMES6
026A     0016    DMES6     DMES    '2RTHE DELAY TIME IS   'E
0275     0000    DMESX     BSS     0
0275 0   000F              DC      DMESX-DME10
0276     001F    DME10     DMES    '2RNOW ENTER MIN.VAL. H0 IN MV'E
0285     0000    DMESX     BSS     0
0285 0   0010              DC      DMESX-DME11
0286     0020    DME11     DMES    '2RNOW ENTER MAX.DIFF. U1 IN MV.'E
0296     0000    DMESX     BSS     0
0296 0   000F              DC      DMESX-DME12
0297     001C    DME12     DMES    '2RNOW ENTER LIMIT OF BAD PT.'E
02A5     0000    DMESX     BSS     0
02A5 0   000F              DC      DMESX-DME13
02A6     0016    DME13     DMES    '2RTHE MIN.VALUE H0 IS'E
02B1     0000    DMESX     BSS     0
02B1 0   000F              DC      DMESX-DME14
02C2     001F    DME14     DMES    '2RTHE MAX.DIFF. U1 IS'E
02D0     0000    DMESX     BSS     0
02D0 0   000D              DC      DMESX-DME15
02DF     001A    DME15     DMES    '2RTHE LIMIT OF BAD PT. IS'E
02E9     0000    DMESX     BSS     0
02E9 0   0000    PRINT     DC      *-*         PRINTING SUBROUTINE
02EA 20  02255103          LIBF    BINDC       BINARY TO DECIMAL
02EB 1   02E6              DC      BNOUT
02EC 20  08593509          LIBF    HOLPR       HOLLERITH TO PRINTER
02ED 0   0000              DC      /0000
02EE 1   02E6              DC      BNOUT
02EF 1   02F9              DC      PTOUT
02F0 0   0006              DC      6
02F1 20  23A17155          LIBF    TYPEN       PRINT OUT NUMBER
02F2 0   2002              DC      /2002
02F3 1   02F8              DC      PTOUT-1
02F4 0   0000              DC      /0000
02F5 20  23A17155          LIBF    TYPEN
02F6 0   0002              DC      /0002
02F7 0   70ED              MDX     *-3
02F8 01  4C02002D          BSC  I  PRINT       END OF SUBROUTINE PRINT
02FC     0006    BNOUT     BSS     6
02FC 0   0001    ONE       DC      1
02FD 0   0002    TWO       DC      2
02FE 0   0003    THREE     DC      3
02FF 0   0004    FOUR      DC      4
0300 0   0005    FIVE      DC      5
0301 0   0006    SIX       DC      6
0302 0   0003              DC      3
0303     0003    PTOUT     BSS     3
0306 0   0012              DC      DMESR-DMES9
0307
104 14.093 02          1442 NOT READY 001C        DMES9 DMES    '2R'AACSY3'B CONST
ANTS WILL BE '
0328     0008              DMES    MODIFIED'E
032F     0000    DMESR     BSS     0
```

THIS DOCUMENT IS BEST QUALITY PRACTICABLE.
THE COPY FURNISHED TO DDC CONTAINED A
SIGNIFICANT NUMBER OF PAGES WHICH DO NOT
REPRODUCE LEGIBLY.

```
0300    0000                END     START
     NO ERRORS IN ABOVE ASSEMBLY.
CHANG
DUP FUNCTION COMPLETED
```

```
// JOB   0000011111
// ASM CNVRT
*LIST
                        ************************************************
                        *       PROGRAM : CNVRT                        *
                        *  THIS PROGRAM CONVERTS THE DATA IN MV. TO    *
                        *  (PPM) FOR CHANNEL 1 (SEDIMENT CONCENTRATION)*
                        *  AND 1000*(FT/S) FOR CHANNEL 3 (VERTICAL VELOCIT*
                        *  Y) THROUGH THE SCALING PROCEDURE.           *
                        *  PROGRAMED BY LOCHER AND NAKATO              *
                        ************************************************
0000 01 C4000013C  START LD    L  DEC10     SET UP WORD COUNT TO
0002 01 D4000204        STO   L  INFOM      GET INFORMATION
0004 20 04262495        LIBF     DISKN      READ FIL20
0005 0  1000            DC       /1000
0006 1  0204            DC       INFOM
0007 0  0140       WDCNT DC      320
0008 20 04262495        LIBF     DISKN
0009 0  0100            DC       /0100
000A 1  0204            DC       INFOM
000B 0  70FC            MDX      *-4
000C 0  C0FA            LD       WDCNT      LOAD WORD COUNT ON FIL27
000D 01 D4000346        STO   L  CB@CD
000F 20 04262495        LIBF     DISKN      READ FIL27 TO GET UNSCALED
0010 0  1000            DC       /1000      (MEAN + PERIODIC)
0011 1  0346            DC       CB@CD
0012 0  0000            DC       /0000
0013 20 04262495        LIBF     DISKN
0014 0  0100            DC       /0100
0015 1  0346            DC       CB@CD
0016 0  70FC            MDX      *-4
0017 01 C4000208        LD    L  PONTS
0019 0  1001            SLA      1
001A 01 D4000140        STO   L  TNPTS
001C 0  1010            SLA      16         SET UP ZERO IN A-REG.
001D 01 94000208        S     L  PONTS      SUBTRACT NO. OF PTS.
001F 01 D400013F        STO   L  MNPTS      MINUS NO. OF PONTS
0021 01 6580013F        LDX   I1 MNPTS      DO LOOP FOR CHANNEL1
0023 01 C4000348   LOOP1 LD    L  AREAE-1    LOAD (MEAN + PERI)
0025 01 84000142        A     L  ZERO1      ADD UNSCALED ZERO VOLY
0027 01 A4000143        M     L  SCALE      SCALING
0029 01 D4000144   ARRAG STO   L  AREAG
002B 01 74010024        MDX   L  LOOP1+1,1
002D 01 7401002A        MDX   L  ARRAG+1,1
002F 0  7101            MDX    1 1          INCREASE INDEX REG.1 BY 1
0030 0  70F2            MDX      LOOP1      GO TO LOOP1
0031 0  C0F2            LD       LOOP1+1
0032 01 94000208        S     L  PONTS
0034 0  D0EF            STO      LOOP1+1
0035 0  C0F4            LD       ARRAG+1
0036 01 94000208        S     L  PONTS
0038 0  D0F1            STO      ARRAG+1
0039 01 C4000488        LD    L  ADRE       CALCUL. ADRESS 3.CH.
003B 01 84000140        A     L  TNPTS
003D 01 9400013A        S     L  DEC1
003F 0  D003            STO      LOOP2+1
0040 01 6680013F        LDX   I2 MNPTS      DO LOOP FOR CHANNEL 3
0042 00 C4000000   LOOP2 LD    L  *-*        LOAD MEAN + PERIODIC
0044 01 A4000143        M     L  SCALE
0046 01 D40001A4   ARRAH STO   L  AREAH
0048 01 74010043        MDX   L  LOOP2+1,1
004A 01 74010047        MDX   L  ARRAH+1,1
004C 0  7201            MDX    2 1          RAISE INDEX REG.2 BY 1
004D 0  70F4            MDX      LOOP2
```

```
004E 0  C0F7                LD      ARRAH
004F 01 94000208            S    L  PONTS
0051 0  D0F5                STO     ARRAH+1
0052 20 23A17171            LIBF    TYPE1       PRINT RUNNO
0053 1  020A                DC      CLICK
0054 0  0001                DC      1
0055 01 0C0000E4            XIO  L  IOCCA       READ DATA ENTRY SWITCH
0057 01 E40000E7            AND  L  MASC2       TEST FOR SWITCH 2
0059 0  4820                BSC     Z           SKIP IF DES 2 IS NOT SET
005A 0  700D                MDX     SKIPP       SKIPP OUTPUT CHANNEL 1
005B 20 26663A15            LIBF    WRTYN       WRITE MESSAGE FOR SEDIMENT
005C 0  2001                DC      /2001
005D 1  0489                DC      DMES1-1
005E 0  0000                DC      /0000
005F 20 26663A15            LIBF    WRTYN
0060 0  0001                DC      /0001
0061 0  70FD                MDX     *-3
0062 01 C4000208            LD   L  PONTS
0064 0  D002                STO     NOP
0065 20 23A17171            LIBF    TYPE1       TYPE OUT SED. CONCENTRATION
0066 1  0144                DC      AREAG       IN PPM UNIT
0067 0  0000        NOP     DC      *-*
0068 20 26663A15    SKIPP   LIBF    WRTYN       WRITE MESSAGE FOR V-COMP
0069 0  2001                DC      /2001
006A 1  049A                DC      DMES2-1
006B 0  0000                DC      /0000
006C 20 26663A15            LIBF    WRTYN
006D 0  0001                DC      /0001
006E 0  70FD                MDX     *-3
006F 01 C4000208            LD   L  PONTS
0071 0  D002                STO     NNOP
0072 20 23A17171            LIBF    TYPE1       TYPE OUT V-COMP.
0073 1  01A4                DC      AREAH       IN 1000*(FT/S) UNIT
0074 0  0000        NNOP    DC      *-A*
0075 01 0C0000E4            XIO  L  IOCCA       READ DATA ENTRY SWITCH
0077 01 E40000E6            AND  L  MASC
0079 0  4808                BSC     +
007A 0  7067                MDX     OUT
007B 20 03059115            LIBF    CARDN       FEEDS 1 CARD
007C 0  3000                DC      /3000
007D 0  0000                DC      0
007E 20 03059115            LIBF    CARDN
007F 0  0000                DC      /0000
0080 0  70FD                MDX     *-3
0081 01 C400020A            LD   L  CLICK       PUNCH RUNNO
0083 20 02255103            LIBF    BINDC
0084 1  00E9                DC      OUTPT
0085 01 C4000209            LD   L  WAVES       PUNCH NO OF WAVES
0087 20 02255103            LIBF    BINDC
0088 1  00EF                DC      OUTPT+6
0089 01 C400013D            LD   L  DEC12
008B 0  D05C                STO     AREA
008C 20 03059115            LIBF    CARDN
008D 0  2000                DC      /2000
008E 1  00E8                DC      AREA
008F 0  0000                DC      0
0090 20 03059115            LIBF    CARDN
0091 0  0000                DC      /0000
0092 0  70FD                MDX     *-3
0093 01 C400013E            LD   L  DEC72       PUNCH MEAN AND
0095 0  D052                STO     AREA        PERIODIC ON CARDS
0096 01 65800208            LDX  11 PONTS
0098 0  620C        PUNCH   LDX  2  12          12 VALUES PER CARD
0099 01 C40001A4    CONV    LD   L  AREAH
009B 20 02255103            LIBF    BINDC
009C 1  00E9        OTP     DC      OUTPT
```

```
009D 01 7406009C          MDX   L  OTP,6      FIELD FOR NEXT VALUE
009E 01 7401009A          MDX   L  CONV+1,1    NEXT VALUE.
00A1 0  72FF              MDX   2  -1
00A2 0  70F6              MDX      CONV
00A3 20 03059115          LIBF     CARDN
00A4 0  2000              DC       /2000
00A5 1  00E8              DC       AREA
00A6 0  0000              DC       0
00A7 20 03059115          LIBF     CARDN
00A8 0  0000              DC       /0000
00A9 0  70FD              MDX      *-3
00AA 01 74B8009C          MDX   L  OTP,-72     RESTORES 1. OUTPUT AD.
00AC 0  71F4              MDX   1  -12
00AD 0  70EA              MDX      PUNCH
00AE 01 C4000208          LD    L  PONTS       PRINTOUT OF REST
00B0 0  1890              SRT      16
00B1 01 AC000138          D     L  DEC12
00B3 0  1090              SLT      16
00B4 01 B4000139          CMP   L  ZERO
00B6 0  7002              MDX      GOON
00B7 0  7024              MDX      RSTOR
00B8 0  7023              MDX      RSTOR
00B9 01 D4000141    GOON  STO   L  REST
00BB 01 A4000138          M     L  DEC6
00BD 0  1090              SLT      16
00BE 01 D40000E8          STO   L  AREA
00C0 0  C0D9              LD       CONV+1      SET ADRESS IN AREAH
00C1 0  D006              STO      CONVV+1
00C2 01 84000141          A     L  REST
00C4 0  D0D5              STO      CONV+1
00C5 01 66800141          LDX   12 REST
00C7 00 C4000000    CONVV LD    L  *-*
00C9 20 02255103          LIBF     BINDC
00CA 1  00E9        OTTP  DC       OUTPT
00CB 01 740600CA          MDX   L  OTTP,6
00CD 01 740100C8          MDX   L  CONVV+1,1
00CF 0  72FF              MDX   2  -1
00D0 0  70F6              MDX      CONVV
00D1 20 03059115          LIBF     CARDN
00D2 0  2000              DC       /2000
00D3 1  00E8              DC       AREA
00D4 0  0000              DC       0
00D5 20 03059115          LIBF     CARDN
00D6 0  0000              DC       /0000
00D7 0  70FD              MDX      *-3
00D8 0  C0F1              LD       OTTP        RESTORES OTTP
00D9 01 940000E8          S     L  AREA
00DB 0  D0EE              STO      OTTP
00DC 01 C400009A    RSTOR LD    L  CONV+1      RESTORES ADR. IN CONV+1
00DE 01 94000208          S     L  PONTS
00E0 01 D400009A          STO   L  CONV+1
00E2 30 059C98C0    OUT   CALL     EXIT
00E4    0000              BSS   E  0
00E4 0  0000        IOCCA DC       /0000       READ DATA ENTRY SW.
00E5 0  0740              DC       /0740
00E6 0  0001        MASC  DC       /0001
00E7 0  0002        MASC2 DC       /0002       MASK FOR DES 2
00E8 0  0000        AREA  DC       *-A*         OUTPUT AREA FOR CARDS
00E9    0050        OUTPT BSS      80
0139 0  0000        ZERO  DC       0
013A 0  0001        DEC1  DC       1
013B 0  0006        DEC6  DC       6
013C 0  0068        DEC10 DC       104
013D 0  000C        DEC12 DC       12
013E 0  0048        DEC72 DC       72
013F 0  0000        MNPTS DC       *-*
```

```
0140 0  0000          TNPTS DC      *-*
0141 0  0000          REST  DC      *-*
0142 0  0000          ZERO1 DC      0          ZERO SHIFT CHAN.1
0143 0  2717          SCALE DC      10007
0144    0060          AREAG BSS     96         PPM FOR SED. CONC.
01A4    0060          AREAH BSS     96         1000*(FT/S)FOR V-COMP.
0204 31 00253CB0      INFOM DSA     FIL20
0207 0  0000          DELAY DC      *-*
0208 0  0000          PONTS DC      *-*
0209 0  0000          WAVES DC      *-*
020A 0  0000          CLICK DC      *-*
020B    0060          AREAB BSS     96
026B    00DB          AREAF BSS     219
0346 31 00253CB7      CBQCD DSA     FIL27
0349    013F          AREAE BSS     319
0488 1  0349          ADRE  DC      AREAE
0489 0  0010                DC      DMESA-DMES1
048A    0008          DMES1 DMES    '2RPRESSURE '
048F    0013                DMES    (MEAN AND PERIODIC)'E
0499 0  8105                DC      /8105
049A    0000          DMESA BES     0
049A 0  0015                DC      DMESB-DMES2
049B    0014          DMES2 DMES    '2RVELOCITY COMPONENT'
04A5    0014                DMES    (MEAN AND PERIODIC)'E
04AF 0  8105                DC      /8105
04B0    0000          DMESB BES     0
04B0    0000                END     START
    NO ERRORS IN ABOVE ASSEMBLY.
CNVRT
DUP FUNCTION COMPLETED
 // JOB   0000011111
 // END OF ALL JOBS
```

```
// JOB   0000011111
// ASM CONVT
*LIST
                        ********************************************************
                        *     PROGRAM : CONVT                                  *
                        *  THIS PROGRAM CONVERTS VOLTAGE UNIT OF RANDOM        *
                        *  FLUCTUATIONS FOR PRINTOUT. AND PUNCHES CARDS.       *
                        *  DES1 UP : CARDS ARE PUNCHED                         * *
                        *  DES2 UP : PRINTOUT CHANNEL 1 IS SUPRESSED           *
                        *  PROGRAMMED BY A. MUELLER      MARCH 1977            *
                        ********************************************************
0000 01 C400022C   START LD    L  DEC9       LOAD WORD COUNT ON FIL20
0002 01 D4000234        STO   L  INFOM
0004 20 04262495        LIBF     DISKN       GET INFORMATION
0005 0  1000            DC       /1000
0006 1  0234            DC       INFOM
0007 0  0000            DC       /0000
0008 20 04262495        LIBF     DISKN
0009 0  0100            DC       /0100
000A 1  0234            DC       INFOM
000B 0  70FC            MDX      *-4
000C 01 C4000487        LD    L  WORDC      LOAD WORD COUNT ON FIL22
000E 01 D4000242        STO   L  CPVST
0010 20 04262495        LIBF     DISKN       GET SQUARE VALUE OF
0011 0  1000            DC       /1000       RANDOM FLUCTUATION
0012 1  0242            DC       CPVST
0013 0  0000            DC       /0000
0014 20 04262495        LIBF     DISKN
0015 0  0100            DC       /0100
0016 1  0242            DC       CPVST
0017 0  70FC            MDX      *-4
0018 0  1010            SLA      16          SET A REGISTER ZERO
0019 01 94000238        S     L  PONTS
001B 01 D400022D        STO   L  MNPTS       MINUS NO. OF PONTS
001D 0  1001            SLA      1           MULTIPLY BY TWO
001E 01 D400022E        STO   L  TNPTS       -2* NO. OF PONTS
0020 0  1001            SLA      1
0021 01 D400022F        STO   L  FNPTS       -4* NO. OF PONTS
0023 01 C4000239        LD    L  WAVES
0025 0  1090            SRT      16          SET UP DOUBLE PRECISION
0026 30 051064E3        CALL     EDFLT       FLOAT NO. OF WAVES
0028 20 058A3580        LIBF     ESTO        STORE FLOATED WAVES
0029 1  0230            DC       DVSER
002A 20 23A17171        LIBF     TYPE1       PRINT RUNNO
002B 1  023A            DC       CLICK
002C 0  0001            DC       1
002D 01 0C000112        XIO   L  IOCCA       READ DATA ENTRY SWITCH
002F 01 E4000115        AND   L  MASC2       TEST FOR SWITCH 2
0031 0  4820            BSC      Z           SKIP IF DES 2 IS NOT SET
0032 0  7037            MDX      SKIPP       SKIPP OUTPUT CHANNEL 1
0033 20 26663A15        LIBF     WRTYN       CARRAGE RETURN
0034 0  2001            DC       /2001
0035 1  0488            DC       CARIG.
0036 0  0000            DC       0
0037 20 26663A15        LIBF     WRTYN
0038 0  0001            DC       /0001
0039 0  70FD            MDX      *-3
003A 20 26663A15        LIBF     WRTYN
003B 0  2001            DC       /2001
003C 1  0494            DC       DMES1-1     HEADING FOR CHANNEL 1
003D 0  0000            DC       0
003E 20 26663A15        LIBF     WRTYN
003F 0  0001            DC       /0001
0040 1  003E            DC       *-3
```

```
0041 20 26663A15          LIBF    WRTYN     CARRAGE RETURN
0042 0  2001              DC      /2001
0043 1  0488              DC      CARIG
0044 0  0000              DC      0
0045 20 26663A15          LIBF    WRTYN
0046 0  0001              DC      /0001
0047 0  70FD              MDX     *-3
0048 01 6580022E          LDX  I1 TNPTS     SET UP INDEX REG. 1
004A 01 CC000244    LOOP1 LDD  L  AREAD-1   LOOP FOR CHANNEL 1
004C 30 051064E3          CALL    EDFLT     FLOAT THE VALUE
004E 20 05109940          LIBF    EDIV      DEVIDE BY NO. OF WAVES
004F 1  0230              DC      DVSER
0050 30 05898640          CALL    ESQR      TAKE SQUARE ROOT
0052 20 091899C0          LIBF    IFIX      CONVERT TO INTEGER
0053 01 D4000160    ADO   STO  L  AREAG
0055 01 74010054          MDX  L  ADO+1,1
0057 01 7402004B          MDX  L  LOOP1+1,2
0059 0  7102        LOOPC MDX    1 2
005A 0  70EF              MDX     LOOP1
005B 01 C4000238          LD   L  PONTS
005D 0  D002              STO     NPON
005E 20 23A17171          LIBF    TYPE1     PRINTOUT 1.CHANNEL
005F 1  016C              DC      AREAG
0060 0  0000        NPON  DC      *-*
0061 0  C0F2              LD      ADO+1     RESTORES ADR. IN AREAG
0062 01 94000238          S    L  PONTS
0064 01 D4000054          STO  L  ADO+1
0066 0  C0E4              LD      LOOP1+1
0067 01 84000226          A    L  TNPTS
0069 0  D0E1              STO     LOOP1+1
006A 20 26663A15    SKIPP LIBF    WRTYN     CONVERSION CHANNEL 3
006B 0  2001              DC      /2001
006C 1  0488              DC      CARIG
006D 0  0000              DC      0
006E 20 26663A15          LIBF    WRTYN
006F 0  0001              DC      /0001
0070 0  70FD.             MDX     *-3
0071 20 26663A15          LIBF    WRTYN     HEADING FOR CHANNEL 3
0072 0  2001              DC      /2001
0073 1  04A2              DC      DMES2-1
0074 0  0000              DC      0
0075 20 26663A15          LIBF    WRTYN
0076 0  0001              DC      /0001
0077 0  70FD              MDX     *-3
0078 20 26663A15          LIBF    WRTYN     CARRAGE RETURN
0079 0  2001              DC      /2001
007A 1  0488              DC      CARIG
007B 0  0000              DC      0
007C 20 26663A15          LIBF    WRTYN
007D 0  0001              DC      /0001
007E 0  70FD              MDX     *-3
007F 01 6580022E.         LDX  I1 TNPTS
0081 01 C4000485          LD   L  ADRD      SETS ADR. FOR 3.CHANNEL
0083 01 9400022F          S    L  FNPTS
0085 01 94000486          S    L  DEC1
0087 0  D001              STO     LOOP2+1
0088 00 CC000000    LOOP2 LDD  L  *-*       LOOP FOR CHANNEL 3
008A 30 051064E3          CALL    EDFLT     FLOAT THE VALUE
008C 20 05109940          LIBF    EDIV      DIVISION ROUTINE
008D 1  0230              DC      DVSER.
008E 30 05898640          CALL    ESQR      SQUARE ROOT
0090 20 091899C0          LIBF    IFIX      CONVERTS TO INTEGER
0091 01 D40001CC    AD1   STO  L  AREAH     FIELD FO INT. VALUE
0093 01 74010092          MDX  L  AD1+1,1
0095 01 74020089          MDX  L  LOOP2+1,2
0097 0  7102        LOOPB MDX    1 2
```

```
0098 0  70EF              MDX     LOOP2
0099 01 C4000238          LD   L  PONTS
009B 0  D002              STO     NPPON
009C 20 23A17171          LIBF    TYPE1       PRINTOUT 3.CHANNEL
009D 1  01CC              DC      AREAH
009E 0  0000        NPPON DC      *-*
009F 0  C0F2              LD      ADI+1       RESTORES 1.ADR. IN AREAH
00A0 01 94000238          S    L  PONTS
00A2 0  D0EF              STO     ADI+1
00A3 01 0C000112          XIO  L  IOCCA       READ DATA ENTRY SWITCH
00A5 01 E4000114          AND  L  MASC
00A7 0  4808              BSC     +
00A8 0  7066              MDX     OUT
00A9 20 03059115          LIBF    CARDN       FEEDS 1 CARD
00AA 0  3000              DC      /3000
00AB 0  0000              DC      0
00AC 20 03059115          LIBF    CARDN
00AD 0  0000              DC      /0000
00AE 0  70FD              MDX     *-3
00AF 01 C400023A          LD   L  CLICK       PUNCH RUNNO
00B1 20 02255103          LIBF    BINDC
00B2 1  0117              DC      OTPUT
00B3 01 C4000239          LD   L  WAVES
00B5 20 02255103          LIBF    BINDC
00B6 1  011D              DC      OTPUT+6
00B7 01 C4000169          LD   L  DEC12
00B9 0  D05C              STO     AREA
00BA 20 03059115          LIBF    CARDN
00BB 0  2000              DC      /2000
00BC 1  0116              DC      AREA
00BD 0  0000              DC      0
00BE 20 03059115          LIBF    CARDN
00BF 0  0000              DC      /0000
00C0 0  70FD.             MDX     *-3
00C1 01 C400016A          LD   L  DEC72       PUNCH MEAN AND
00C3 0  D052              STO     AREA        PERIODIC ON CARDS
00C4 01 65800238          LDX  11 PONTS
00C6 0  620C        PUNCH LDX   2 12          12 VALUES PER CARD
00C7 01 C40001CC    CONV  LD   L  AREAH
00C9 20 02255103          LIBF    BINDC
00CA 1  0117        OTP   DC      OTPUT
00CB 01 740600CA          MDX  L  OTP,6       FIELD FOR NEXT VALUE
00CD 01 740100C8          MDX  L  CONV+1,1    NEXT VALUE
00CF 0  72FF              MDX   2 -1
00D0 0  70F6              MDX     CONV
00D1 20 03059115          LIBF    CARDN
00D2 0  2000              DC      /2000
00D3 1  0116              DC      AREA
00D4 0  0000              DC      0
00D5 20 03059115          LIBF    CARDN
00D6 0  0000              DC      /0000
00D7 0  70FD              MDX     *-3
00D8 01 74B800CA          MDX  L  OTP,-72     RESTORES 1. OUTPUT AD.
00DA 0  71F4              MDX   1 -12
00DB 0  70EA              MDX     PUNCH
. 00DC 01 C4000238          LD   L  PONTS     PRINTOUT OF REST
00DE 0  1890              SRT     16
00DF 01 AC000169          D    L  DEC12
00E1 0  1090              SLT     16
00E2 01 B4000167          CMP  L  ZERO
00E4 0  7002              MDX     GOON
00E5 0  7023              MDX     RSTOR
00E6 0  7022              MDX     RSTOR
00E7 01 D400016B    GOON  STO  L  REST
00E9 01 A4000168          M    L  DEC6
00EB 0  1090              SLT     16
```

```
00EC 01 D4000116          STO  L  AREA
00EE 0  C0D9              LD      CONV+1      SET ADRESS IN AREAH
00EF 0  D0D6              STO     CONVV+1
00F0 01 8400016B          A    L  REST
00F2 0  D0D5              STO     CONV+1
00F3 01 6680016B          LDX  12 REST
00F5 00 C4000000  CONVV   LD   L  *-*
00F7 20 02255103          LIBF    BINDC
00F8 1  0117      OTTP    DC      OTPUT
00F9 01 740600F8          MDX  L  OTTP,6
00FC 01 740100F6          MDX  L  CONVV+1,1
00FD 0  72FF              MDX   2 -1
00FE 0  70F6              MDX     CONVV
00FF 20 03059115          LIBF    CARDN
0100 0  2000              DC      /2000
0101 1  0116              DC      AREA
0102 0  0000              DC      0
0103 20 03059115          LIBF    CARDN
0104 0  0000              DC      /0000
0105 0  70FD              MDX     *-3
0106 0  C0F1              LD      OTTP        RESTORES OTTP
0107 0  900E              S       AREA
0108 0  D0EF              STO     OTTP
0109 01 C40000C8  RSTOR   LD   L  CONV+1      RESTORES ADR. IN CONV+1
010B 01 94000238          S    L  PONTS
010D 01 D40000C8          STO  L  CONV+1
010F 30 059C98C0  OUT     CALL    EXIT
0112    0000              BSS  E  0
0112 0  0000      IOCCA   DC      /0000       READ DATA ENTRY SW.
0113 0  0740              DC      /0740
0114 0  0001      MASC    DC      /0001
0115 0  0002      MASC2   DC      /0002       MASK FOR DES 2
0116 0  0000      AREA    DC      *-*         OUTPUT AREA FOR CARDS
0117    0050      OTPUT   BSS     80
0167 0  0000      ZERO    DC      0
0168 0  0006      DEC6    DC      6
0169 0  000C      DEC12   DC      12
016A 0  0048      DEC72   DC      72
016B 0  0000      REST    DC      *-*
016C    0060      AREAG   BSS     96          STOR. 1. CHANNEL
01CC    0060      AREAH   BSS     96          STOR. 2. CHANNEL
022C 0  0009      DEC9    DC      9
022D 0  0000      MNPTS   DC      *-*
022E 0  0000      TNPTS   DC      *-*
022F 0  0000      FNPTS   DC      *-*
0230    0003      DVSER   BSS     3
0234    0000              BSS  E  0
0234 31 06253CB0  INFOM   DSA     FIL20       INFORMATIONF FOR EXP.CONST
0237 0  0000      DELAY.  DC      *-*
0238 0  0000      PONTS   DC      *-*
0239 0  0000      WAVES   DC      *-*
023A 0  0000      CLICK   DC      *-*
023B    0006              BSS     6
0242    0000              BSS  E  0
0242 31 06253CB2  CPVST   DSA     FIL22       USES FIL22 AND FIL23
0245    0240      AREAD   BSS     576         SQUARE OF RANDOM FLUCTU.
0485 1  0245      ADRD    DC      AREAD
0486 0  0001      DEC1    DC      1
0487 0  0240      WORDC   DC      576
0488 0  0001      CARIG   DC      1
0489 0  8181              DC      /8181
048A 0  0008              DC      8
048B    0008      OUTPT   BSS     8
0493 0  2121              DC      /2121
0494 0  000D              DC      DMESA-DMES1
0495    0018      DMES1   DMES    '2RRMS VALUES OF PRESSURE'E
```

```
04A1 0  8105                    DC      /8105
04A2    0000            DMESA   BES     0
04A2 0  001B                    DC      DMESB-DMES2
04A3    001B            DMES2   DMES    '2RMS VALUES OF THE RANDOM '
04B0    0019                    DMES    COMPONENT OF THE VELOCITY'E
04C0 0  8105                    DC      /8105
04BE    0000            DMESB   BES     0
04BE    0000                    END     START
    NO ERRORS IN ABOVE ASSEMBLY.
)CONVT
)UP FUNCTION COMPLETED
// JOB   0000011111
// END OF ALL JOBS
```